

Characterization of genetic modulators of PARP inhibitor sensitivity: molecular mechanisms and therapeutic implications

Ph.D. Thesis

Hasan Mamar

Supervisor: Gyula Timinszky, M.D., Ph.D.

Co-supervisor: Roberta Fajka-Boja, Ph.D.

**HUN
REN**



Doctoral School of Biology
Faculty of Science and Informatics
University of Szeged

Laboratory of DNA damage and nuclear dynamics
Institute of Genetics
Biological Research Centre, Szeged

Szeged, 2024

Table of Contents

List of abbreviations	4
1. Introduction	6
1.1. Personalized medicine in cancer treatment.....	6
1.2. Synthetic lethality in cancer therapy.....	7
1.3. BRCA1 and BRCA2 functions to maintain genomic integrity.....	9
1.3.1. Role of BRCA1 and BRCA2 in DSB repair through homologous recombination repair pathway	9
1.3.2. BRCA1 and BRCA2 in DNA replication	11
1.4. ADP-ribosylation and PARP inhibitors	13
1.4.1. PARP1 as the main catalyzer of ADP-ribosylation.....	13
1.4.2. PARP inhibitors in cancer therapy	15
1.5. Hallmarks of PARP inhibitor sensitivity.....	17
1.5.1. Homologous recombination deficiency	17
1.5.2. PARPi-induced ssDNA gap accumulation.....	18
1.6. Mechanisms of PARP inhibitor resistance.....	19
1.6.1. Secondary Reversion Mutations in HR Genes	20
1.6.2. Restoration of HR Gene Expression.....	21
1.6.3. HR rewiring due to loss of factors of NHEJ pathway	21
1.7. Identification of regulators of PARP inhibitor sensitivity	22
2. Aims	24
3. Materials and Methods	25
3.1. Cell lines and cell culture.....	25
3.2. RNA Interference and Plasmid Transfection	26
3.3. PARP1 recruitment to sites of laser irradiation.....	26
3.4. Immunofluorescence.....	27
3.5. Alkaline comet assay	28
3.6. BrdU comet post-replication repair assay.....	28
3.7. DNA fiber assay.....	29
3.8. Cell survival assays.....	30
3.9. Flow cytometry for intracellular markers and cell cycle analysis	30
3.10. Western blotting	31
3.11. Statistical analysis	31

4.	Results	32
4.1.	Deciphering the role of ALC1 in inducing PARP inhibitor sensitivity.....	32
4.1.1.	Loss of ALC1 underlies sensitivity to PARP inhibitors and increased genomic instability	32
4.1.2.	PARP inhibitor toxicity in ALC1-deficient cells is due to enhanced PARP1 trapping. 35	
4.1.3.	Loss of ALC1 impairs both HR and NHEJ.....	37
4.1.4.	Overexpression of the oncogene ALC1 drives resistance to PARP inhibitors in BRCA-deficient cells.	38
4.2.	Investigating the molecular mechanism underlying PARP inhibitor sensitivity in POLE4-deficient cells.	39
4.2.1.	Deletion of the accessory subunits of DNA polymerase epsilon leads to PARP inhibitor sensitivity	39
4.2.2.	Sensitivity of POLE4 KO to PARP inhibitors is dependent on the presence of PARP1 with no defects in its recruitment kinetics	40
4.2.3.	POLE4 loss reduces replication fork speed and causes accumulation of PARPi-induced ssDNA gaps	42
4.2.4.	POLE4 as a protector against replication stress induced by PARPi or ATRi44	
4.2.5.	PARPi-induced replication stress is driven by PIKKs	49
4.2.6.	Sensitivity of POLE4 KO to PARP inhibitors is independent of BRCA1 status 52	
5.	Discussion.....	54
6.	Summary.....	59
7.	Összefoglaló	62
8.	Acknowledgment.....	65
9.	References	67
10.	List of Publications	88
11.	Appendix.....	89
12.	Declaration.....	93
13.	Co-authors declaration.....	94

List of abbreviations

53BP1: p53 Binding Protein 1

ALC1: Amplified in liver cancer 1.

ARH: ADP-ribosyl hydrolase.

ARTD: ADP-ribosyltransferase diphtheria-toxin like.

ARTs: ADP-ribosyltransferases.

ATM: Ataxia-telangiectasia mutated.

ATR: Ataxia-telangiectasia mutated and RAD3-related.

BARD1: BRCA1-associated RING domain.

BER: Base excision repair.

BRCA: BReast CAncer Susceptibility protein.

CtIP: CtBP-interacting protein.

DNA-PK: DNA-dependent protein kinase.

DSB: DNA double strand breaks.

dsDNA: Double stranded DNA.

FANC: Fanconi anemia.

HPF1: Histone PARylation factor 1.

HR: Homologous recombination.

HU: Hydroxyurea.

ICLs: Interstrand crosslinks.

KO: Knockouts.

LIG3: Ligase 3.

MARylation: Mono-ADP-ribosylation.

MMEJ: Micro-homology end-joining.

NAD⁺: Nicotinamide adenine dinucleotide.

NER: Nucleotide excision repair.

NHEJ: Non-homologous end joining.

PALB2: Partner And Localizer of BRCA2.

PARG: Poly(ADP-ribose) Glycohydrolase.

PARPi: PARP inhibitors.

PARylation: Poly-ADP-ribosylation.

PCNA: Proliferating cell nuclear antigen.

PDX: Patient-derived xenograft.

PIKK: Phosphatidylinositol 3-kinase-related kinase.

POLE3: DNA polymerase epsilon accessory subunit 3.

POLE4: DNA polymerase epsilon accessory subunit 4.

POL β : DNA polymerase β .

POL ϵ : DNA polymerase epsilon.

PRIMPOL: Primase/polymerase.

PRR: Post-replicative repair.

RPA: Replication protein A.

SLFN11: Schlaffen 11.

ssDNA: Single stranded DNA.

TARG1: Terminal ADP-ribose protein glycohydrolase.

UV: Ultraviolet.

γ H2AX: Phosphorylated histone variant H2AX.

1. Introduction

1.1. Personalized medicine in cancer treatment

If evolution is the survival of the fittest, then perhaps cancer is outperforming us, humans. It is *immortal*. Yet, this continues to haunt us, as this immortality causes our own mortality. Our encounter with cancer dates to prehistoric times, when we first noticed irregular lumps suspiciously appearing on the body. Since then, what could be the longest battle in our lifetime has commenced and it is yet to be over (1, 2).

Different strategies were adopted to manage cancer, from surgery and excision to radiation and cytotoxic compounds. The main slogan for a long time was “one disease requires one treatment”. During the twentieth century, scientists ramped up their efforts screening through countless chemical compounds hoping to discover what Nobel laureate Paul Erlich once described as the “magic bullet” that would cure cancer, once and for all (3).

It took limitless efforts of thousands of scientists to advance our knowledge in genetics, cell biology and biochemistry to finally realize that what is termed ‘cancer’ is actually numerous diseases driven by various genetic alterations, making every cancer patient a unique case that needs to be carefully studied and understood before a medication is administered. This uniqueness is translated scientifically into what would become a fundamental hallmark of cancer, *heterogeneity*, and to manage these diseases medicine must be *personalized* (4–6).

Personalized medicine started to become a prominent term in the late twentieth century concomitant to the sequencing of the human genome (7). Since then, tremendous efforts have been made to define it, expand it, and put it in practice. The National Human Genome Research Institute in the United States defines personalized medicine as “an emerging practice of medicine that uses an individual's genetic profile to guide decisions made in regard to the prevention, diagnosis, and treatment of disease” (8). In the context of cancer treatment, personalized medicine is divided into two types, the first one is immunotherapy, where medical intervention aims to harness the power of the patient’s immune system to unleash a decisive attack that would wipe out the tumor. The second type is the targeted drug therapy, small molecules or biologics that are designed to hit specific targets in or on the cancer cells. The rationale here is to exploit the same genetic alterations that drive

tumorigenesis and use them as hallmarks to differentiate malignant cells from normal ones, therefore, pave the way for targeted drug intervention that would eliminate the cancer cells with minimal side effects (9).

1.2. Synthetic lethality in cancer therapy

Targeted cancer therapy aims to exploit the very same feature that gives the cancer cell an edge over its neighboring normal ones and turns that feature into *Achilles' heel* by designing a drug that would eliminate only those cells where this feature is present, thus, achieving precision therapy. This can be achieved through two main modalities, first one is by leveraging the phenomenon of “oncogene addiction” (10), that is when a tumor relies on a gain-of-function mutation that upregulates a certain pathway which becomes essential for the tumor’s survival. By inhibiting this pathway, the addicted tumor is precisely eliminated (10). The second possibility for targeted therapy concerns tumors that carry non-oncogenic cancer-specific mutation and become dependent on the activity of another partner gene (11). This partner gene or its protein product becomes ideal target for drugs, as inhibiting it would be lethal for such tumors, a phenomenon termed as *synthetic lethality*, where two mutations with a viable phenotype for either of them alone lead to a lethal phenotype if they are present together (11).

This concept was first described in the mid twentieth century via genetic studies on fruit flies (12) and was observed later on in yeast as well (13). While this concept is highly attractive for developing targeted therapy (14), it has remained difficult to identify for several reasons. Firstly, since by definition the combination of these genetic alterations is not viable, it is challenging to detect it and characterize it (11). Secondly, for a synthetic lethal interaction to be adopted as a basis for developing a drug, it needs to be *highly penetrant*, that is such interaction is not dependent on the genetic background of the tumor (15). Such highly penetrant interactions are the exception rather than the rule, which made it very difficult to identify synthetic lethality with common oncogenes, as often these cases tend to be very specific to the genetic background of the patient. Therefore, it is crucial to draw a line between synthetic lethal interactions identified in the lab and those that can be expanded to have applicability by the bedside (11).

Due to these limitations only one family of drugs, so far, that are developed based on a synthetic lethal interaction has made it all the way from experimental discovery in 2005 (16, 17), to clinical trials and approvals to be used in the clinics by the United States Food and Drug Administration and the European Medicines Agency. That is the Poly ADP-ribose Polymerase (PARP) inhibitors (PARPi) and their synthetic lethality with Breast Cancer Susceptibility protein (BRCA) (**Fig. 1**).

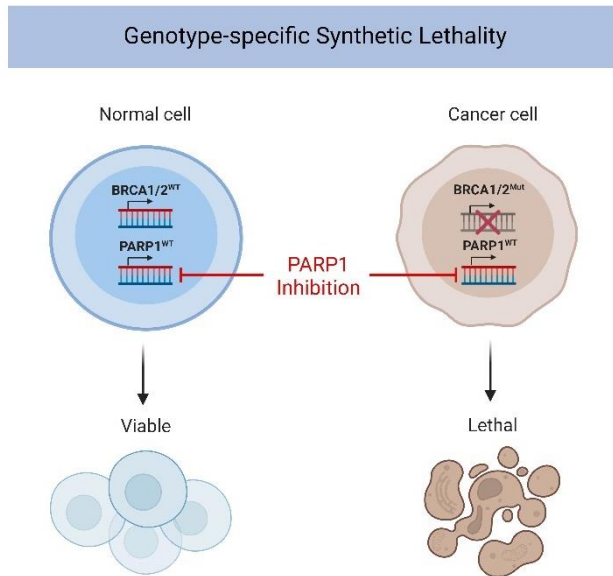


Figure 1: Synthetic lethal interaction between BRCA1/2 and PARP1

A schematic representation of the synthetic lethal interaction demonstrating that cells with wild-type BRCA1 or BRCA2 are viable despite the status of PARP1. On the other hand, inactivating mutations in either BRCA1 or BRCA2 predispose to cancer and render cells sensitive to PARP inhibitors.

The following sections will discuss the two branches of this synthetic lethal interaction, BRCA1 and BRCA2 roles in maintaining genomic integrity, as well as ADP-ribosylation as a posttranslational modification largely mediated by PARP1, the main target of PARPi. Specifically, I will discuss the activity of BRCA1 and BRCA2 in ensuring faithful repair of DNA double strand breaks (DSB) through their crucial functions within homologous recombination, a major pathway for repairing DSB and maintaining genomic stability. Furthermore, PARP1 functions in DNA damage response and replication along with PARPi mode of action will be introduced.

1.3. BRCA1 and BRCA2 functions to maintain genomic integrity

1.3.1. Role of BRCA1 and BRCA2 in DSB repair through homologous recombination repair pathway

Our genome's integrity faces constant challenges from various sources, including environmental factors like high-energy radiation and mutagenic chemicals (18, 19). Additionally, DNA replication itself is fraught with risks, as the process to replicate billions of nucleotides is hardly to go without serious challenges including potential hindrances to the DNA polymerase machinery from secondary DNA structures, replication-transcription conflicts and DNA lesions, which can result in stalled or collapsed replication forks. Failure to repair DNA damage or to resume stalled replication forks can lead to mutations or genomic instability, ultimately contributing to cancer formation (20, 21).

Among the diverse array of DNA lesions, DSB stand out as the most serious threat to genomic integrity, arising from direct exogenous insults or due to collapsed replication forks. To counteract DSB, several evolutionarily conserved pathways of DSB repair have emerged, each with distinct mechanisms, including homologous recombination (HR) and non-homologous end joining (NHEJ) (22, 23) (**Fig. 2**). In NHEJ, a protein complex comprising mainly of Ku70-Ku80 proteins and DNA-dependent protein kinase (DNA-PK) binds to the DNA broken ends, recruiting additional proteins to trim the ends, fill in any gaps, and finally seal the breaks by ligating the ends (24). While NHEJ is highly efficient in repairing DSB, it often results in deletions or insertions leading to genomic instability. On the other hand, HR is considered the most faithful mechanism for repairing DSB as it maintains genomic stability (25–27), by relying on a homology sequence to serve as a template for restoring the missing part of the DNA. Due to the fact that HR requires the sister chromatid as a template for DSB repair, its function is predominantly limited to the S and G2 phases of the cell cycle (28, 29).

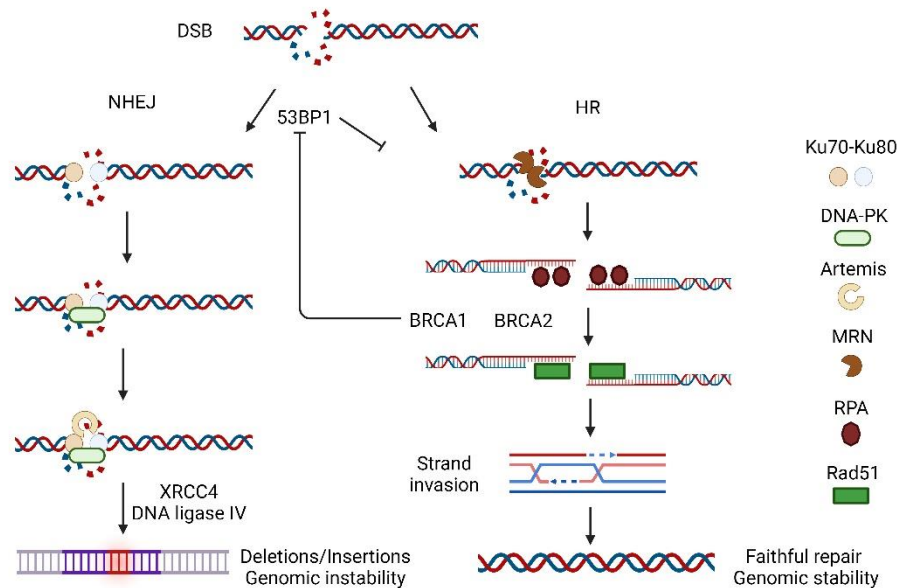


Figure 2: The two main pathways for DSB repair

DSB in the cell are repaired through two main pathways. In non-homologous end joining (NHEJ), 53BP1 blocks DNA end resection promoting NHEJ, where Ku70-Ku80 bind DNA ends and recruit DNA-PK. The DNA ends are processed by Artemis then ligated through the activity of XRCC4 and Ligase IV. This process could result in insertions or deletions of DNA, eventually causing genomic instability. In homologous recombination (HR), 53BP1 is blocked by BRCA1 which allows for DNA end resection by the MRN complex consisting of MRE11-RAD50-NBS1. The single-stranded DNA is covered by RPA to protect it from nuclease activity, this is followed by RPA-Rad51 exchange mediated by BRCA1 and BRCA2. The Rad51 filaments lead the DNA homology search and strand invasion which eventually allow for faithful repair of DSB restoring the original DNA sequence and maintaining genomic stability.

During HR, DSB ends undergo nucleolytic degradation in a process called end resection. This results in deletion of around hundreds of nucleotides to generate a 3' single-stranded DNA (ssDNA) overhang. The 3' ssDNA overhang is covered by replication protein A (RPA), which is later exchanged by the recombinase Rad51 (30–34). This sequential occupancy of DSB end resected DNA is explained by different binding affinity of RPA and Rad51 to ssDNA. The strong binding affinity of RPA to ssDNA facilitates “smoothing” of these DNA stretches from any secondary structures to allow for unhindered recruitment of Rad51 (35). Considering that Rad51 binding affinity to ssDNA is only slightly higher than to double-stranded DNA (dsDNA) (36, 37), the RPA coating step prevents creation of Rad51-dsDNA structure which is dysfunctional for homology search and strand invasion (38–40).

BRCA1 is fundamental to HR execution. The first evidence of BRCA1 role in DSB repair by HR came from observing a colocalization of BRCA1 and the recombinase Rad51 at nuclear foci induced by ionizing radiation (41). Additionally, it was reported that BRCA1 deletion in mouse and human cells resulted in failure to mount Rad51 foci at sites of DNA damage (42, 43), a crucial event in HR. Moreover, BRCA1 is implicated in the DNA end resection of DSB, as it associates with the MRE11–RAD50–NBS1 nuclease complex and the end resection factor CtBP-interacting protein (CtIP) (44, 45). Similar to BRCA1, loss of BRCA2 leads to defective HR repair (46, 47), due to its main role of regulating the formation of Rad51 filaments (32, 33). A protein complex comprised of BRCA1 along with its obligate binding partner BRCA1-associated RING domain 1 (BARD1), BRCA2-Sem1 and partner and localizer of BRCA2 (PALB2) functions to ensure the exchange of RPA and Rad51 on ssDNA (48), a crucial step in HR that precedes the homology search and strand invasion. BRCA1-BARD1 complex physically binds Rad51 (49) and BRCA1 interacts with PALB2 which facilitates recruitment of BRCA2 to DNA damage sites to assemble Rad51 (50, 51). Impairment in BRCA1-PALB2 interaction leads to defective HR (50, 51).

1.3.2. BRCA1 and BRCA2 in DNA replication

Replication of our genome is a vulnerable process even under normal conditions due to its complexity. Challenges such as DNA lesions, replication-transcription conflicts or difficult-to-replicate regions slow down or stall replication forks leading to replication stress (20, 52). Stalling of replication forks necessitates the restart of these forks to finalize duplication of the genetic material prior to mitotic entry to prevent lethal DNA breakages. Stalled forks can be triggered by uncoupling of the helicase-polymerase within the replication machinery as well as endogenous DNA damage, which results in ssDNA gaps and subsequent replication stress (53, 54).

A defining feature of BRCA1-deficient cells is the replication stress underlined by impairment in resolving stalled replication forks (5, 55). The first evidence of BRCA1 role in mitigating replication stress was described in a study utilizing hydroxyurea (HU), an agent that blocks ribonucleotide reductase activity, causing nucleotide pool depletion (56). In HU-treated cells, BRCA1 and Rad51 colocalize at S phase-specific foci indicated by Proliferating

cell nuclear antigen (PCNA), likely revealing stalled replication forks (56). BRCA1 was also shown to be recruited to stalled replication forks along with the MRE11–RAD50–NBS1 nuclease complex and the helicase Bloom syndrome protein (57), where it protects stressed forks from MRE11-mediated nucleolytic degradation (58). Multiple players of the SNF2 helicase family, specifically SMARCAL1, ZRANB3 and HLTF, mediate stalled fork remodeling in a process called ‘fork regression’ to produce a branched structure with a single DNA end, that is degraded by MRE11 when either BRCA1 or BRCA2 is absent (59).

BRCA2 is also crucial for preserving stalled forks from degradation by MRE11 (60) and EXO1 (61). HU treatment in BRCA2-deficient cells results in severe MRE11-dependent fork degradation (58, 61–63), which is rescued by inhibiting MRE11 function or reintroduction of BRCA2 (58). This function of BRCA2 at stalled replication forks is regulated by BRCA1 and PALB2, since downregulating either of them impairs this function resulting in destabilization of the replication forks (59, 64, 65). Moreover, fork recovery in Rad51-independent manner is also mediated by BRCA2 and PLAB2 which directly interact with Pol η and recruit it to sites of stalled and collapsed replication forks to initiate DNA synthesis (66).

Another source of replication stress is the physical hindrance by secondary structures that impede fork progression. Among such structures is R-loop, an RNA-DNA hybrid which reflects replication-transcription conflict. Ongoing replication machinery colliding with accumulated R-loops causes collapse of the replication fork and DSB (67). It has been shown that BRCA1 promotes R-loop resolution (68) by working together with senataxin, an RNA-DNA hybrid helicase that plays role in resolution of R-loop structures (69). In a similar fashion, BRCA1 and BRCA2 are important for resolving interstrand crosslinks (ICLs), which hinder DNA replication. These ICLs induced by chemical agents such as platinum salts or due to byproducts of cellular metabolism lead to a sensitive phenotype in BRCA-deficient tumors (70, 71).

Overall, the important role of BRCA1 and BRCA2 in maintaining genomic stability through their functions in DSB repair or replication is also highlighted by their tumor suppressor roles and the adverse effects of their loss of function (48, 72–74). Meta-analyses have demonstrated that carriers of BRCA1 pathogenic mutations have a mean cumulative breast

cancer risk of 57% by age 70, while carriers of BRCA2 mutations have a risk of 49% (75). Similarly, the mean cumulative ovarian cancer risk by age 70 for BRCA1 mutation carriers is 40% and for BRCA2 mutation carriers is 18% (75). Therefore, the possibility of selective targeting of BRCA-deficient tumors with PARPi offered a breakthrough in the field of personalized cancer treatment and encouraged further research to expand the applicability of these drugs.

1.4. ADP-ribosylation and PARP inhibitors

1.4.1. PARP1 as the main catalyzer of ADP-ribosylation

ADP-ribosylation is a posttranslational modification of proteins defined by metabolizing the enzyme cofactor nicotinamide adenine dinucleotide (NAD⁺) for the addition of mono-ADP-ribose (MAR) or poly-ADP-ribose (PAR) to proteins or nucleic acids. Proteins can be modified on glutamate, aspartate (76), serine (77), threonine (78), arginine (79, 80) and cysteine (81). Furthermore, recent reports demonstrated that both DNA (82, 83) and RNA (84–86) can be ADP-ribosylated as well. ADP-ribosyltransferases (ARTs) are the main writers of ADP-ribosylation. Most of the mammalian ARTs are classified under the ADP-ribosyltransferase diphtheria-toxin like (ARTD) subfamily (87). In humans, there are 17 ARTDs (88), which were previously called PARP. However, considering that only PARP1, PARP2, TNKS1, and TNKS2 are able to catalyze PAR chain while all other family members catalyze MAR, it was suggested that ART should be used as a unified nomenclature, while PARP would be adopted to differentiate among the different ART members (87).

As with other posttranslational modifications, ADP-ribosylation is reversible through a group of ADP-ribose hydrolase enzymes. These enzymes differ in their hydrolase ability based on whether they can recognize and cleave MAR or PAR chain. Poly(ADP-ribose) glycohydrolase (PARG) specifically cleaves the glycosidic bonds between ADP-ribose units hydrolyzing the PAR chains in an exo- or endo-glycosidic manner (89, 90). While PARG is the main enzyme reversing Poly-(ADP-ribosylation) (PARylation) by hydrolyzing ~90% of PAR chains, it cannot cleave the protein-bound proximal ADP-ribose unit (89, 91). The remaining ADP-ribose unit attached to the protein is cleaved by the MAR-erasers terminal ADP-ribose protein glycohydrolase (TARG1) (92), MacroD1 or MacroD2 (93, 94). Those MAR-erasers specifically hydrolyze the ester bond between terminal ADP-ribose and the

aspartate and glutamate residues (95). Importantly, TARG1 possesses the ability to cleave the entire PAR chain attached to glutamate residues (92, 96). The ADP-ribosyl hydrolase (ARH) family includes three enzymes, ARH1-3. Among them ARH3 has the strongest catalytic activity with the ability to hydrolyze the O-glycosidic bond of both MAR and PAR linked to serine residues (97, 98).

PARP1 is the main catalyzer of ADP-ribosylation and the most studied one. It is a highly abundant nuclear protein which is involved in many cellular processes (99). PARP1 is well-investigated for its role in the DNA damage response and repair. It has the ability to recognize and bind ssDNA breaks and promote the recruitment of XRCC1, a scaffold protein pivotal in the repair of ssDNA breaks (100). PARP1 is directly involved in the regulation of multiple repair pathways including base excision repair (BER), nucleotide excision repair (NER) as well as HR and NHEJ (99). Mechanistically, PARP1 is among the first responders to DNA lesions, it rapidly recruits to damage sites and gets activated modifying itself along with other proteins in the vicinity of the lesions (88, 99), leading to massive opening of the chromatin environment to allow for DNA repair proteins to be recruited and initiate the repair process (101). PARP1's role in regulating chromatin structure can be attributed directly to its ADP-ribosylation activity on histones (101) or indirectly by mobilizing PAR-binding chromatin remodelers such as Amplified in Liver Cancer 1 (ALC1) (102, 103). This process requires beside PARP1 activity, the presence of histone PARylation factor 1 (HPF1) to mediate serine ADP-ribosylation which is a crucial step to guarantee timely and efficient repair of DNA lesions (77, 101, 104).

Beside DNA lesions, PARP1 plays a role in DNA replication as it can bind stalled forks and reduce replication speed to mitigate replication stress. Consequently, inhibiting PARP1 has been shown to speed up replication forks causing genomic stress (105). In unperturbed scenarios, PARylation is restricted to S-phase (106), as PARP1 can recognise and bind unligated Okazaki fragments, where PARylation serves as a signal to promote their processing and ligation, therefore PARP1 promotes nascent DNA maturation on the lagging strand (106, 107). On the leading DNA strand, inhibiting PARP1 is a source of ssDNA gaps due to the upregulation of primase-polymerase (PRIMPOL)-mediated repriming of DNA synthesis upon encountering a replication obstacle (108). Additional to its function in

replication and DNA repair, PARP1 has been implicated in plethora of cellular processes, including regulation of other posttranslational modifications, gene expression, ribosome biogenesis, RNA processing and cell death. While these processes are outside the scope of this thesis work, they were discussed more in detail in these excellent reviews (99, 109).

1.4.2. PARP inhibitors in cancer therapy

PARPi as a term usually refers to compounds that mainly target and inhibit PARP1 and PARP2 by binding to the catalytic pocket of the enzyme and outcompeting NAD⁺, therefore blocking the enzymatic function (110, 111).

Due to the role of PARP1 in the DNA damage response, PARPi were first developed in the 1990s as sensitizers in combination with other therapeutic strategies (112, 113), including sensitization to DNA-methylating agents and the topoisomerase 1 poisons, such as camptothecin. Furthermore, *in vivo* preclinical studies with a combination of the PARP inhibitor, Rucaparib, and the alkylating drug temozolomide showed profound tumor regression (114, 115). This laid the groundwork for the first clinical trial of this combination for the treatment of patients with cancer, however, the outcome of the treatment proved the combination to be highly toxic (116, 117). Although further studies explored the potential of combining PARPi with platinum-based drugs (118) as well as ionizing radiation (117, 119), no approval has been granted to a combination of either conventional chemotherapy or radiotherapy with PARPi.

At the same time, mounting evidence pointed to the importance of PARP1 activity at sites of DNA damage repaired by HR pathway, and how cells lacking factors implicated in the repair of ssDNA breaks, such as XRCC1, became dependent on HR functionality (120, 121). This justified the notion that inhibiting PARP1 in cells lacking functional HR may lead to their selective killing, a hypothesis that gained more importance in the context of cancer therapy as BRCA1 and BRCA2 genes were established as tumor suppressors crucial for the seamless activity of HR pathway (122). Building on these data, two landmark studies in 2005 illustrated experimentally the sensitivity of BRCA-deficient tumor models to PARPi (16, 17). These studies demonstrated the possibility of exploiting a feature of tumors (BRCA deficiency) for selective treatment, paving the way for a new strategy in cancer therapy.

Following these preclinical studies, clinical trials began to assess the efficacy of PARPi as a single agent in the treatment of ovarian and breast cancers with BRCA deficiency, which led in 2014 to the approval of the first PARPi, Olaparib, as a maintenance therapy for patients with germline BRCA mutations and platinum-sensitive ovarian cancer.

PARPi block ADP-ribosylation and impair PARP1 dynamics at the sites of DNA damage. Faithful repair of DNA breaks requires a delicate balance between PARP1 recruitment to the damage site and its timely release (123) (**Fig. 3**). The main mechanism by which PARPi toxicity is explained is based on the fact that upon PARP1 recruitment to the site of DNA damage, PARPi inhibit its catalytic activity preventing its automodification which is important for PARP1 release from the damage site. This would cause increased retention of chromatin-bound PARP1 which is termed as ‘PARP1 trapping’. The PARP1-DNA complexes form physical barriers to replication forks leading to its collapse upon collision with these barriers and causing DSB (99, 124). Therefore, the mode of action of PARPi which underlies their cytotoxicity is through trapping of inhibited PARP1 on chromatin rather than just blocking ADP-ribosylation (124).

However, this definition of PARP1 trapping is being challenged recently by a new model suggesting that the affinity of PARP1 binding to the damage site is governed by modulation of its allostery (125). This model proposes to classify PARPi ability to ‘trap’ PARP1 based on their capability to remain engaged with the catalytic pocket of PARP1 (off-rate), an inhibitor with low off-rate such as Veliparib will favor rapid release of PARP1 from the damage site compared to an inhibitor with higher off-rate such as Talazoparib (111, 126, 127). It should be noted, however, that in order to translate this model into a clinical aspect, that is to correlate the inhibitor’s ability to retain PARP1 on damage site with its potency in the context of inducing cell death, HPF1 should be taken into consideration for its direct role in promoting PARP1 activity. This is in light of a recent study demonstrating that cytotoxicity of PARPi correlates better with the off-rate of a PARP1-HPF1 complex as compared to PARP1 alone (128). Taken together, the ‘trapping’ model of PARP1 on the DNA lesion can be better resembled by continuous recruitment of PARP1 molecules in a rate that exceeds their release rather than the physical stalling of a molecule on the lesion.

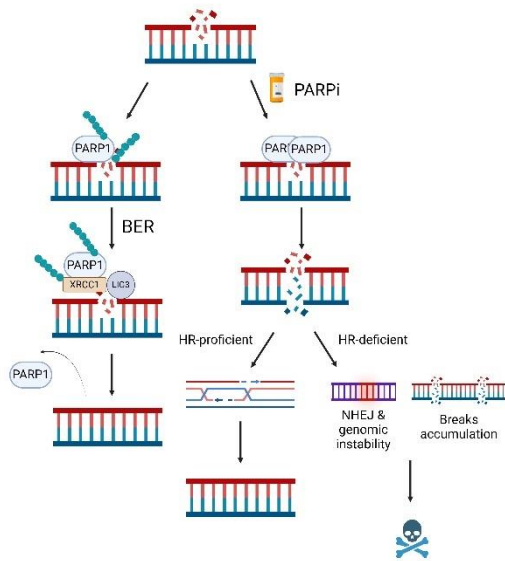


Figure 3: The role of PARP1 in ssDNA break repair

A representation of PARP1 role in the base-excision repair pathway (BER). PARP1 is recruited to sites of single-stranded DNA breaks and catalyzes ADP-ribosylation of neighboring proteins to facilitate recruitment of other repair factors such as XRCC1 and LIG3, which mediate repair of the breaks. Moreover, PARP1 ADP-ribosylates itself to promote its dissociation from the DNA break. Upon PARP inhibitor (PARPi) treatment, ADP-ribosylation is blocked and PARP1 retention on the damage site is increased leading to DSB, which can be repaired faithfully in HR-proficient genetic background. However, if HR is compromised, the DSB either persist or are repaired by NHEJ resulting in genomic instability which underlies the cytotoxicity of PARPi in HR-deficient genetic background.

So far, four PARPi (Olaparib, Rucaparib, Niraparib and Talazoparib) have been granted regulatory approval to be used in the clinic to treat patients with breast, ovarian, pancreatic, or prostate cancers, characterized by impairment in their HR, while continuous research is ongoing to identify other hallmarks of PARPi sensitivity and expand their usage at the bedside.

1.5. Hallmarks of PARP inhibitor sensitivity

1.5.1. Homologous recombination deficiency

The first model to explain the synthetic lethality of PARPi and BRCA-deficient tumors demonstrated that PARPi treatment led to persistence of unrepaired ssDNA breaks, and upon colliding with these breaks, replication forks collapsed causing DSB. In the absence of functional BRCA1/2, cells were unable to faithfully repair these breaks undermining their viability (16, 17). This led to the approval of Olaparib as the first PARPi to be used in the clinics for patients with ovarian and breast cancers carrying germline inactivating mutations in BRCA1 or BRCA2.

Considering that PARPi sensitivity depends on deficiency in the HR pathway due to BRCA mutations, HR deficiency is suggested to be a feature that correlates with PARPi sensitivity,

and logically mutations in genes that cause defective HR are expected to confer susceptibility to PARPi, or to underlie the ‘BRCAness’ phenotype, which describes a phenotype of HR-defective tumors that do not exhibit germline mutations of either BRCA1 or BRCA2. Moreover, large-scale sequencing efforts of cancer specimens reveal somatic mutations in genes involved in HR pathway in ovarian (129), pancreatic (130, 131) and advanced prostate cancers (132).

In support of this hypothesis, more studies demonstrate that BRCA status does not perfectly align with the outcome of Olaparib treatment, with functional assays showing that nearly half of investigated ovarian cancers are HR-defective regardless of their BRCA mutations (133–135). Furthermore, inactivation of other genes that maintain functional HR including PALB2, ATM, ATR, CHK1, CHEK2, DSS1/Sem1, RAD51, NBS1 and the Fanconi anemia (FANC) family of genes results in PARPi sensitivity (136). Consequently, Olaparib was approved for treatment of platinum-sensitive ovarian cancer regardless of BRCA status in 2017, and then as a first-line maintenance therapy for ovarian cancer in 2019 (110).

On the basis of these data, several genomic and functional approaches have been developed to assess the activity of HR repair pathway in a tumor specimen. This includes establishing a mutational signature for BRCAness tumors, that is a pattern of genomic scars that the tumor harbors due to its inability to engage HR (137–139). Another genomic approach is to employ sequencing of gene panels that include HR-essential genes (140). Functional methodologies can also be used to measure HR efficiency by directly monitoring the localization of key factors of the HR pathway such as Rad51 (134, 141). These techniques can serve as powerful tools in order to predict tumors’ response to PARPi treatment.

1.5.2. PARPi-induced ssDNA gap accumulation

A recently emerging model to explain PARPi sensitivity is the accumulation of unprocessed ssDNA gaps during replication. This is supported by the observation that cells deficient of the helicase FANCI showed PARPi resistance despite being defective in HR. This phenotype correlates with suppression of ssDNA gaps in these cells (107). Importantly, high levels of ssDNA gaps are detected in BRCA-deficient cells but not in BRCA-proficient ones (107).

The source of these gaps is linked to two main processes. The first one is the defective Okazaki fragment processing (106). The discontinuous synthesis of DNA on the lagging strand during replication results in the formation of Okazaki fragments which are recognized by PARP1. Then, PARP1 activity mediates the recruitment of XRCC1 which associates with Ligase 3 (LIG3) and DNA polymerase β (POL β) to process and ligate these fragments finalizing synthesis of the DNA lagging strand (106). Not surprisingly, elevated activity of PARP1 can be detected in S-phase of the cell cycle when the PAR chain hydrolase PARG is inhibited (106). Consistently, PARPi were found to interfere with the maturation of newly synthesized DNA strands (142). These studies propose that interfering with lagging strand synthesis causes accumulation of ssDNA gaps that is a source of susceptibility to PARPi treatment.

The second source of ssDNA gaps arising in BRCA-deficient cells is linked to the DNA leading strand and mediated by activity of the primase/polymerase PRIMPOL. A recent study showed that upon PARPi treatment ssDNA gaps form behind stalled replication forks due to activity of PRIMPOL repriming the replication machinery past the stalled fork leaving ssDNA gaps behind it (108). In the following S-phase, BRCA-deficient cells fail to restrain replication fork progression leading to collision with these persistent lesions and causing DSB in a trans cell cycle manner (108).

Collectively, PARP1 plays a crucial role in ensuring seamless maturation of DNA strand during replication and interfering with this role through inhibiting PARP1 leads to ssDNA gaps arising on both DNA strands, which primes for cytotoxicity of PARPi treatment in BRCA-deficient cells (107, 108, 142).

1.6. Mechanisms of PARP inhibitor resistance

Although PARPi have revolutionized cancer therapy and led to permanent positive outcomes in many patients, cases of innate and acquired resistance pose a challenge to the efficacy of the treatment and demand comprehensive understanding of the underlying mechanisms and how to overcome them. Those can be divided into mechanisms that are independent of the HR status, and ones that function through restoring the activity of this pathway. Mechanisms of HR-independent PARPi resistance include upregulation of drug efflux pumps, loss of

schlafen 11 (SLFN11) and PARG deficiency, which are extensively discussed in recent reviews (142–144). However, it is noteworthy that only the mechanisms arising from reactivation of HR either through reversion mutations, BRCA1 hypomorphs or rewiring of HR pathway due to loss of NHEJ factors have been observed clinically or in patient-derived xenograft (PDX) models (143), therefore those ones will be further discussed here.

1.6.1. Secondary Reversion Mutations in HR Genes

Reversion mutations in BRCA genes to restore their functionality in HR were among the first means of resistance to be described against PARPi and/or platinum therapy (144–146). Those are mostly genetic alterations that override the original mutation to restore BRCA function either partially or completely as shown by rescuing Rad51 foci formation upon such reversion mutations (147). Not surprisingly, these resistance-driving events have been identified in many tumors from patients undergoing PARPi treatment, especially in ovarian cancer patients where a meta-analysis of reversion mutations in BRCA genes identified 23% of such events in relapsed ovarian cases after PARPi or platinum therapy (148). Importantly, comprehensive analysis of tumor samples with reversion mutations implicated the mutagenic micro-homology end-joining (MMEJ) repair in generating these alterations with a frequency reaching 30% in BRCA1 and almost 60% in BRCA2 deficient cases (148). Many of these reversion mutations were predicted to encode tumor neoantigens, indicating a potential mechanism to target these resistant tumors with immunotherapy (149).

Consistent with restoration of HR function as the driver of PARPi resistance, reversion events were identified on cancers that had HR deficiency due to mutations in other HR genes including Rad51C, Rad51D (150) and PALB2 (151). Considering that PARPi are now approved to be used for treatment of certain cancers regardless of the BRCA status, it is important to exploit the progress in large-scale DNA sequencing and non-invasive liquid biopsies (152) to provide timely and accurate data regarding the status of fundamental HR genes and the frequency of reversion mutations in a way that could inform better clinical practices and improve therapy outcome for those patients.

1.6.2. Restoration of HR Gene Expression

One mechanism that was identified for impairing HR in breast and ovarian cancers is silencing of essential genes in the pathway such as BRCA1 and Rad51C by hypermethylation of their promoters (153, 154), which correlated with PARPi sensitivity (155, 156). Similar observation was detected for PARPi sensitivity driven by deficiency of XRCC3 in prostate cancer as a result of promoter methylation (157). This suggests that gene expression in these tumors can be restored by loss of promoter hypermethylation leading to induction of PARPi resistance.

While resistance to therapy through this mechanism was observed in ovarian cancer when comparing biopsies before and after platinum therapy due to restoration of BRCA1 expression (158), such phenotype has not been reported yet clinically in the case of post PARPi treatment. Nevertheless, PARPi resistance was observed in PDX models of ovarian cancer due to loss of Rad51C promoter methylation (159) as well as PDX models of breast cancers due to reactivation of BRCA1 either by loss of hypermethylation or by novel gene fusion that puts BRCA1 under transcription regulation of a heterologous promoter (160, 161).

1.6.3. HR rewiring due to loss of factors of NHEJ pathway

Since NHEJ can be active regardless of cell cycle phase and HR is limited to S and G2, these two repair pathways are competing for DSB repair in S and G2. If BRCA1 is active, it blocks recruitment of the NHEJ factors 53BP1-RIF1 to sites of DNA damage, preventing the cells from repairing DSB through NHEJ and committing to HR pathway (162). With this in mind, loss of BRCA1 impairs HR and promotes DSB repair by NHEJ which causes genomic instability. However, concomitant loss of both BRCA1 and 53BP1 overrides HR impairment and drives PARPi resistance (163–165). The mechanism underlying this restored resistance is explained by the ability of NHEJ to repair DSB with minimal DNA resection of the break ends, while extensive end resection is crucial for HR functionality. A complex of 53BP1-SHLD3-RIF1 can bind the ends of DSB shielding it from nuclease activity, hindering DNA end resection and committing the cell to NHEJ. Therefore, in BRCA1-deficient cells, loss of 53BP1 prevents association of the 53BP1-SHLD3-RIF1 complex with the break site,

facilitating end resection by nucleases including MRE11, CtIP, EXO1 and DNA2 leading to BRCA1-independent HR repair (166, 167). In a similar fashion, loss of another NHEJ factor, REV7 also drives PARPi resistance in BRCA1-deficient background by promoting DNA end resection mediated through the activity of CtIP nuclease, therefore restoring HR functionality (168).

Crucially, PARPi resistance through restoration of DNA end resection was detected only in BRCA1-deficient background and not in cells lacking BRCA2. This is because the function of BRCA2 in mediating the exchange of RPA by Rad51 on the ssDNA overhangs is downstream of the DNA end resection step (163–165).

So far, PARPi resistance through rewiring of HR has been identified clinically only in the case of 53BP1 loss (147), calling for further studies to uncover the clinical impact of losing other factors of NHEJ on the outcome of PARPi therapeutic regimen. Moreover, it emphasizes the importance of investigating molecular mechanisms to overcome PARPi resistance induced by loss of 53BP1.

1.7. Identification of regulators of PARP inhibitor sensitivity

The breakthrough in cancer treatment strategies by the discovery of PARPi synthetic lethality with BRCA-deficient tumors calls for extensive studies to identify other genes and pathways that could exhibit synthetic lethality with PARPi and therefore lays the ground for expanding their therapeutic applications. Advances in genetic engineering and next-generation sequencing made it possible to conduct high throughput genetic screens with PARPi, which aimed to identify genetic alterations that regulate PARPi sensitivity (169–171). Similarly, we conducted a comprehensive CRISPR-based knockout screen using the GeCKOv2 whole-genome gRNA library (172) in wild-type HeLa cells along with the PARPi, Olaparib (173). This approach aimed to enrich the population of cells resistant to Olaparib while depleting those with heightened sensitivity. Among the genes identified to underlie sensitivity to Olaparib upon their deletion are, the PAR-binding chromatin remodeler ALC1/CHD1L and the accessory subunits of DNA polymerase epsilon POLE3 and POLE4 (173).

ALC1 is a chromatin remodeler classified as a member of the SNF2 family, with an ability to be activated by binding PAR chains via its C-terminal Macro domain and catalyzes

chromatin remodeling by nucleosome sliding through its ATPase domain (174, 175). Moreover, ALC1 overexpression leads to excessive chromatin relaxation upon DNA damage (176), while its deletion interferes with the repair of ssDNA breaks by impairing BER and NER repair pathways (177, 178). Clinically, ALC1 is an oncogene associated with poor prognosis and amplified in different solid tumors including hepatocellular carcinoma (179, 180), non-small cell lung cancer (181) and ovarian cancer (182). Furthermore, ALC1-depleted cells exhibit enhanced sensitivity to oxidative damage by H₂O₂ as well as other genotoxic stress inducers such as ultraviolet radiation (UV), and phleomycin (102, 178).

POLE3 and POLE4 are the accessory subunits of DNA polymerase epsilon (POLE ϵ), a protein complex responsible for executing replication of DNA leading strand (183). It comprises of four subunits, POLE1 is the catalytic subunit which associates with POLE2 along with POLE3 and POLE4. Yeast studies showed that the yeast orthologues of POLE1 and POLE2, Pol2 and Dpb2 are indispensable for survival, which is not the case for Dpb3 (POLE4 in mammals) or Dpb4 (POLE3 in mammals) (184). Loss of the accessory subunits in yeast decreases the processivity of the Pol2-Dpb2 subcomplex rather than stalling replication completely, as a result of weak DNA binding leading to recurrent dissociation from the DNA template, therefore leaving gaps on the DNA leading strand (185). The importance of these accessory subunits in stabilizing the POLE ϵ complex is highlighted by the sensitivity to replication stress inducers upon their loss (186, 187). POLE3 and POLE4 are crucial for ensuring symmetrical histone segregation upon DNA replication through their H3-H4 histone chaperon activity (188, 189). In line with their role within the chromatin environment, yeast studies demonstrated a role of these accessory subunits in regulating heterochromatin silencing (190, 191).

Taking into account the results of our CRISPR screen, as well as the known functions of ALC1, POLE3 and POLE4 in maintaining genomic stability, this work aimed to investigate the molecular mechanisms underlying the roles of these proteins in modulating PARPi sensitivity.

2. Aims

By employing CRISPR gene editing technique, along with molecular, cellular, biochemical and immune-based assays performed in well-characterized cancer cell lines, this work aimed to advance our understanding of the molecular mechanisms underlying PARPi sensitivity and resistance from a fundamental science perspective, with a potential clinical impact in the context of diagnosis and/or drug target identification.

Specifically, we worked towards:

- Validating three of the top candidates identified in our CRISPR screen (ALC1, POLE3, POLE4) in the context of PARPi sensitivity.
- Characterizing the molecular mechanism by which PARPi sensitivity is induced when ALC1 and POLE4 are deleted.
- Investigating whether targeting these genes (ALC1 and POLE4) enhances the sensitivity of BRCA-deficient cells to PARPi and overcomes acquired resistance due to loss of 53BP1.

3. Materials and Methods

3.1. Cell lines and cell culture

U2OS and HeLa cell lines utilized in this work were cultured in DMEM (Biosera) supplemented with 10% FBS, 100 µg/ml penicillin, 100 U/mL streptomycin and 1% NEAA and maintained at 37°C in a 5% CO₂ incubator unless otherwise stated.

For experiments concerning the ALC1 project, BRCA2^{+/ Δ 11} (BRCA2^{+/-}), BRCA2 ^{Δ 11/ Δ 11} (BRCA2^{-/-}) were kind gift from Scott E Kern lab (192), U2OS YFP-ALC1, U2OS PARP1 KO, and U2OS ALC1 KO #1 were generated earlier (176). Additional U2OS ALC1 KO cells were generated in this work using wild-type U2OS cells as the parental cell line. U2OS ALC1/PARP1 double knockout cells were generated by knocking out ALC1 in PARP1 KO U2OS cells.

RPE-1 p53 KO and RPE-1 p53/BRCA1 double KO cells were kind gift from Alan D. D'Andrea lab (193) and grown using DMEM-F12 (Biosera) supplemented with 10% FBS, 100 µg/ml penicillin, 100 U/mL streptomycin.

POLE3 KO and POLE4 KO cell lines were engineered in this study from wild-type HeLa cells using CRISPR/Cas9 technology. The HeLa cell line was authenticated by STR profiling (Eurofins Genomics) and had 100% match with HeLa (amelogenin + 12 loci) using the Cellosaurus cell line database (194).

The sgRNA sequences for CRISPR/Cas9 targeting are:

sgPOLE3: 5'-GTACAGCACGAAGACGCTGG-3'

sgPOLE4: 5'-GTCGGGATCTGCCTTCACCA-3'

ALC1 KO sgRNA Exon 9 Top: 5'-CACCGACCACCTGACTGAGGCTAG-3'

ALC1 KO sgRNA Exon 9 Bottom: 5'-AAACCTAGCCTCAGTCAGGTGGTC-3'

ALC1 KO sgRNA Exon 13 Top: 5'-CACCGTATATCATATCATACTGG-3'

ALC1 KO sgRNA Exon 13 Bottom: 5'-AAACCCAGGTATGATATGATATAC-3'

3.2. RNA Interference and Plasmid Transfection

pSpCas9(BB)-2A-Puro (PX459) V2.0 utilized to produce the knockouts was provided from Feng Zhang lab (Addgene, plasmid #62988) (195). The piRFP670-ALC1, and piRFP670-ALC1 E175Q (196); pmEGFP-ALC1 and pmCherry-ALC1 G750E (175); and pmCherry-ALC1, pmCherry-ALC1 K77R, pmCherry-ALC1 E175Q (176) plasmids were previously described. Plasmid transfections were done with Xfect (Takara) following to the manufacturer's guidelines.

RNA interference experiments with siRNA (sequences in Table S1) were performed with Dharmafect (Dharmacon) or RNAiMAX (Lipofectamine) transfection reagents following the manufacturers' protocol. Downregulation was verified by western blotting using specific antibodies (detailed in Table S2).

For rescue experiments of POLE4 KO, the cells were transfected with pmEGFP-C1 and either pcDNA5-FRT-TO or pcDNA5-FRT-TO-POLE4 using TransIT®-LT1 Transfection Reagent (Mirus) 24-48 h prior treatment. POLE4 expression was verified by Western blotting.

3.3. PARP1 recruitment to sites of laser irradiation

Cells were grown in 8-well Lab-Tek II chambered cover glass 30 (Thermo Scientific) and transfected 48 h prior to imaging with GFP-tagged PARP1 or GFP-tagged PARP1 chromobody (Chromotek). For sensitization, growth medium was changed to medium containing 0.15 $\mu\text{g}/\text{mL}$ Hoechst 33342 for 1 hour at 37 °C. Before imaging, the sensitizing medium was then replaced with CO₂-independent imaging medium (Phenol Red-free Leibovitz's L-15 medium (Life Technologies) supplemented with 20% fetal bovine serum, 2 mM glutamine, 100 $\mu\text{g}/\text{mL}$ penicillin and 100 U/mL streptomycin). For PARP inhibition conditions, cells were treated with Olaparib (30 nM) for 30 min prior to imaging.

Live-cell imaging experiments were conducted on a Ti-E inverted microscope from Nikon equipped with a CSU-X1 spinning-disk head from Yokogawa, a Plan APO 60x/1.4 N.A. oil-immersion objective lens and a sCMOS ORCA Flash 4.0 camera. Laser microirradiation at 405 nm was performed along a 16 μm -line through the nucleus using a single-point scanning

head (iLas2 from Roper Scientific) coupled to the epifluorescence backboard of the microscope. The laser power at 405 nm was measured before each experiment to maintain consistency across the experiments and set to 125 μ W at the sample level. Cells were kept at 37 °C with a heating chamber. Protein recruitment was quantified using a custom-made Matlab (MathWorks) routine.

3.4. Immunofluorescence

For non-denaturing BrdU staining, cells were cultured with 20 μ M BrdU-containing medium for 48 h, the medium was then changed to 10 μ M Olaparib-containing medium for 24 h. Cells were washed with PBS, pre-extracted with 0.5% Triton X-100 in PBS for 5 min at 4°C then fixed with 4% paraformaldehyde (PFA) for 15 min at 4°C. Permeabilization was done using 0.5% Triton X-100 in PBS for 10 min followed by blocking with 5% FBS in 0.1% Triton X-100 for 45 min at room temperature, then incubated with primary antibody (Table S2) diluted in blocking solution overnight at 4°C.

For Rad51 experiments, cells were challenged with 10 μ M Olaparib-containing medium for 48 h prior to washing with PBS and pre-extraction with pre-extraction buffer (10 mM Tris-HCl, 2.5 mM MgCl₂, 0.5% NP-40, 100 \times Protease inhibitor cocktail (Roche)) for 5 min at 4°C. Fixation was done using 4% PFA for 15 min at 4°C followed by permeabilization, blocking and antibody incubation as described earlier.

Following overnight incubation with the primary antibodies (Table S2), cells were washed three times with 0.1% Triton X-100 and incubated at room temperature with fluorescently tagged secondary antibody (Table S2) for 1 h. Next, cells were washed with 0.1% Triton X-100 and counterstained with DAPI (1 μ g/mL in PBS) for 10 minutes.

Z-stacks of images were acquired on a Zeiss LSM800 confocal microscope with a Plan-Apochromat 20x/0.8 M27 or a water immersion Plan-Apochromat 40x/1.2 DIC M27 objective controlled by the ZEN 2.3 software. Fluorescence excitation was performed using diode lasers at 405 nm for DAPI, 488 nm for Alexa Fluor 488, 561 nm for Alexa Fluor 555 and 650 nm for Alexa Fluor 647. Images were analyzed after generating maximum intensity projections of the z-stacks using custom CellProfiler pipelines (197).

3.5. Alkaline comet assay

U2OS WT or ALC1 KO cells were treated or not with 1 μ M Olaparib for 1 hour before irradiation. X-ray irradiation was conducted at 90 kV and 150 mA with a dose of 2 Gy using a Trakis XR-11 x-ray machine. Cells were collected 30 min after x-ray treatment and washed with 1 \times PBS. Cells were embedded in 1% low-gelling-temperature agarose (approximately 5000 cells/ml) and rapidly dropped onto 1% agarose-covered surface of precoated microscope slides. After agarose has solidified, samples were lysed in alkaline lysis solution [1.2 M NaCl, 100 mM Na₂EDTA, 0.1% sodium lauryl sarcosinate, and 0.26 M NaOH (pH > 13)] overnight at 4°C in the dark. Samples were then washed with rinse solution [0.03 M NaOH and 2 mM Na₂EDTA (pH ~ 12.3)] for 20 min. Microscope slides were then submerged in an electrophoresis chamber containing fresh rinse solution, and electrophoresis was run for 25 min at a voltage of 0.6 V/cm (198). Comets were visualized by Hoechst staining. One hundred comet images from each slide were analyzed in Fiji (ImageJ) (199) after generating the maximum intensity projections of z-stacks. The tail moment lengths—the distance between the centers of the nucleus and the tail—were plotted.

3.6. BrdU comet post-replication repair assay

Cells were plated in 24-well plate at a density of 3x10⁵ cells/well. Next day the cells were pulse-labeled with 25 μ M of the nucleotide analog BrdU, and incubated at 37 °C for 30 min. Then, the cells were washed with PBS and challenged or not with hydroxyurea (4 mM) for 3 h. Cells were then harvested (corresponding to 0 h repair) or left to perform post-replicative repair for additional 3 h. Cells were embedded in 0.75% low melting agarose and layered onto microscope slides (pre-coated with 1% agarose), covered with coverslips, and left to solidify for 5 minutes at 4°C.

The following steps were performed as described previously (200) with a slight modification detailed below. The alkaline lysis was done in 0.3 M NaOH, 1 mM EDTA, pH 13 for 2 hours in Coplin jars. The DNA was left to unwind for 40 minutes in this ice-cooled electrophoresis buffer. The electrophoresis was subsequently performed at 1 V/cm (25 V, 300 mA) for 30 minutes in the same buffer at 10 °C.

Next, the slides were washed with neutralization buffer (0.4 M Tris-HCl, pH 7.4), blocked with PBS containing 1% BSA for 20 minutes at room temperature and incubated with the primary antibody (Table S2) for 2 h at room temperature. The primary antibody was washed off and slides were incubated with secondary antibody (Table S2) for 2 hours at room temperature then mounted by Fluoromount mounting solution containing DAPI, covered with coverslips and stored at 4°C until microscopy. Imaging was done with Zeiss Axioscope Z2 fluorescent microscope. Scanning of images was done using automated scanning platform of Metasystem and the quantitation of comets was done by Metasystems Neon Metafer4 software. Three independent experiments were done with duplicate slides, 150-300 comet/slides were scored.

3.7. DNA fiber assay

Exponentially growing cells were pulse labelled with 25 μ M IdU for 20 min in 37°C, washed twice with prewarmed PBS and then labeled with 250 μ M CldU (chlorodeoxyuridine) in the presence or absence of Olaparib (10 μ M), cells were collected, and DNA fiber spreads were prepared as described previously (201). Briefly, 2 μ l of cells resuspended in PBS (10^6 cells/ml) were spotted onto clean glass slides. Cells were lysed with lysis solution (0.5% sodium dodecyl sulphate (SDS) in 200 mM Tris-HCl (pH 7.5), 50 mM EDTA), then tilted at 15° to the horizontal, allowing a stream of DNA to run slowly down the slide. Next, slides were air-dried for 20 minutes and fixed in methanol-acetic acid (3:1) and let dry for 10 minutes. Fixed fibers were rehydrated in water for 5 minutes and denatured (2.5 M HCl for 1 h) and blocked in blocking buffer (1% bovine serum albumin and 0.1% Tween20) for 1h. Incubation with the two primary antibodies (Table S2) was done for 2 hours in humidified chamber at room temperature. Slides were washed and incubated with the secondary antibodies (Table S2) for 90 minutes in humidified chamber at room temperature. DNA fibers were imaged using Axioscope Z2 fluorescent microscope (Zeiss, Germany) with a 60x objective. The lengths of DNA tracks corresponding to IdU and CldU labelling were measured using the Zen (Zeiss) software. In each experiment, a minimum of 200 independent fibers were analyzed per experiment. All measurements of 4 independent experiments were summarized in a dot plot created in GraphPad10.2.

3.8. Cell survival assays

For work concerning ALC1 experiments, clonogenic cell survival assays were performed with U2OS WT, ALC1 KO, PARP1 KO, and ALC1/PARP1 double knockout. Cells were seeded in defined numbers and treated with Olaparib, Veliparib, or Niraparib (Selleckchem; 30, 300, and 3000 nM) for 24 hours, then washed and incubated for 14 days. The obtained colonies were fixed with methanol:acetic acid (3:1) and stained with crystal violet (Sigma-Aldrich). The fraction of the surviving cells was calculated and normalized to nontreated conditions.

For POLE4-related work, POLE4 KO, POLE3 KO and their parental wild-type cells were seeded in defined numbers in 96-well plates and treated for one week with Olaparib (0, 0.45, 0.9, 1.8, 3.7, 7.5, 15, 30 μ M), Rucaparib (0, 0.45, 0.9, 1.8, 3.7, 7.5, 15 μ M), Talazoparib (0, 15, 31, 62, 125, 250 nM), or ATRi (0, 0.6, 1.2, 2.5, 5, 10 μ M) (Table S3). For experiments with the combination of ATRi and Olaparib, 1 μ M Olaparib was used along with 0.6 μ M of ATRi. For experiments with RNAi-induced BRCA1 depletion the concentrations of Olaparib were 0, 0.3, 0.6, 1.2, 2.5, 5 and 10 μ M. After 7 days of incubation, the supernatants were aspirated and resazurin (Sigma) solution was added (25 μ g/ml in Leibowitz's L-15, Gibco). The fluorescent resorufin product was measured after 30-60 min using a Biotek Synergy H1 microplate reader with a 530/590 filter set. The fraction of the surviving cells was calculated and normalized to nontreated conditions.

3.9. Flow cytometry for intracellular markers and cell cycle analysis

Cells were harvested with TrypLe Select (Gibco), washed with PBS and fixed with ice-cold ethanol. For labelling the intracellular markers, the cells were permeabilized and blocked with 0.5% Triton X-100 and 5% FBS in PBS, and then incubated with the appropriate primary antibody (Table S2) overnight at 4 °C. Next, the cells were washed two times with PBS, and incubated with fluorescently tagged secondary antibodies (Table S2) for 2 h at room temperature. Finally, the DNA staining solution was added (10 μ g/mL propidium-iodide and 10 μ g/mL RNase in PBS) for 15 min at room temperature. The samples were analyzed with CytoFLEX S flow cytometer (Beckman Coulter Life Sciences) or

FACSCalibur (Becton Dickinson). The measurements were evaluated with Kaluza Analysis software (Beckman Coulter Life Sciences).

3.10. Western blotting

Protein samples were prepared for SDS–polyacrylamide gel electrophoresis in 4× sample buffer (10% SDS, 300 mM Tris-HCl, 10 mM β-mercaptoethanol, 50% glycine, and 0.02% bromophenol blue). Separated proteins were blotted onto nitrocellulose or PVDF membranes, blocked for 1 hour at RT in 5% low-fat milk or 5% BSA in 0.1% Tris-buffered saline, and incubated with primary antibodies (dilution specified in Table S2) overnight at 4°C. Horseradish peroxidase-conjugated secondary antibodies were used for 1 hour at room temperature. Membranes were developed with enhanced chemiluminescence using Odyssey Fc Imaging System (LI-COR Biotechnology).

3.11. Statistical analysis

All experiments were done at least in triplicates and for immunofluorescence experiments at least 200 cells were scored. A minimum of 10 cells were irradiated in live-cell imaging experiments. Graphing and statistical analysis were done using GraphPad Prism versions 6 and 7. Statistical analysis of cell survival experiments was done using two-way ANOVA. PARP1 recruitment experiments were analyzed using Mann-Whitney unpaired t-test. Statistics for immunofluorescence experiments were performed using one-way ANOVA. Asterisks represent *p* values, which correspond to the significance (**p* < 0.05, ***p* < 0.01, ****p* < 0.001 and *****p* < 0.0001).

4. Results

4.1. Deciphering the role of ALC1 in inducing PARP inhibitor sensitivity

4.1.1. Loss of ALC1 underlies sensitivity to PARP inhibitors and increased genomic instability

To confirm the influence of ALC1 depletion on PARPi sensitivity, we utilized CRISPR/Cas9 gene editing to create ALC1 knockout (ALC1 KO) cell lines in U2OS cells (**Fig. 4A**) and tested their sensitivity to Olaparib. All tested clones of ALC1 KO cell lines exhibited sensitivity to Olaparib, even at low doses, validating their synthetic lethality with PARPi (**Fig. 4B**). To investigate whether the synthetic lethality between ALC1 KO and PARPi necessitated the presence of the PARP1 protein, we generated ALC1/PARP1 double knockout cell lines (**Fig. 4B**). Consistent with prior findings, PARP1 KO cells were resistant to Olaparib treatment (**Fig. 4B**). Consequently, PARP1 loss in ALC1 KO cells reduced their sensitivity to PARPi as well (**Fig. 4B**). These outcomes align with the requirement of PARP1 for PARPi toxicity (124). Moreover, ALC1 KO cells demonstrated sensitivity to other PARP inhibitors, such as Veliparib and Niraparib, which exhibit differing trapping potentials compared to Olaparib (**Fig. 4C, D**) (202). Importantly, the sensitivity of ALC1 KO cells to PARPi treatment was partially reversed when complemented with wild-type ALC1 (**Fig. 4E**), whereas complementation with a PAR-binding mutant of ALC1, incapable of recruitment to DNA damage sites, or ATPase-deficient mutants of ALC1, which recruit to DNA damage sites similar to wild-type ALC1 but cannot remodel the chromatin, failed to rescue sensitivity. Collectively, these findings highlight the critical role of ALC1 in conferring resistance to PARPi.

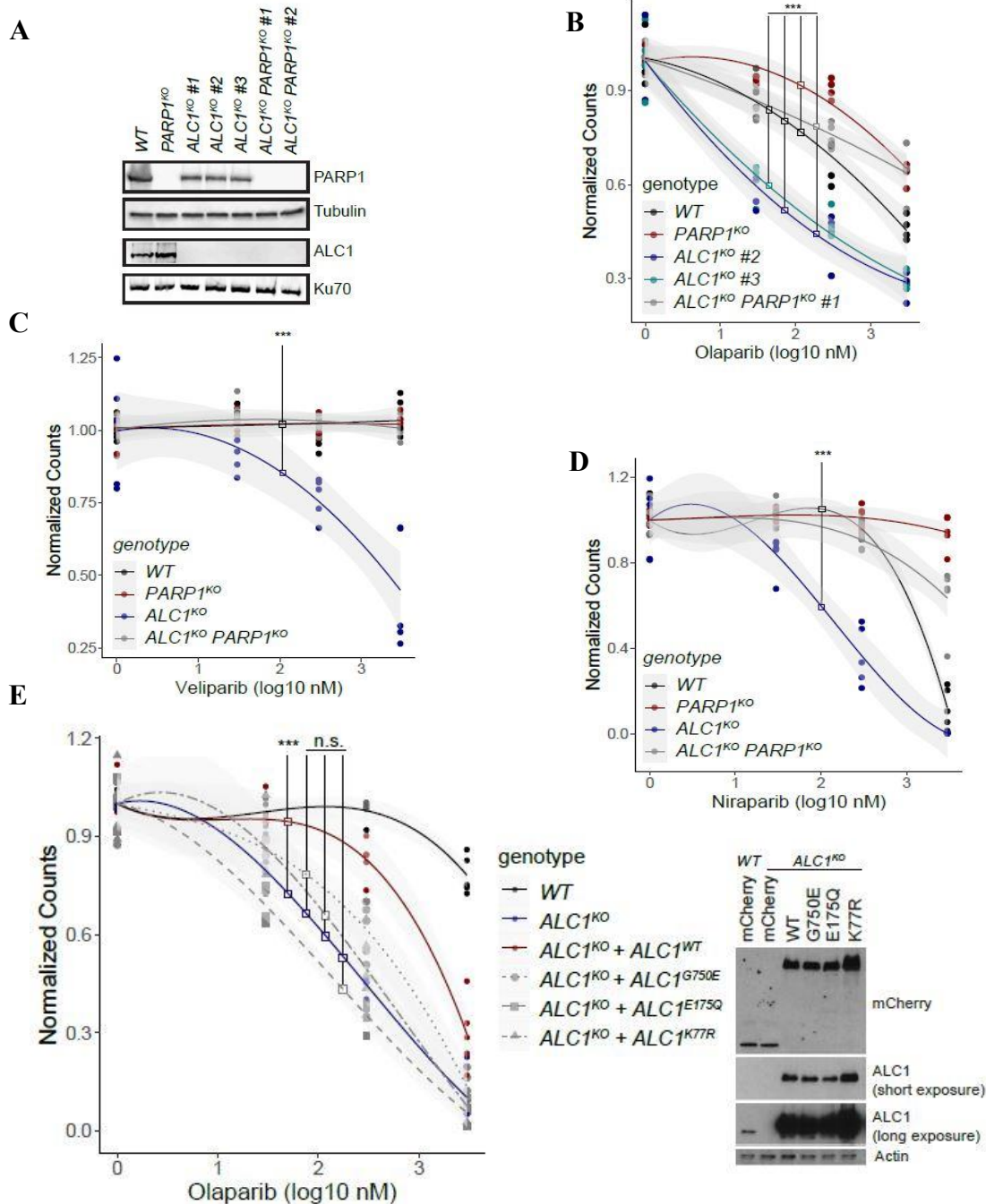


Figure 4: ALC1 deficiency leads to PARPi sensitivity

(A) Western blot analysis of wild-type U2OS, PARP1 KO, ALC1 KO, and ALC1/PARP1 double KO showing levels of PARP1 and ALC1. Tubulin and Ku70 were used as loading controls. (B-D) Clonogenic cell survival assays showing ALC1 KO sensitivity to 24h treatment of (B) Olaparib, (C) Veliparib and (D) Niraparib. This sensitivity was PARP1-dependent. The graphs were derived from three independent experiments. All data points are shown. Asterisks indicate p -values obtained by two-way ANOVA (** $p < 0.001$). (E) (Left) Clonogenic cell survival assay of wild-type U2OS and ALC1 KO transfected with mCherry-ALC1 variants. The treatment was done for 24h. All data points are depicted. Asterisks indicate p -values obtained by two-way ANOVA n.s. Not significant, *** $p < 0.001$). (Right) Western blot validating the expression of mCherry and ALC1 variants. Actin was used as a loading control.

We then aimed to investigate whether PARPi induces DNA lesions in ALC1 KO cells which could alter their cell cycle progression and eventually cause the observed sensitivity. To that end, we utilized flow cytometry to investigate the effect of PARPi treatment on cell cycle progression in ALC1 KO cells. Our analysis revealed that 24h exposure to Olaparib caused significant accumulation of ALC1 KO cells in the G2/M phase, indicative of cell cycle arrest (**Fig. 5A**). Conversely, Olaparib-resistant ALC1/PARP1 double knockout cells displayed normal cell cycle distribution under PARPi treatment, similar to that of wild-type cells (**Fig. 5A**). Such cell cycle arrest could reflect accumulation of DNA lesions upon PARPi treatment. To test this hypothesis, we stained cells for the phosphorylated histone variant H2AX (γ H2AX), as an indicator of DSB. Indeed, ALC1 KO cells showed striking increase of γ H2AX staining upon Olaparib treatment compared to wild-type cells (**Fig. 5B**). Interestingly, this phenotype was dependent on the presence of PARP1, as PARP1 KO and ALC1/PARP1 double knockouts had similar γ H2AX levels compared to wild-type cells (**Fig. 5B**). To probe for the source of this elevated DNA damage signaling in ALC1 KO upon PARPi treatment, we investigated the levels of DNA breaks by alkaline comet assay. Indeed, this assay showed longer tail moment in ALC1 KO cells compared to wild-type only upon Olaparib treatment (**Fig. 5C**), indicating elevated levels of DNA breaks.

Taken together, these results provide evidence that ALC1 deficiency leads to substantial accumulation of DNA breaks in response to PARPi treatment, which underlies the observed synthetic lethality.

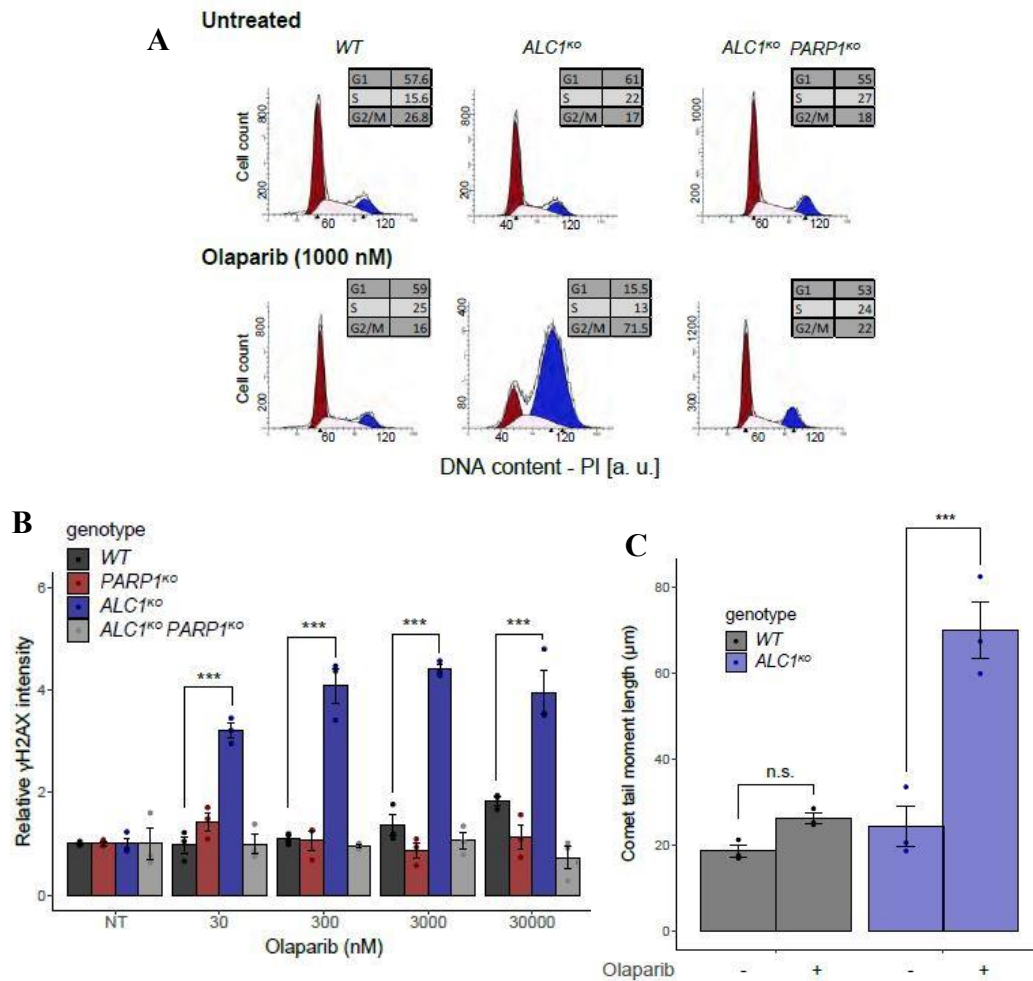


Figure 5: PARPi treatment causes accumulation of DSB and cell cycle arrest

(A) FACS measurement showing cell-cycle profile of the indicated genotypes treated or not with 1 μ M of Olaparib for 24h. The numbers in the boxes represent the distribution of the cells in G1, S and G2/M. (B) Immunostaining of γ H2AX in the indicated genotypes after 12h treatment with Olaparib. Asterisks indicate p - values obtained by linear regression (***) $p < 0.001$. (C) Comet tail length obtained from alkaline comet assay of ALC1 KO and their U2OS wild-type with or without 1 μ M of Olaparib treatment for 1h prior to X-ray irradiation (2 Gy). Graph includes datapoints from 100 comets/condition. (Mean \pm SEM) ($n=3$) Asterisks indicate p - values obtained by linear regression (n.s Not significant, *** $p < 0.001$).

4.1.2. PARP inhibitor toxicity in ALC1-deficient cells is due to enhanced PARP1 trapping.

To uncover the molecular mechanisms underlying sensitivity of ALC1 KO to PARPi, we assessed whether PARP1 is being trapped at DNA lesions in ALC1 KO, reflecting a role of ALC1 in mobilizing PARP1 from DNA damage sites. Therefore, we monitored the dynamics of GFP-PARP1 at sites of laser microirradiation in live cell imaging. In wild-type cells, GFP-PARP1 was rapidly recruited to sites of laser-induced damage, followed by a timely release,

which was delayed upon PARPi treatment (**Fig. 6**). Notably, while GFP-PARP1 was recruited efficiently to damage sites in ALC1 KO cells, its release was significantly delayed compared to wild-type cells even without Olaparib (**Fig. 6**). Olaparib further enhanced the retention of GFP-PARP1 in ALC1 KO cells (**Fig. 6**), confirming ALC1's role in regulating PARP1 dynamics at sites of DNA damage. These results demonstrate that loss of ALC1 leads to PARP1 trapping potentiated by PARPi and supports a role of ALC1 in mobilizing PARP1 from sites of DNA damage.

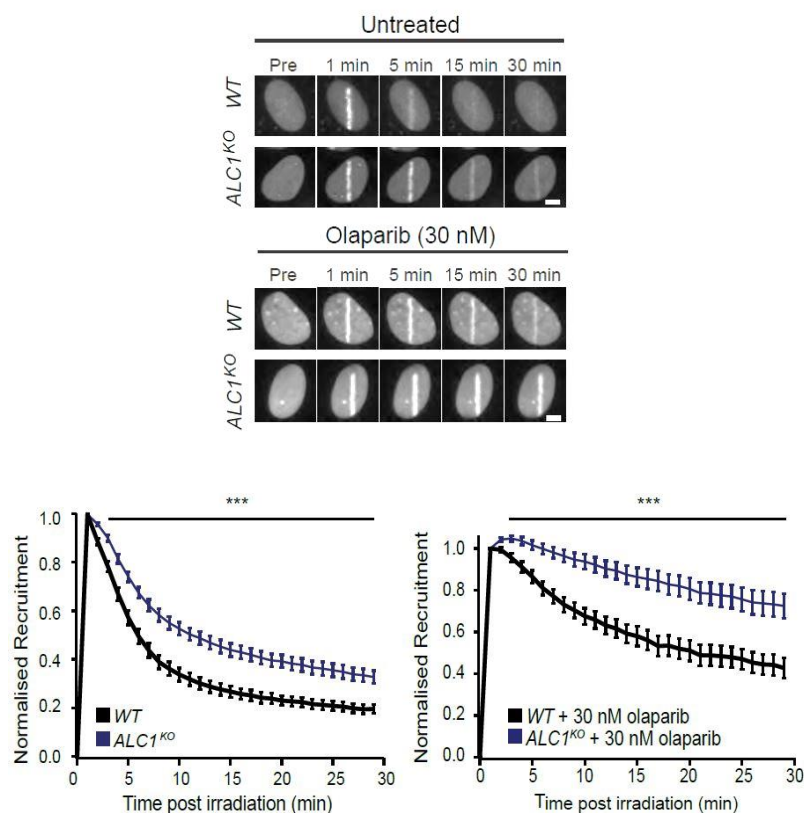


Figure 6: ALC1 KO suffer from increased PARP1 trapping at DNA damage sites

(Top) Representative images of GFP-PARP1 recruitment at sites of DNA damage induced by laser microirradiation in both wild-type and ALC1 KO with and without 30 nM of Olaparib. Scale bar, 5 μ m. **(Bottom)** Quantification of GFP-PARP1 retention at sites of laser induced damage in the indicated genotypes challenged with the indicated treatment. *p*-values were obtained by Mann-Whitney unpaired t-test (n.s. Not significant, *** $p < 0.001$).

4.1.3. Loss of ALC1 impairs both HR and NHEJ

We then aimed to elucidate how ALC1 deficiency affects the DSB repair pathway choice, as sensitivity to PARPi has been shown to stem from an unbalanced pathway choice for repairing DSB. In cells compromised for their HR, PARPi toxicity arises due to the upregulation in activity of the error-prone NHEJ pathway (203). Conversely, resistance to PARPi upon loss of 53BP1 in BRCA1-deficient cells results from the rewiring of HR, in a phenotype called synthetic viability (204). To investigate how ALC1 influences the choice between these two repair pathways, we downregulated BRCA1, 53BP1 or both of them in wild-type and ALC1 KO cells and probed their sensitivity to Olaparib. Consistent with previous reports, depleting BRCA1 in wild-type cells induced sensitivity to Olaparib (**Fig. 7**). As expected, compromising NHEJ by downregulating 53BP1 did not significantly affect wild-type survival upon Olaparib treatment (**Fig. 7**), while targeting 53BP1 in BRCA1-depleted cells reduced their PARPi sensitivity (**Fig. 7**), mimicking the synthetic viable phenotype reported earlier (205). In contrast to wild-type scenario, downregulating either BRCA1, 53BP1 or both of them in ALC1 KO cells neither enhanced nor reduced their sensitivity to PARPi (**Fig. 7**). These data demonstrate that ALC1 acts upstream of the HR-NHEJ pathway choice.

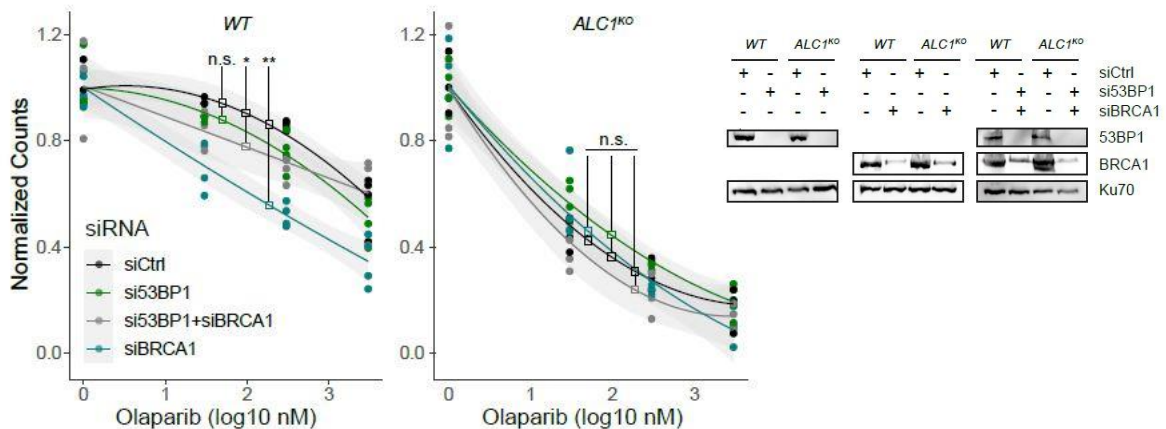


Figure 7: ALC1 acts upstream of both HR and NHEJ

(Left) Clonogenic cell survival assay of WT and ALC1 KO cells transfected with the indicated siRNA and subjected to 24h treatment of Olaparib. The figures were derived from three independent experiments. All data points are represented. Asterisks indicate *p*- values obtained by two-way ANOVA (n.s Not significant, * *p*<0.05, ** *p*<0.01). **(Right)** Immunoblots validating the downregulation of the indicated proteins upon transfection with the indicated siRNA, Ku70 was used as a loading control.

4.1.4. Overexpression of the oncogene ALC1 drives resistance to PARP inhibitors in BRCA-deficient cells.

Overexpression of the oncogene ALC1 has been reported in cancer and correlated with poor prognosis (179–181). Considering our results that ALC1 deficiency induced PARPi sensitivity (Fig. 4), we addressed whether its overexpression modulates this phenotype. Indeed, cells stably overexpressing ALC1 fused to YFP were more resistant to Olaparib than wild-type cells (Fig. 8A), and while depleting BRCA1 in wild-type cells induced Olaparib sensitivity (Fig. 8A), this was not the case in YFP-ALC1 cells (Fig. 8A). Moreover, while BRCA2-deficient cells were sensitive to Olaparib compared to their wild-type (Fig. 8B), transient overexpression of ALC1 induced resistance to PARPi to a similar level as of the wild-type cells (Fig. 8B). These results support the notion to use ALC1 protein levels as a biomarker to guide the outcome of PARPi therapy.

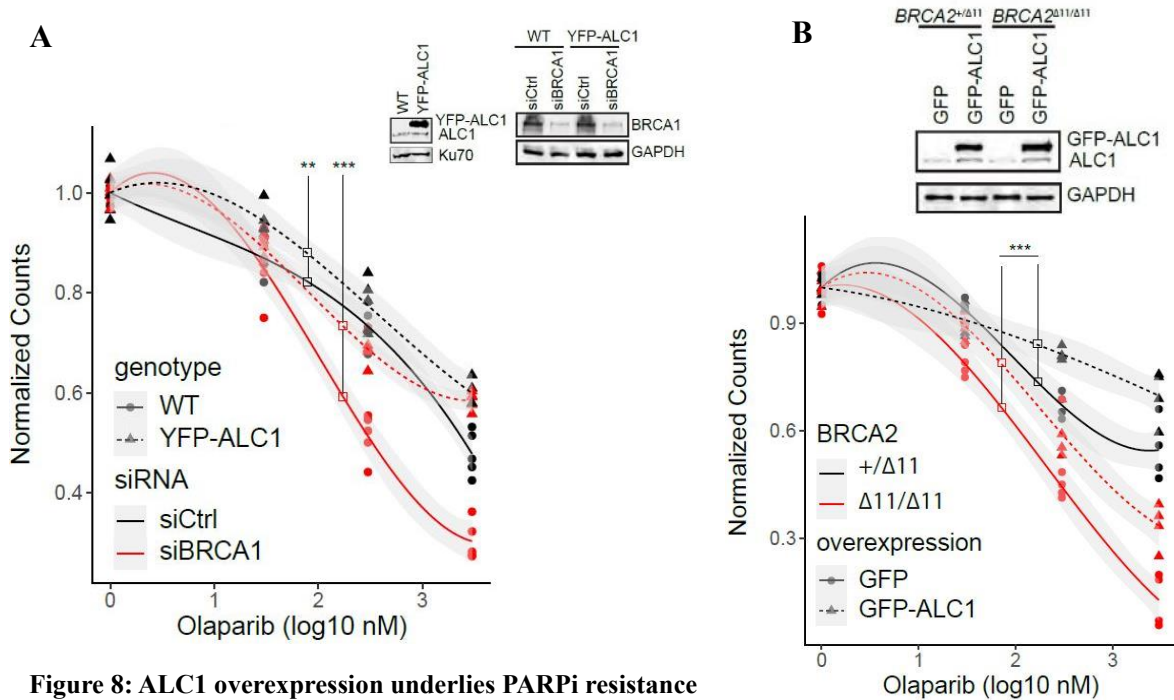


Figure 8: ALC1 overexpression underlies PARPi resistance

(A) (Top) Western blots of BRCA1 and ALC1 in U2OS YFP-ALC1 and their wild-type after transfection with the indicated siRNA. Ku70 and GAPDH were used as loading controls. **(Bottom)** Clonogenic cell survival assay of U2OS wild-type and U2OS YFP-ALC1 cells transfected with siCTRL or siBRCA1 and treated with the indicated concentrations of Olaparib for 24h. The figure is derived from three independent experiments. All data points are represented. Asterisks indicate p - values obtained by two-way ANOVA (** $p < 0.01$, *** $p < 0.001$).

(B) (Top) Western blot of ALC1 in BRCA2^{+/ Δ 11} (BRCA2^{+/-}) and BRCA2 ^{Δ 11/ Δ 11} (BRCA2^{-/-}) cells after transfection with GFP or GFP-ALC1. GAPDH was used as a loading control. **(Bottom)** Clonogenic cell survival assay of BRCA2^{+/ Δ 11} (BRCA2^{+/-}) and BRCA2 ^{Δ 11/ Δ 11} (BRCA2^{-/-}) cells transfected with GFP or GFP-ALC1 and treated with the indicated concentrations of Olaparib for 24h. The figure is derived from three independent experiments. All data points are represented. Asterisks indicate p - values obtained by two-way ANOVA (*** $p < 0.001$).

4.2. Investigating the molecular mechanism underlying PARP inhibitor sensitivity in POLE4-deficient cells.

4.2.1. Deletion of the accessory subunits of DNA polymerase epsilon leads to PARP inhibitor sensitivity

Our initial screen along with other reports (171, 206) identified deletion of the accessory subunits of POL ϵ , POLE3 and POLE4 to sensitize cells to the PARPi. To validate this, we utilized CRISPR/Cas9 to create knockouts (KO) of POLE3 and POLE4 in HeLa cells (**Fig. 9A**). As anticipated, POLE3 KO and POLE4 KO exhibited heightened sensitivity to Olaparib treatment in cell survival assays (**Fig. 9B**). Moreover, POLE3 and POLE4 KOs demonstrated sensitivity to other PARP inhibitors, such as Talazoparib and Rucaparib, indicating that this sensitive phenotype can be extended to other PARPi (**Fig. 9C, D**).

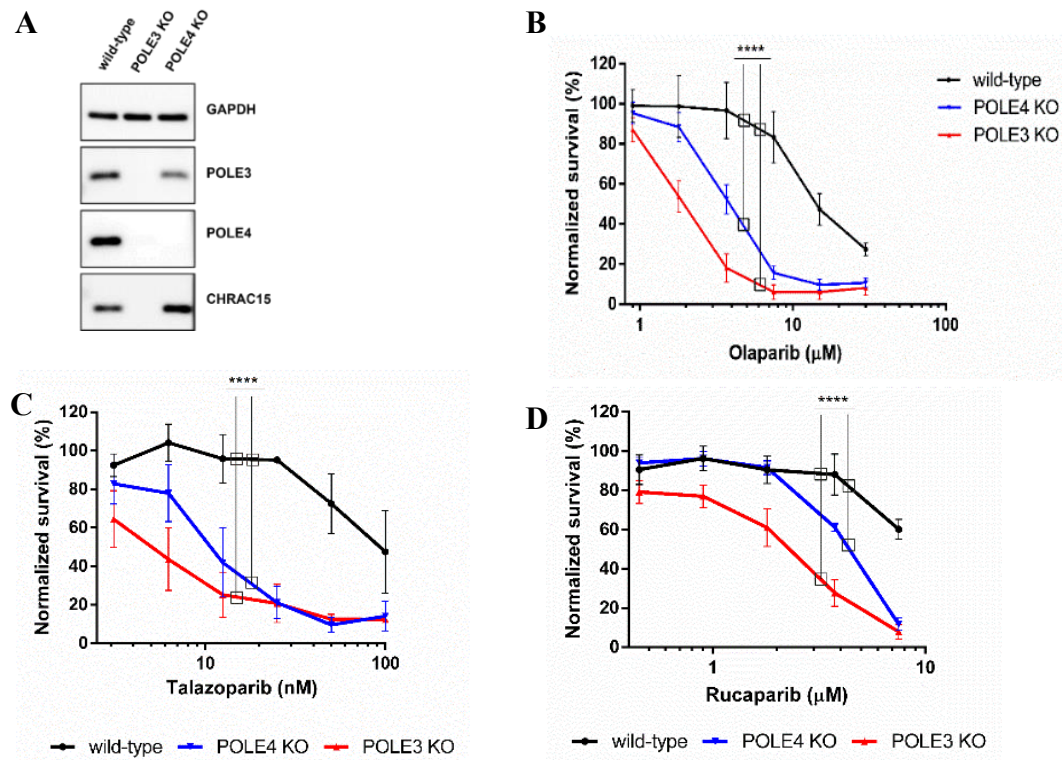


Figure 9: POLE3 KO and POLE4 KO are sensitive to PARPi treatment

(A) Immunoblot of POLE3, POLE4 and CHRAC15 in POLE4 KO, POLE3 KO and their HeLa parental cell line. GAPDH was used as a loading control. (B-D) Cell survival assay showing sensitivity of POLE3 KO and POLE4 KO to (B) Olaparib, (C) Talazoparib and (D) Rucaparib compared to their HeLa parental cell line. The treatment was changed once during the 7-day long experiment. Asterisks indicate p -values obtained by two-way ANOVA (**** $p < 0.0001$).

The formation of a heterodimer between POLE3 and POLE4 is crucial for their stability (171). Consequently, loss of either subunit abolished or significantly reduced the expression of the other (**Fig. 9A**). POLE3 serves as a shared subunit between the POL ϵ holoenzyme and the CHRAC complex, that is, it forms a heterodimer with either POLE4 or CHRAC15, respectively. Therefore, we aimed to assess the consequence of deleting POLE3 on those two subcomplexes. Knocking out POLE3 led to loss of both POLE4 and CHRAC15 proteins (**Fig. 9A**). To avoid potential confounding phenotypes stemming from the absence of both POLE3-POLE4 and POLE3-CHRAC15 heterodimers, we opted to further investigate the effects of PARPi treatment specifically in POLE4 KO cells.

4.2.2. Sensitivity of POLE4 KO to PARP inhibitors is dependent on the presence of PARP1 with no defects in its recruitment kinetics

The efficacy of PARPi relies on the presence of PARP1 in cells (124), with recent studies also indicating a necessity of PARP2 (207, 208). To probe whether the sensitivity of POLE4 KO to PARPi required the presence of PARP1 or PARP2, we utilized RNAi to target either or both factors. Cell survival assays revealed that only PARP1 downregulation was adequate to rescue the sensitivity of POLE4 KO (**Fig. 10A**). Conversely, depleting PARP2 failed to diminish PARPi sensitivity in POLE4 KO or enhance survival of these cells when co-depleted with PARP1 compared to the phenotype observed with PARP1 depletion alone (**Fig. 10A**), indicating that the Olaparib-induced sensitivity of POLE4 KO relies on PARP1 rather than PARP2, consistent with PARP1 trapping on their respective lesions.

To assess PARP1 dynamics in real-time, we monitored the recruitment and release kinetics of endogenous PARP1 at sites of DNA lesions induced by laser microirradiation using a GFP-tagged PARP1 chromobody (209). Live-cell imaging experiments revealed that PARP1 was efficiently recruited to damage sites followed by timely release in a similar fashion both in wild-type and POLE4 KO cells (**Fig. 10B, C**). Olaparib treatment reduced the release kinetics of PARP1 from damage sites, as expected, but again with no significant difference between wild-type and POLE4 KO cells (**Fig. 10B, C**), indicating that POLE4 does not interfere with PARP1 kinetics at DNA lesions.

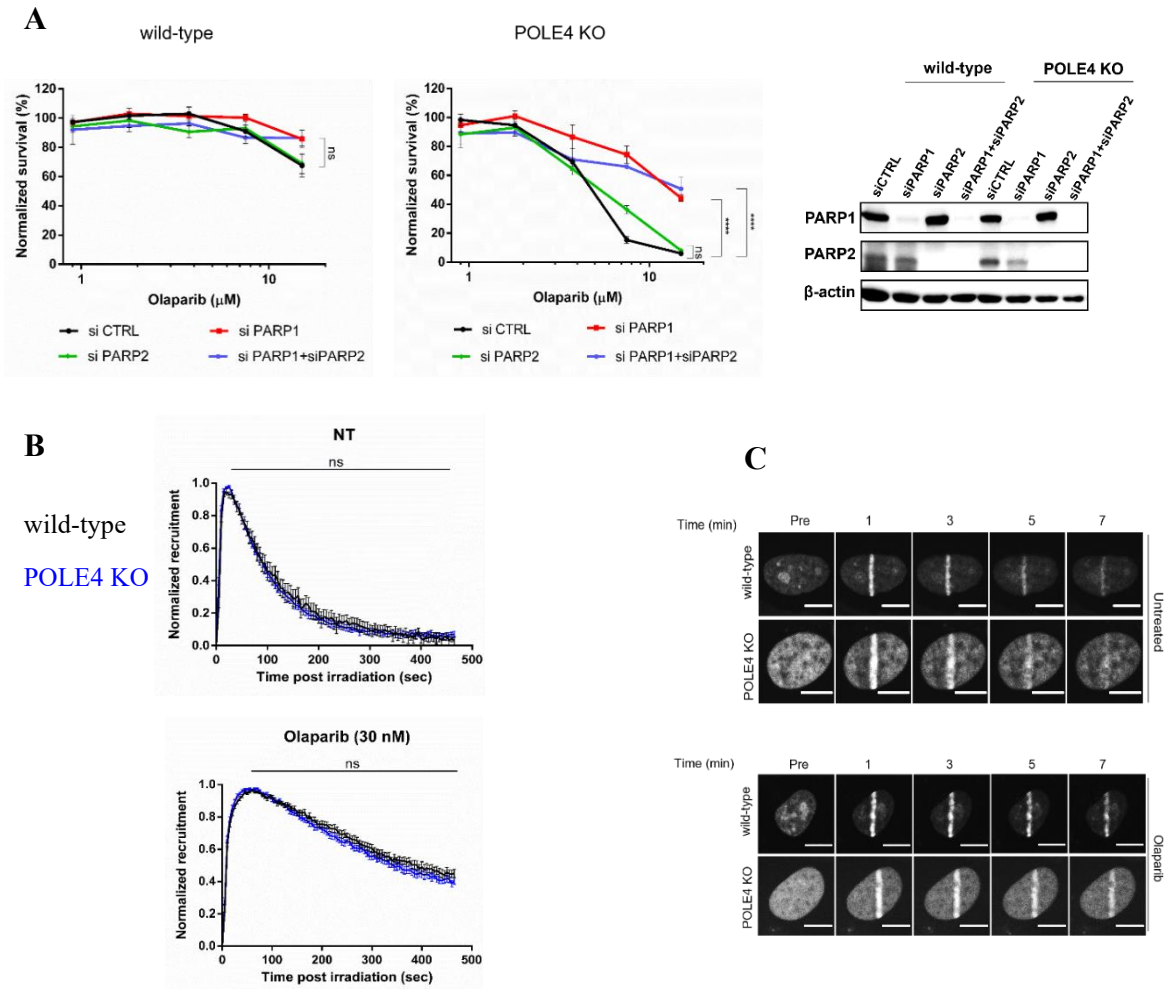


Figure 10: Sensitivity of POLE4 KO to PARPi is PARP1 dependent

(A) (Left) Cell survival assay of POLE4 KO and their parental HeLa cell line transfected with the indicated siRNA. The treatment was changed once during the 7-day long experiment. Mean \pm SEM ($n=3$). Asterisks indicate p -values obtained by two-way ANOVA (ns. Not significant and **** $p < 0.0001$). **(Right)** Immunoblot of PARP1 and PARP2 levels in POLE4 KO and their parental HeLa cell line upon transfection with the indicated siRNA. β -actin was used as a loading control. **(B)** Quantification of recruitment of GFP-tagged PARP1 chromobody at sites of laser-induced damage in POLE4 KO and their parental HeLa cell line without treatment **(Top)** or with Olaparib treatment **(Bottom)**. All data points included \pm SEM. The figure is a representative experiment of three independent replicates ($n=3$). Measurements were analyzed using Mann-Whitney unpaired t-test. (ns. Not significant). **(C)** Representative images of GFP-tagged PARP1 chromobody in the indicated cell lines upon the indicated treatment. Scale bar, 10 μ m.

In summary, these findings indicate that the sensitivity of POLE4 KO to PARPi, although dependent on PARP1 presence, is not due to dysregulated PARP1 kinetics at DNA damage sites.

4.2.3. POLE4 loss reduces replication fork speed and causes accumulation of PARPi-induced ssDNA gaps

PARPi treatment speeds up DNA replication (105). Moreover, the accessory subunits of POL ϵ are pivotal for stable progression of the POL ϵ complex (185). To probe for replication speed in POLE4 KO cells and the effect of PARPi in this context, we performed a DNA fiber assay. In this assay, cells were first pulse labeled with the nucleotide analog IdU for 20 minutes, followed by pulse labeling with another nucleotide analog, CldU, for the same duration, with or without PARPi treatment (**Fig. 11A, B**). Consistent with previous findings, PARPi treatment accelerated fork speed in wild-type cells, as evidenced by higher CldU/IdU ratios compared to untreated cells (**Fig. 11A**). Interestingly, loss of POLE4 alone slightly reduced replication speed compared to wild-type cells, as shown by the shorter track lengths (**Fig. 11 B**). This reduction in fork speed was further potentiated by PARPi treatment (**Fig. 11A, B**), suggesting accumulation of replicative defects in POLE4 KO due to PARPi treatment.

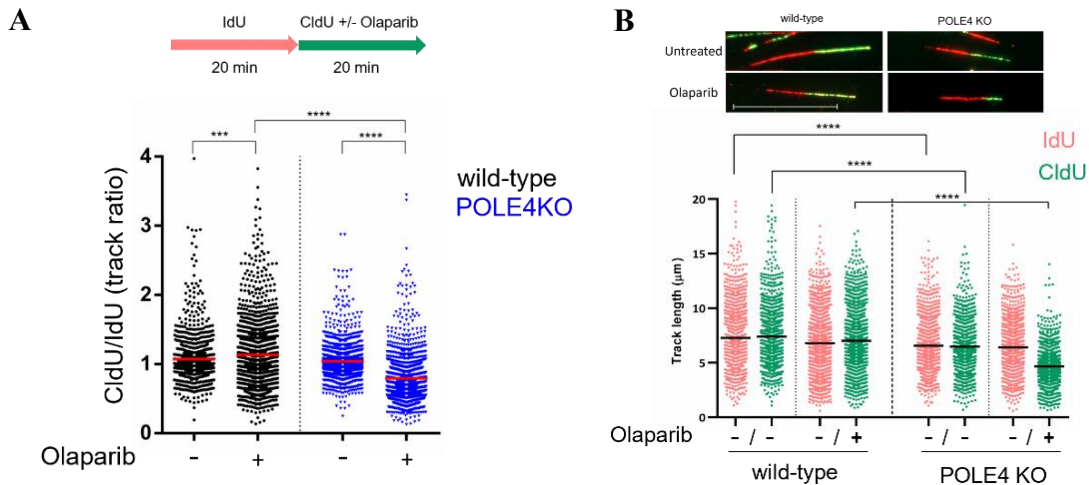


Figure 11: POLE4 deficiency slows down replication fork speed

(**A, B**) DNA fiber assay of POLE4 KO and their parental HeLa cell line with or without 20 μM of Olaparib treatment. (**A**) (**Top**) Illustration of the experimental protocol. (**Bottom**) Ratio of CldU/IdU labelled fibers from four independent experiments. (**B**) (**Top**) Representative images of DNA fibers of the indicated cell lines under the indicated conditions. Scale bar, 20 μm . (**Bottom**) The length of the DNA tracks obtained from four independent experiments. Asterisks indicate p -values obtained by one-way ANOVA (***) $p < 0.001$, **** $p < 0.0001$).

Considering that PARPi lead to elevated levels of ssDNA gaps behind replication forks (108), we probed for such gaps in POLE4 KO. To that end, we utilized the non-denaturing BrdU immunostaining assay, which relies on the inability of a specific antibody against BrdU to bind to the epitope in native conditions unless there is a single-stranded DNA gap opposite it, rendering the intensity of BrdU staining as an equivalent of the levels of ssDNA gaps in the cell (107, 108). The assay revealed a substantial increase in the intensity of BrdU staining in POLE4 KO cells following Olaparib treatment compared to their wild-type. This heightened BrdU intensity suggests major levels of unprocessed ssDNA gaps in these cells (Fig. 12A, B).

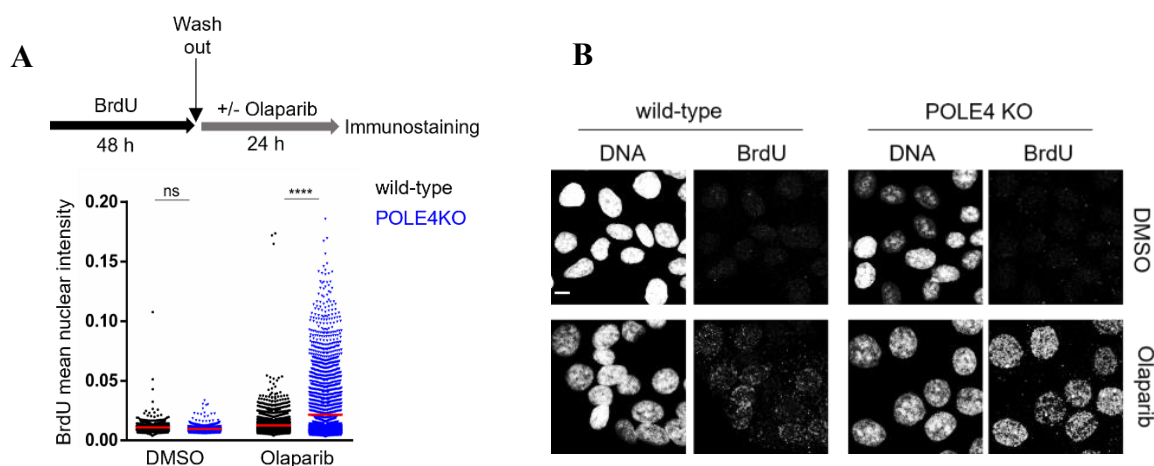


Figure 12: PARPi induces accumulation of ssDNA gaps in POLE4 KO

(A) Immunofluorescence of non-denaturing BrdU experiment. (Top) Representation of the experimental protocol. (Bottom) Mean intensity of BrdU in POLE4 KO and their parental HeLa cell line treated or not with 10 μ M of Olaparib for 24h. Asterisks indicate p -values obtained by one-way ANOVA (ns. Not significant, **** $p < 0.0001$). (B) Representative images of the experiment in (A). Scale bar, 10 μ m.

Defects in post-replicative repair (PRR) lead to increased levels of unprocessed ssDNA gaps. To test whether POLE4 deficiency impairs this process, we employed a previously established variation of BrdU comet assay to assess PRR (200). In this assay, BrdU pulse-labelled cells are treated with HU to induce replicative ssDNA gaps, then the cells are left to recover from the treatment and repair these gaps before scoring the comet tails with a specific antibody against BrdU. This assay revealed that wild-type cells challenged with HU accumulated post-replicative gaps, which were reduced after 3h recovery period, as indicated

by the percentage of comet tail DNA (**Fig. 13A, B**). In POLE4 KO cells, the levels of post-replicative gaps were higher than in wild-type cells upon HU treatment (**Fig. 13A, B**). Although there was some reduction, this phenotype persisted even after 3h recovery time (**Fig. 13A, B**), indicating the importance of POLE4 in ensuring seamless PRR.

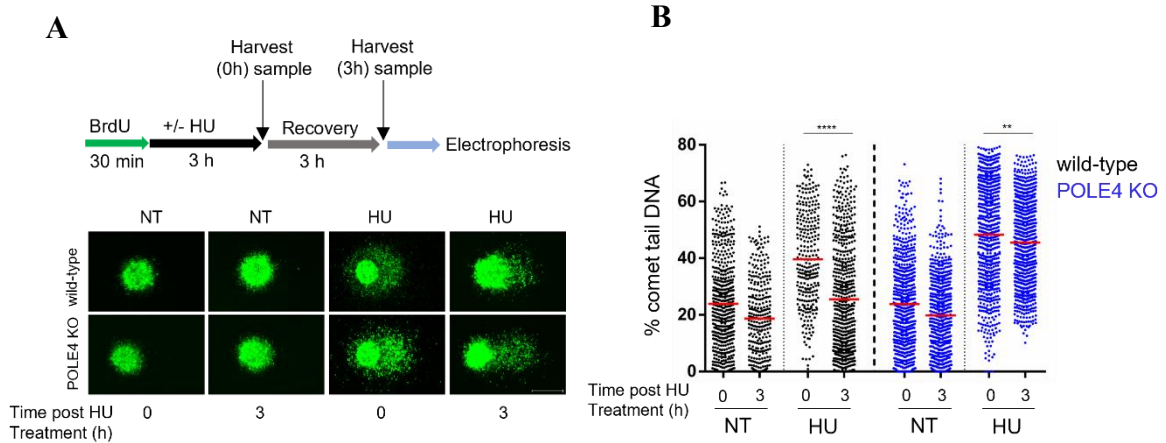


Figure 13: Loss of POLE4 impairs post-replicative repair

(A) (Top) Illustration of the post-replicative comet assay. (Bottom) Representative images of the experiment. Scale bar 20 μ m. (B) Quantified percentage of comet tail DNA in POLE4 KO and their parental HeLa cell line after being treated or not with hydroxyurea (HU) according to the illustration in (A). The figure is a representative of three independent experiments. Asterisks indicate *p*-values obtained by one-way ANOVA (** *p* < 0.01, **** *p* < 0.0001).

Collectively, these findings indicate that POLE4 deficiency disrupts the replication profile by reducing fork speed, which is potentiated in the presence of PARPi, resulting in the accumulation of ssDNA gaps as a result of inefficient post-replicative gaps processing.

4.2.4. POLE4 as a protector against replication stress induced by PARPi or ATRi

Unrepaired ssDNA gaps lead to replication stress and cell cycle arrest (210). Therefore, we probed for POLE4 KO cell cycle profile by flow cytometry. POLE4 KO cells suffered from moderate G2/M arrest, which was strongly exacerbated by PARPi treatment (**Fig. 14A**), suggesting mild replication stress in POLE4 KO potentiated by PARP inhibition. When cells go under replication stress, the Ataxia-telangiectasia mutated and RAD3-related (ATR) as a member of the phosphatidylinositol 3-kinase-related kinase (PIKK) family, regulates origin

firing, cell cycle progression and replication speed (206). To investigate upregulation of ATR activity in POLE4 KO cells, we probed for the autophosphorylation of Threonine 1989 (T1989), an indicator of ATR activity (211). Immunoblotting showed slight elevation in ATR activity in POLE4-deficient cells compared to wild-type, which was markedly increased upon PARPi treatment (**Fig. 14B**). This signal was suppressed by ATRi (**Fig. 14B**). These data indicate that replication stress in POLE4 KO signals through upregulated ATR activity.

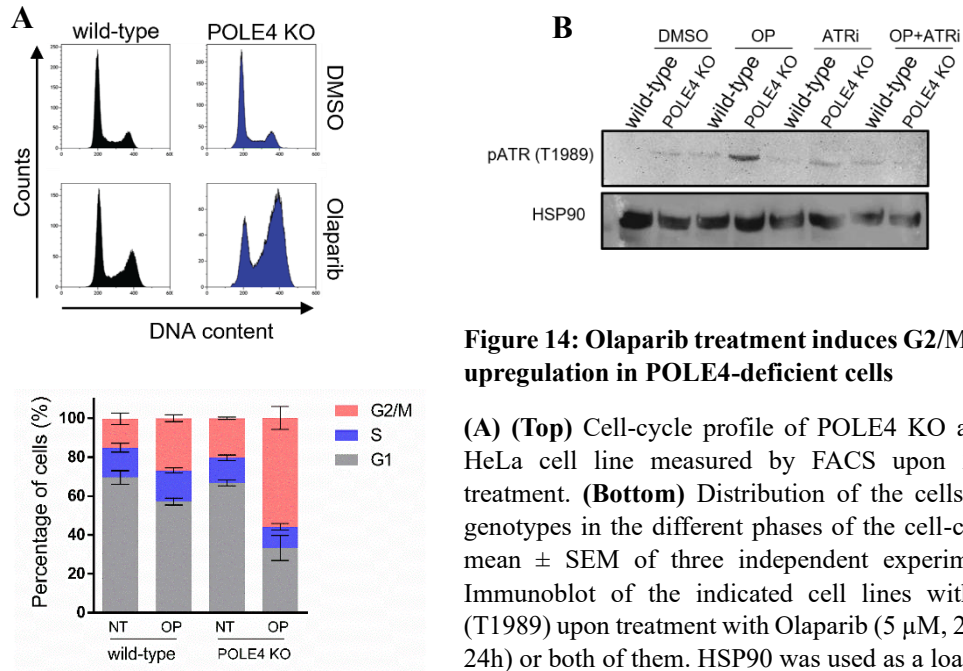


Figure 14: Olaparib treatment induces G2/M arrest and ATR upregulation in POLE4-deficient cells

(A) (Top) Cell-cycle profile of POLE4 KO and their parental HeLa cell line measured by FACS upon 24h of Olaparib treatment. **(Bottom)** Distribution of the cells of the indicated genotypes in the different phases of the cell-cycle presented as mean \pm SEM of three independent experiments, (n=3). **(B)** Immunoblot of the indicated cell lines with the anti-pATR (T1989) upon treatment with Olaparib (5 μ M, 24h), ATRi (5 μ M, 24h) or both of them. HSP90 was used as a loading control.

RPA binds ssDNA and is phosphorylated upon replication stress on multiple residues by PIKKs, where Serine 33 (S33) is phosphorylated early on upon mild replication stress, and Threonine 21 (T21) upon severe replication stress (212). In line with mild replication stress upon the loss of POLE4, we detected pRPA (S33) signal in untreated POLE4 KO cells, which was potentiated by PARPi (**Fig. 15A**). The pRPA (S33) signal was reversed by ATRi, confirming that it is an ATR target (212). Furthermore, the important role of ATR in signaling replication stress in POLE4 KO is mirrored by their sensitivity to ATRi (**Fig. 15B**), providing evidence for a synthetic lethality between ATR inhibition and loss of POLE4, consistent with earlier reports (171, 206).

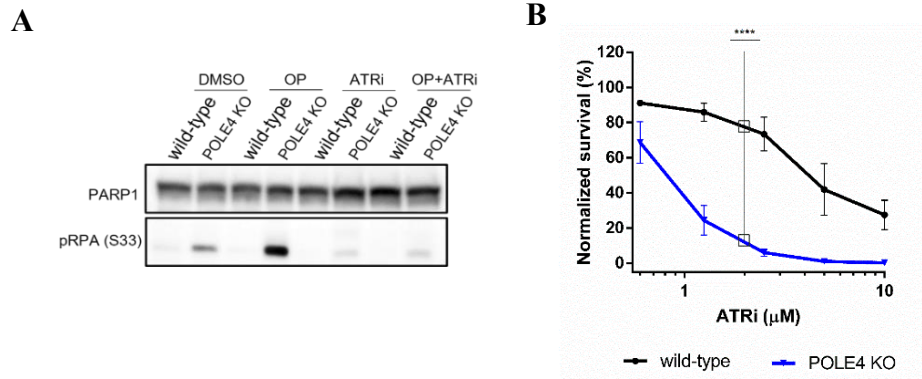


Figure 15: Susceptibility to replication stress upon loss of POLE4

(A) Immunoblot showing the levels of pRPA (S33) in the indicated genotypes upon treatment with Olaparib (5 μM, 24h), ATRi (5 μM, 24h) or both of them. PARP1 was used as a loading control. (B) Cell survival assay showing sensitivity of POLE4 KO to ATRi treatment compared to their parental HeLa cell line. The treatment was changed once during the 7-day long experiment. Mean ± SEM (n=3). Asterisks indicate *p*-values obtained by two-way ANOVA (**** *p*< 0.0001).

Failure to mitigate replication stress in POLE4 KO upon PARPi caused a striking increase in the pRPA (T21) signal, which correlated with the population of cells accumulated in G2/M in comparison to wild-type cells (Fig. 16A). The sensitivity of POLE4 KO to ATRi was also reflected by induced pRPA (T21) signal (Fig. 16A), supporting severe replication stress, which could be converted to replication catastrophe phenotype as a result of DSB accumulation. To test this hypothesis, we quantified the levels of γH2AX upon the DNA alkylating agent, methyl methanesulfonate (MMS) treatment as a positive control. As expected, MMS treatment led to elevation of γH2AX signal, albeit with no significant difference between wild-type and POLE4 KO cells (Fig. 16B). Although Olaparib neither caused DSB in wild-type nor in POLE4 KO as shown by low γH2AX levels (Fig. 16B), ATRi led to a surge in the percentage of γH2AX positive cells only in POLE4 KO (Fig. 16B) differentiating the cellular response of POLE4 KO to PARPi and ATRi. The conversion of ATRi-induced ssDNA gaps to DSB has been reported and correlated with the activation of other PIKKs, such as DNA-PK and Ataxia-telangiectasia mutated (ATM) (213).

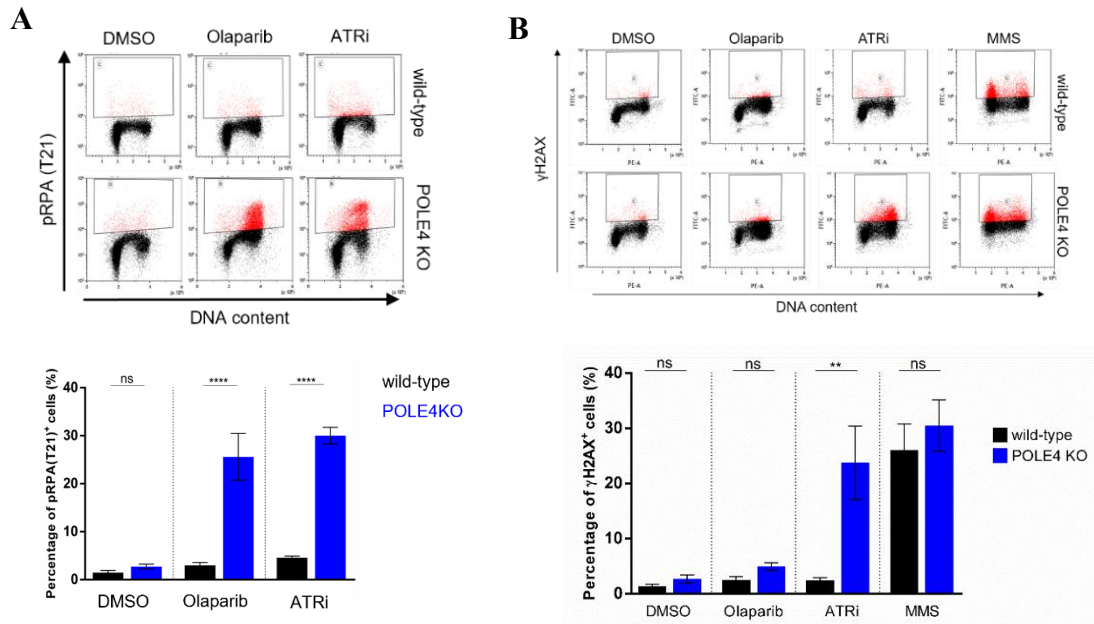


Figure 16: Severe replication stress in POLE4 KO upon PARPi or ATRi treatment

(A) (Top) FACS experiment showing staining of pRPA (T21) correlated to the DNA content (propidium iodide) in the indicated genotypes after 24h treatment with Olaparib (5 μ M), ATRi (5 μ M) or DMSO. (Bottom) Bar chart of the percentages of pRPA (T21) positive cells from three independent experiments. Asterisks indicate *p*-values obtained by one-way ANOVA (ns. Not significant, **** *p* < 0.0001). (B) (Top) FACS experiment showing staining of γ H2AX correlated to the DNA content (propidium iodide) in the indicated genotypes after 24h treatment with Olaparib (5 μ M), ATRi (5 μ M) or 1h treatment with MMS (0.1%). (Bottom) Bar chart of the percentages of γ H2AX positive cells from three independent experiments. Asterisks indicate *p*-values obtained by one-way ANOVA (ns. not significant, ** *p* < 0.01).

To confirm that POLE4 protects against the observed replication stress phenotype, we co-transfected POLE4 KO cells with an empty vector or untagged POLE4 expressing plasmid along with a GFP-expressing plasmid, then we challenged the cells with either PARPi or ATRi and monitored the levels of pRPA (T21). During FACS analysis we gated the transfected cells into two populations: GFP+ population likely to express POLE4 as well, and GFP- population likely to lack POLE4 expression (Fig. 17A). We detected pRPA (T21) signal upon either PARPi or ATRi in both GFP positive and negative populations of cells co-transfected with the GFP expressing plasmid and empty vector (Fig. 17B), confirming that GFP expression alone does not reduce replication stress in POLE4 KO. On the other hand, in cells co-transfected with the plasmids expressing GFP and POLE4 and treated with either

PARPi or ATRi, pRPA (T21) was detected only in the GFP- population corresponding to no POLE4 expression. Importantly, in the GFP+ population, where POLE4 was expressed, the replication stress phenotype was rescued (**Fig. 17A, B**). Similarly, sensitivity of POLE4 KO to PARPi was partially reversed by transient expression of POLE4 as compared to the empty vector control (**Fig. 17C, D**). Altogether, these results demonstrate that POLE4 protects against replication stress associated with inhibition of either PARP or ATR.

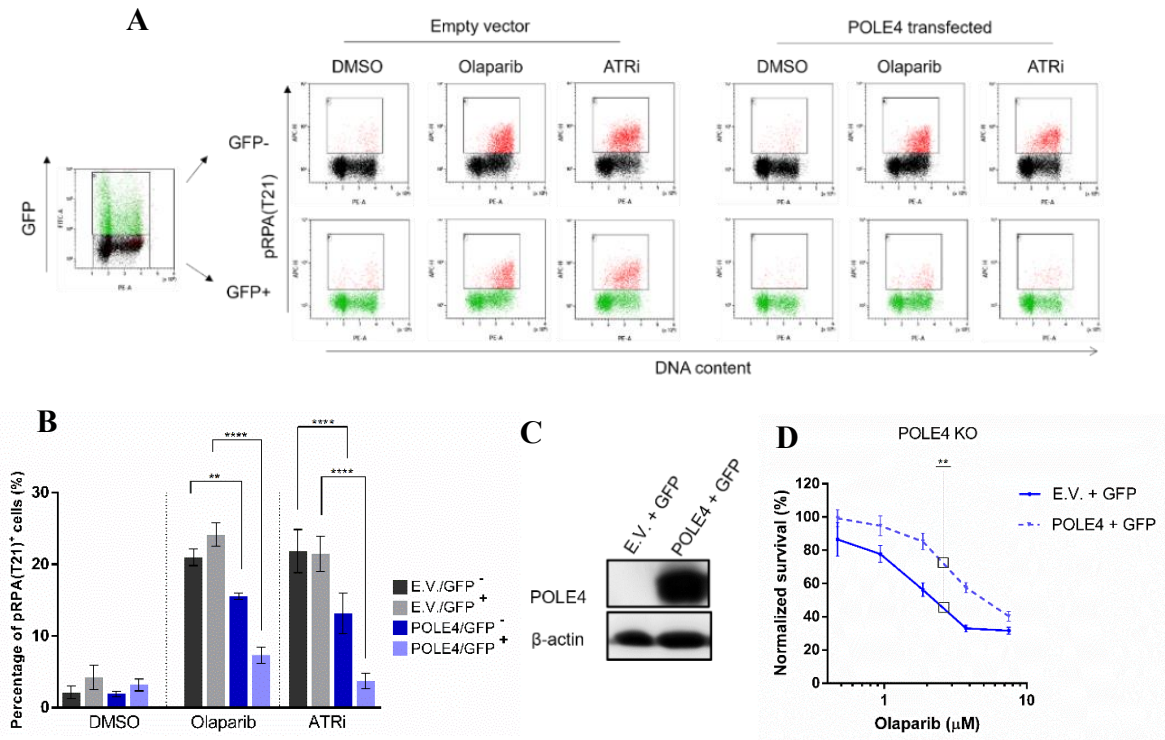


Figure 17: POLE4 suppresses replication stress induced by PARPi or ATRi

(**A, B**) FACS experiment showing staining of pRPA (T21) correlated to the DNA content (propidium iodide) in POLE4 KO after transfection with GFP and either empty (E.V.) or POLE4-expressing plasmid, followed by 16h treatment with Olaparib (5 μM), ATRi (5 μM) or DMSO. Cells gated to GFP positive and negative populations during FACS analysis. (**A**) Representative FACS images of the experiments. (**B**) Percentages of pRPA (T21) positive cells. Data are mean ± SEM from three independent experiments. Asterisks indicate *p*-values obtained by one-way ANOVA (** *p* < 0.01, **** *p* < 0.0001). (**C**) Immunoblot verifying POLE4 expression in POLE4 KO after transfection with (E.V.) or POLE4-expressing plasmid. β-actin was used as loading control. (**D**) Cell survival assay showing sensitivity of POLE4 KO cells to Olaparib after being transfected with the indicated constructs. The treatment was changed once during the 6-day long experiment. Data are mean ± SEM (n=3) of triplicate samples from one out of three independent experiments. Asterisks indicate *p*-values obtained by two-way ANOVA (** *p* < 0.01).

4.2.5. PARPi-induced replication stress is driven by PIKKs

Our findings point to the involvement of other members of the PIKK family in signaling replication stress in POLE4 KO cells. To investigate this further, we examined the activity of ATM and DNA-PK. In wild-type cells, immunoblotting showed that the activity of DNA-PK, as indicated by its autophosphorylation, remained unchanged upon treatment with Olaparib and/or ATRi (**Fig. 18**). However, in POLE4 KO, DNA-PK activity was significantly increased after 24 hours of treatment with ATRi alone or in combination with Olaparib (**Fig. 18**). Similarly, phosphorylation of ATM (pATM), an indicator of ATM activation, revealed a modest increase in wild-type cells following treatment with either Olaparib or ATRi alone, but a substantial enhancement when both were combined. Comparatively, pATM levels were further heightened in POLE4 KO cells in response to single treatments of Olaparib or ATRi, as well as their combination (**Fig. 18**). These results underscore the intricate interplay between PIKKs in POLE4 KO cells during replication stress response.

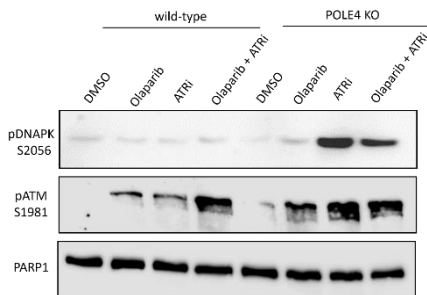


Figure 18: Upregulation of DNA-PK and ATM in POLE4 KO upon treatment with PARPi or ATRi

A representative immunoblot with the indicated antibodies in POLE4 KO and their parental HeLa cells upon treatment with Olaparib (5 μ M, 24h), ATRi (5 μ M, 24h) or both of them. PARP1 was used as a loading control.

Given that pRPA (T21) indicates severe replication stress and is characteristic of the G2/M population of POLE4 KO treated with PARPi, we sought to illustrate the role of the PIKK members in driving this phenotype. ATRi only and no other PIKK inhibitors significantly induced pRPA (T21) in wild-type cells when combined with Olaparib (**Fig. 19**). In POLE4KO, inhibiting ATR alone increased phosphorylation of RPA (T21), whereas neither ATMi nor DNA-PKi drove such phenotype in POLE4 KO (**Fig. 19**). Conversely, all PIKK inhibitors modulated pRPA (T21) signal in POLE4 KO upon Olaparib treatment: ATRi and ATMi potentiated it, while DNA-PKi suppressed it (**Fig. 19**).

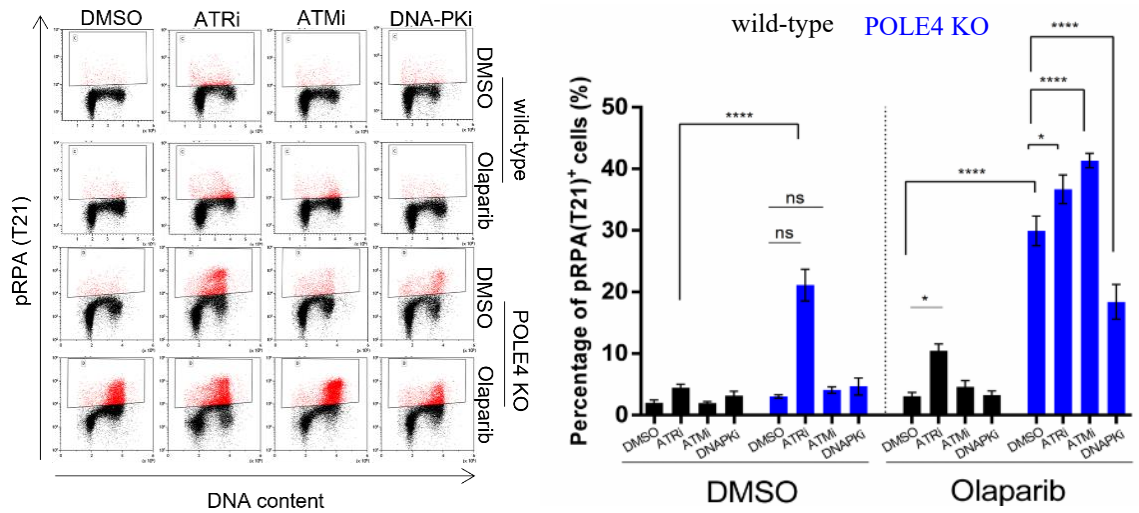


Figure 19: Severe replication stress in POLE4 KO is mediated by PIKK

(Left) FACS experiment showing levels of pRPA (T21) correlated to the DNA content (propidium iodide) of POLE4 KO and their parental HeLa cell line after 24h treatment of Olaparib (5 μ M) and/or DNA-PKi (5 μ M), ATRi (5 μ M) or both. (Right) Bar chart illustrating percentages of pRPA (T21) positive HeLa wild-type or POLE4 KO cells. Mean \pm SEM from four independent experiments. Asterisks indicate *p*-values obtained by one-way ANOVA (ns. Not significant, * *p* < 0.05, **** *p* < 0.0001).

To elucidate whether the population of cells with severe replication stress is blocked in G2 or allowed to enter mitosis with these defects, we co-stained POLE4 KO and wild-type cells with a mitotic marker, which is Serine 10 phosphorylation of histone H3 (pH3S10), along with the pRPA (T21) antibody. The dual staining of pH3(S10) and pRPA (T21) demonstrated that PARPi-induced pRPA (T21)-positive POLE4 KO cells were arrested in G2, unless ATR was inhibited (Fig. 20A), indicating that ATR primarily orchestrates the G2/M transition in POLE4 KO. Curbing ATR activity by chemical inhibition caused premature mitotic entry of cells suffering from replication stress, which explains the replication catastrophe phenotype we observed earlier (Fig. 16B) and the hypersensitivity to ATRi (Fig. 15B). Consistent with this, while challenging POLE4-deficient cells with either PARPi or ATRi alone in a low dose did not have major impact on their survival, their combination synergistically induced cell death in POLE4 KO cells (Fig. 20B). This underscores POLE4 deficiency as a biomarker to co-treatment with ATRi and PARPi, a therapeutic combination currently under evaluation in clinical trials (214).

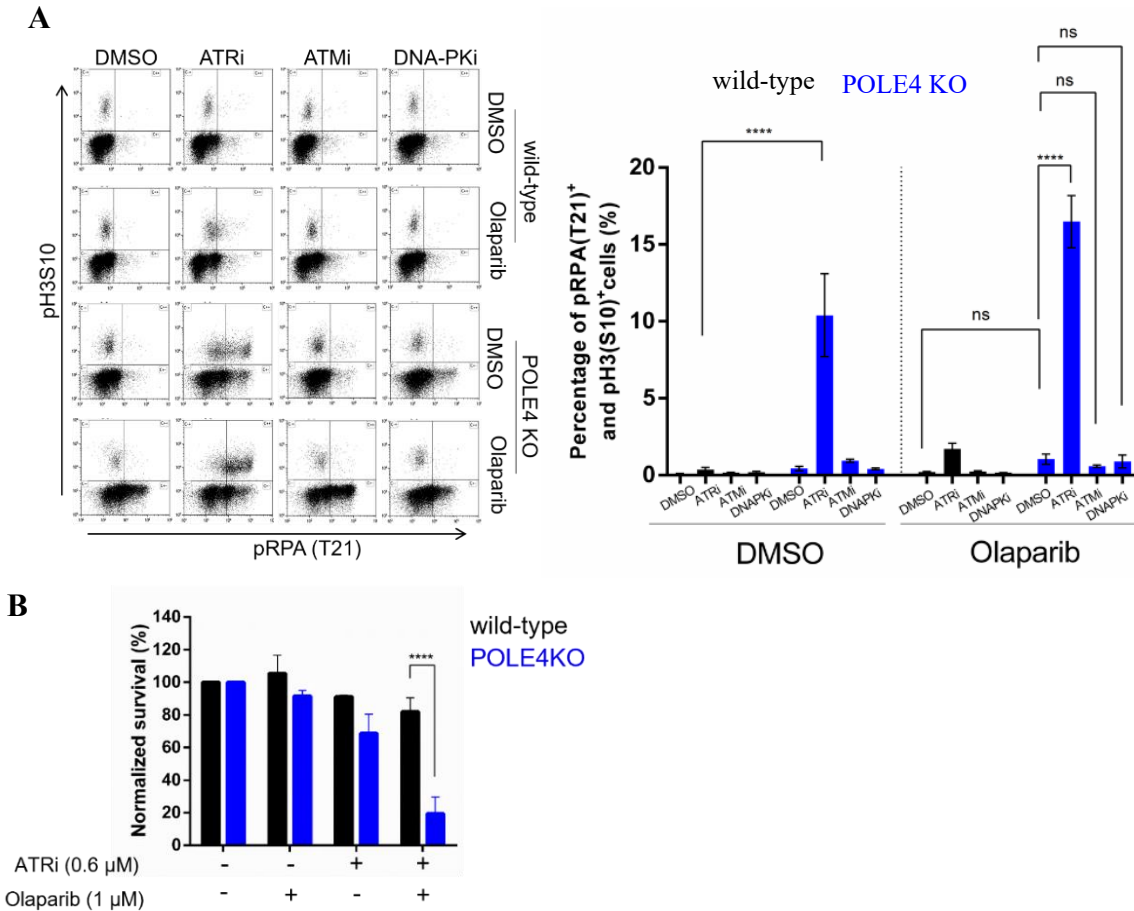


Figure 20: Premature mitotic entry underlies synergistic killing of POLE4 KO upon co-treatment with PARPi and ATRi

(A) (Left) FACS experiment showing mitotic entry indicated by pH3(S10) signal of cells suffering from replication stress indicated by pRPA (T21) signal in POLE4 KO and their parental HeLa cell line after 24h of Olaparib (5 μM) and/or ATRi (5 μM), ATMi (5 μM), DNA-PKi (5 μM) treatment. (Right) Bar chart showing the mean ± SEM of percentages of pRPA (T21)/pH3(S10) double positive cells from three independent experiments. Asterisks indicate *p*-values obtained by one-way ANOVA (ns. Not significant, **** *p* < 0.0001). (B) Cell survival assay of POLE4 KO and their parental HeLa cell line treated with the indicated concentrations of PARPi and/or ATRi. The bars represent normalized survival of the cells. The treatment was changed once during the 7-day experiment. Mean ± SEM (n=3). The figure was derived from three independent experiments. Asterisks indicate *p*-values obtained by two-way ANOVA (**** *p* < 0.0001).

Altogether, these data establish ATR as the major PIKK kinase to regulate mitotic entry of POLE4 KO suffering from replication stress induced by PARPi. Additionally, our results indicate that replication stress phenotype in POLE4-deficient cells are modulated in part by the activity of DNA-PK.

4.2.6. Sensitivity of POLE4 KO to PARP inhibitors is independent of BRCA1 status

Given that PARPi sensitivity was initially associated with BRCA-deficient cells characterized by HR deficiency (16, 17), we sought to investigate whether POLE4 KO are HR defective. To that end, we monitored the ability of POLE4 KO to mount Rad51 foci following PARPi treatment. Rad51 foci formation is a critical step in HR repair as it directs the homology search and strand invasion, thereby mediating homology-directed repair (16, 17). As expected, BRCA1-deficient cells failed to form Rad51 foci upon PARPi treatment compared to BRCA1-proficient controls, consistent with previously reported HR impairment (**Fig. 21A**). Strikingly, POLE4 KO cells demonstrated efficient Rad51 foci formation upon Olaparib treatment, even surpassing the levels observed in their wild-type counterparts (**Fig. 21B**). This phenotype can be explained by the increased presence of ssDNA gaps observed previously in response to PARPi (**Fig. 12A, B**).

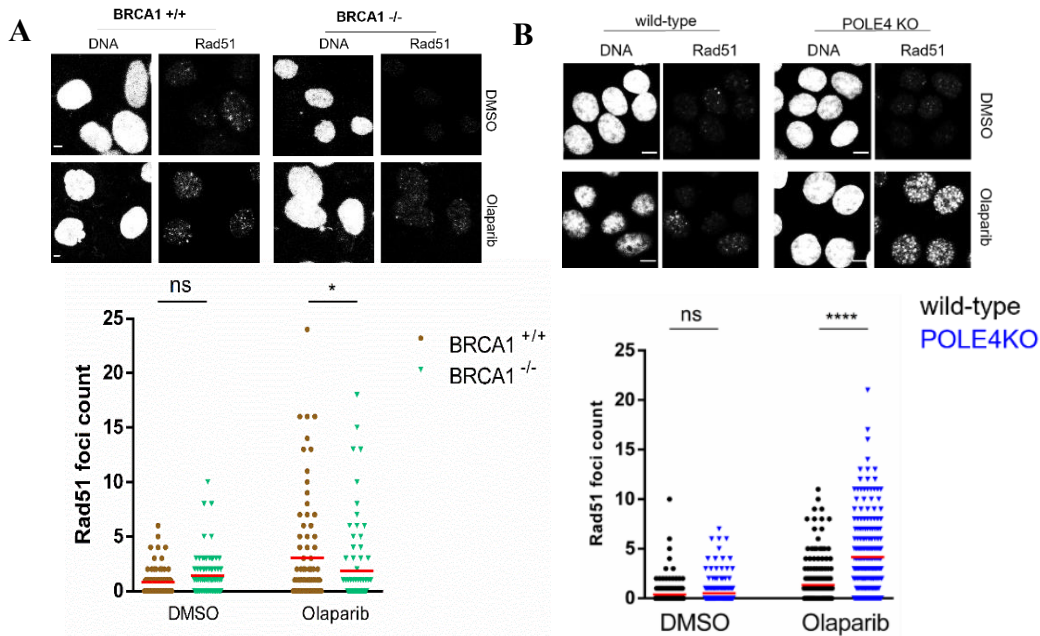


Figure 21: POLE4 KO have functional HR pathway

(A) Immunofluorescence experiment of Rad51 staining in RPE-1 BRCA1-deficient cells and their wild-type after treatment with 10 μ M of Olaparib for 48h. (Top) Representative images of the staining. Scale bar, 10 μ m. (Bottom) Quantification of Rad51 foci count. The experiment is representative of three independent repetitions. Asterisks indicate *p*-values obtained by one-way ANOVA (ns. Not significant, * *p* < 0.05). (B) Immunofluorescence experiment of Rad51 staining in POLE4 KO cells and their parental HeLa cell line after treatment with 10 μ M of Olaparib for 48h. (Top) Representative images of the staining. Scale bar, 10 μ m. (Bottom) Quantification of Rad51 foci count. The experiment is representative of three independent repetitions. Asterisks indicate *p*-values obtained by one-way ANOVA (ns. Not significant, **** *p* < 0.0001).

These results indicate that POLE4 KO have functional HR pathway, therefore, POLE4 and BRCA1 function in parallel rather than in the same route of inducing PARPi sensitivity and targeting both of them would exacerbate PARPi sensitivity. To validate this hypothesis, we depleted BRCA1 in both wild-type and POLE4 KO and applied a low dose of PARPi. Indeed, sensitivity of POLE4 KO depleted from BRCA1 was strikingly higher compared to losing either of them (**Fig. 22A**), supporting the idea of POLE4 serving as a possible target to potentiate PARPi-induced sensitivity of BRCA1-deficient cancers.

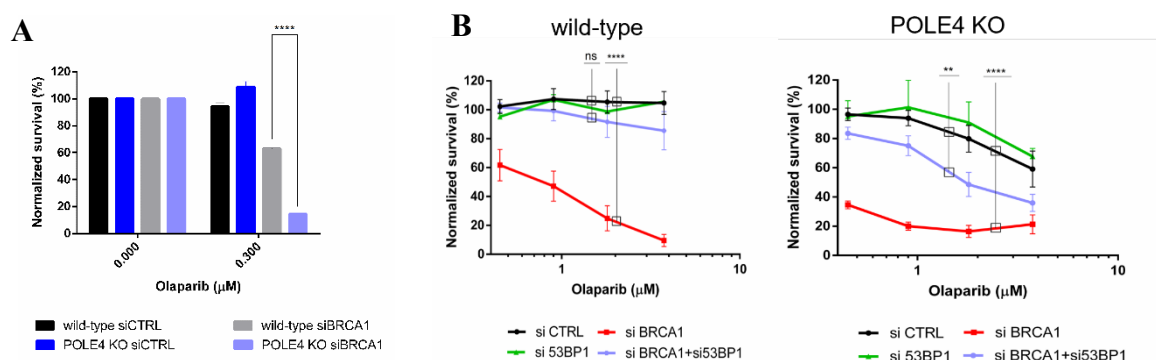


Figure 22: Loss of POLE4 enhances PARPi sensitivity of BRCA1-deficient cells and overcomes acquired resistance associated with restoration of HR

(A) Cell survival assay showing sensitivity of POLE4 KO and their parental HeLa cells to Olaparib after transfection with the indicated siRNA. The treatment was refreshed once during the 7-day long experiment. The figure is derived from three independent experiments, mean \pm SEM. Asterisks indicate p -values obtained by two-way ANOVA (**** $p < 0.0001$). (B) Cell survival assay showing sensitivity of POLE4 KO and their parental HeLa cells to Olaparib after transfection with the indicated siRNA. The treatment was refreshed once during the 7-day long experiment. The figure is derived from three independent experiments, mean \pm SEM. Asterisks indicate p -values obtained by two-way ANOVA (ns. Not significant, ** $p < 0.01$, **** $p < 0.0001$).

Finally, we aimed to elucidate whether POLE4 loss could bypass the synthetic viable phenotype observed in BRCA1-deficient cells upon the loss of the NHEJ factor 53BP1 (163–165). Thus, we employed RNAi to target either BRCA1, 53BP1, or both in wild-type and POLE4 KO cells. As expected, depleting BRCA1 in wild-type cells induced sensitivity to Olaparib, which was reversed by co-depletion of BRCA1/53BP1 (**Fig. 22B**). Importantly, the simultaneous depletion of BRCA1/53BP1 did not rescue PARPi sensitivity in POLE4 KO cells as it did in wild-type cells (**Fig. 22B**), demonstrating that targeting POLE4 hold the potential of exacerbating PARPi-induced synthetic lethality in BRCA1-depleted cells and circumventing the acquired resistance mechanism triggered by HR rewiring upon loss of 53BP1 in BRCA1-compromised cells (162).

5. Discussion

Implementing personalized medicine strategies has been a paradigm shift in the fight against cancer as it allowed for an informed medical intervention for each patient by understanding the molecular mechanisms driving tumor formation, therefore, permitting the selection of the best therapeutic strategy that would offer maximum elimination of malignancies with minimum side effects.

The exploitation of the synthetic lethal interaction between PARPi and BRCA-deficient tumors is one of the most promising and quickly advancing strategies of personalized cancer therapy as it took less than a decade from its experimental discovery (16, 17) to the clinical approval. Since then, this approach has been the epicenter of extensive basic, translational and clinical research to expand our understanding of PARPi, their mode of action, the processes that they interfere with, the genetic backgrounds in which they promote cell death and how this could be implemented in the clinical treatment regimens. Not surprisingly, these efforts yielded the expansion of PARPi applicability beyond BRCA-deficiency to include tumors with mutations in HR-related genes that rendered this pathway inactive, and phenocopied the BRCA-deficiency, a term known as BRCAness (215).

In the current work, we aimed to further increase this knowledge by identifying and validating novel genetic alterations that sensitize cells to PARPi. Furthermore, we worked towards uncovering the molecular mechanisms and pathways that underlie this sensitivity to offer a better understanding of PARPi. Finally, we explored the possibility of overcoming PARPi resistance by targeting the genes identified in this work.

ALC1 was among the top hits we identified in a genome-wide CRISPR knockout screen with the PARPi, Olaparib (173). This PAR-binding chromatin remodeler plays an important role in chromatin relaxation upon DNA damage, which is crucial to guarantee timely and efficient repair process (176). Our data demonstrated that ALC1 deletion induced sensitivity to different PARPi in a PARP1-dependent manner. Mechanistically, we uncovered ALC1 role in mobilizing PARP1 from the sites of DNA lesions and that its deletion even in the context of active ADP-ribosylation resulted in delaying PARP1 release from sites of DNA damage. Importantly, ALC1 KO cells showed increased PARP1 trapping on the damage sites upon

PARPi which caused accumulation of DSB and G2/M cell cycle arrest. This is consistent with the original model of PARPi sensitivity due to enhanced PARP trapping (124).

Clinically, ALC1 is an oncogene that is amplified in different types of solid tumors and associated with poor prognosis (179–182). Moreover, the region where ALC1 gene is located was reported to be amplified in breast cancer (216) and linked to poor response to chemotherapy in ovarian cancer (217). This is also supported by our data showing that ALC1 overexpression reduced the sensitivity of BRCA1 and BRCA2 deficient cells to PARPi treatment. Taken together, our work strongly argues for analyzing ALC1 expression status as a biomarker to predict tumors' response to PARPi treatment. Considering that ALC1 amplification drives tumorigenesis and in light with our current data as well as others (218–220) showing the hypersensitization of cells to PARPi when ALC1 is targeted, ALC1 can serve as an ideal target for selective inhibitors. Indeed, these data justified the development of compounds to target ALC1 which showed therapeutic potentials (221, 222).

Crucially, our results established loss of ALC1 as an inducer of sensitivity to PARPi regardless of HR status, since reactivating HR through loss of 53BP1, which is a common PARPi resistance mechanism (163–165), did not rescue PARPi sensitivity in ALC1 KO as was the case in BRCA1-depleted cells (162) indicating that ALC1 deficiency does not follow the BRCAness phenotype, and supporting the logic that inhibiting ALC1 could synergize with PARPi treatment and potentially re-sensitize resistant cells.

Similarly, our findings indicated that loss of the accessory subunit of DNA polymerase epsilon POLE4 mirrored the phenotype of ALC1 deficiency in the context of HR-independent PARPi sensitivity, paving the way for POLE4 status to be analyzed as a diagnostic tool for identifying PARPi susceptible tumors. This is not only supported by the fact that loss of 53BP1 in POLE4 KO did not rescue PARPi sensitivity, but importantly POLE4 KO cells were able to mount Rad51 foci, a crucial step in HR (16, 17), unlike the case for BRCA1-deficient cells. These data established POLE4 to be parallel to BRCA1, a hypothesis validated by our observation that loss of both POLE4 and BRCA1 increased PARPi sensitivity beyond the levels noticed when either of them were missing alone.

PARPi sensitivity is attributed to trapping of PARP1 and/or PARP2 (124, 207, 208). Our data demonstrated that PARPi sensitivity in genetic backgrounds deficient of either ALC1 or

POLE4 is mainly dependent on the presence of PARP1 rather than PARP2, further supporting the efforts aimed at developing PARP1-specific inhibitors (223, 224). Nevertheless, the underlying mechanisms of PARPi sensitivity in those two genetic backgrounds are different. While ALC1 plays a substantial role in mobilizing PARP1 at the damage site, therefore facilitating the repair process, POLE4 does not impact PARP1 kinetics.

PARPi sensitivity is correlated with abnormal elevation of ssDNA gaps (107, 108), which is a major source of replication stress. Studies in yeast point to a function of the POL ϵ complex in regulating the activity of the S-phase checkpoint by either the catalytic subunit or its accessory one Dpb4 in conditions associated with replication stress (186, 225, 226). Moreover, seamless progression of replication fork requires the presence of both accessory subunits (185), which is supported by reports of defective activation of origins of replication in mice and worms upon POLE4 deletion (187, 227, 228), a phenotype that is exacerbated by agents that induce replication stress (187). Consistent with these reports, our data showed that POLE4-deficient cells have slower replication fork and are susceptible to inducers of replication stress, consolidating the requirement of POLE4 to suppress replication stress.

Increased fork speed due to PARPi treatment leads to replication stress (105). Taking into account that loss of POLE4 produced the opposite phenotype with forks going slower than in wild-type even in PARPi treatment scenario, it is likely that POL ϵ instability as a consequence of POLE4 deficiency (187) resulted in decreased fork speed that only got exacerbated with PARP1 being trapped on the DNA upon PARPi. This scenario along with discontinuous DNA synthesis when the accessory subunits of POL ϵ are missing (185) necessitate an efficient post-replicative repair activity to deal with the generated gaps (229). Considering that POLE4 KO are impaired in this process, this could explain the high levels of ssDNA gaps observed in these cells upon PARPi treatment.

The ATR kinase is critical to protect against replication stress (230). When ssDNA gaps accumulate, RPA binds these structures promoting ATR recruitment (231). This is followed by ATR activation which promotes a cascade of signaling events aimed to regulate DNA replication and cell-cycle progression (232, 233). ATR blocks cells from entering mitosis with unrepaired lesions and slows down the replication speed to mitigate replication stress (234). Loss of POLE4 caused upregulation of ATR activity indicating a replication stress

phenotype which got potentiated upon PARPi treatment. This is also supported by high levels of ssDNA gaps in POLE4 KO treated with Olaparib. These findings demonstrate that POLE4 is important to protect against replication stress.

Consistent with this, the combination of PARPi and ATRi was found to synergistically eliminate BRCA-deficient cells due to premature entry to mitosis (235, 236). A real challenge to combination therapy is the increase of toxic side effects which can be circumvented by identifying biomarkers of sensitivity towards such combination. Our work presents POLE4 as such biomarker to this combination due to two main mechanisms. On one hand, ATRi enhances the replication stress phenotype in PARPi-treated POLE4 KO, as is the case with RNase H2 deficient cells (237, 238). On the other hand, G2-blocked POLE4 KO due to PARPi treatment would be released into mitosis upon inhibiting ATR leading to replication catastrophe as reported with loss of ATM (239, 240) or BRCA deficiency (235, 236).

PIKK share concerted roles in response to replication stress. Moreover, ATM is upregulated upon PARPi treatment (241, 242). This is further validated by our results of ATM activation upon PARPi and/or ATRi in wild-type but to a greater level in POLE4 KO as well. On the other hand, DNA-PK signaling is only upregulated in POLE4 KO and associated with the observed replication stress phenotype. Such DNA-PK activation was reported in HR-deficient cells treated with PARPi (203). These observations support a notion of imbalanced PIKK signaling due to POLE4 loss which contributes to the observed sensitivity.

In summary, the sensitivity of ALC1 KO and POLE4 KO to PARPi treatment is driven by different mechanisms. POLE4 loss slows down replication speed leading to ssDNA gaps behind replication forks and mild replication stress, which the cell could still overcome when ADP-ribosylation is active. However, upon PARPi treatment, replication is further slowed down with massive accumulation of ssDNA gaps leading, driven mainly by inefficient post-replicative repair. This results in severe replication stress signaling involving ATR and DNA-PK which causes cell death. On the other hand, ALC1 KO sensitivity towards PARPi is a consequence of the loss of ALC1's role in regulating PARP1 dynamics at sites of DNA damage. Active ADP-ribosylation could still facilitate PARP1 release from sites of DNA lesions even in genetic backgrounds where ALC1 is missing. Importantly, in case of PARPi treatment, ALC1 loss along with inhibition of ADP-ribosylation lead to enhanced retention of

PARP1 at the damage site, hindering recruitment of repair factors and causing persistence of DNA lesions and eventually cell death (**Fig. 23**).

Finally, this work represents an effort to expand our understanding of targeted cancer therapy with PARPi by exploring how sensitivity to these drugs can be induced by targeting different genes. While both ALC1 KO and POLE4 KO demonstrate HR-independent PARPi sensitivity that could be helpful to evade acquired resistance due to HR restoration, the underlying molecular mechanisms for this sensitivity are different. This offers clear insight into the intertwined nature of the mechanisms by which PARPi induce cytotoxicity. Yet, it projects the promising possibilities to expand the applicability of these inhibitors to uncharted territories in the context of cancer treatment.

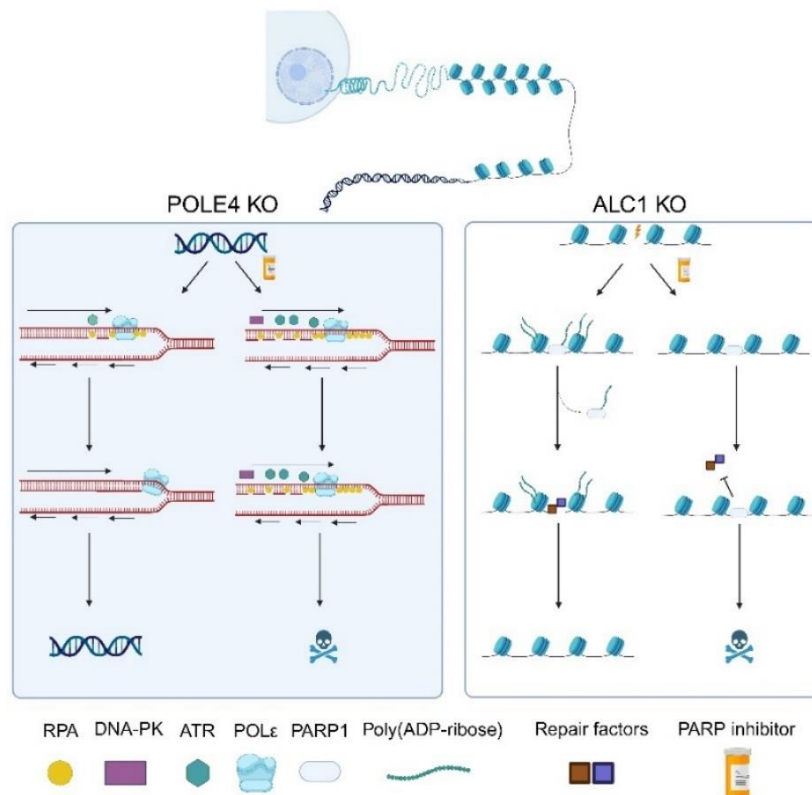


Figure 23: Distinct mechanisms driving PARPi sensitivity in POLE4- and ALC1- deficient cells

In POLE4 KO replication speed is reduced due to decreased processivity of the Pol ϵ complex, leading to mild replication stress, nevertheless, cells recover from it. However, PARPi treatment causes huge elevation of ssDNA gaps, therefore, exacerbating the replication stress phenotypes in POLE4 KO, driven mainly by ATR and DNA-PK, which eventually results in cell death. On the other hand, ALC1 KO susceptibility to PARPi is due to impaired PARP1 dynamics at DNA lesions. When DNA damage occurs in ALC1 KO, PARP1 can be still mobilized - albeit to a slower rate - due to ADP-ribosylation, facilitating repair of the lesion and cell survival. When the cells are challenged with PARPi, ALC1 loss accompanied by abolishing of ADP-ribosylation potentiate PARP1 trapping at the DNA lesions, preventing recruitment of repair factors and leading to accumulation of double-strand breaks and cell death.

6. Summary

The ultimate goal of cancer therapy is to eliminate malignant cells with minimum side effects. This can be better achieved by targeting certain pathways that are essential for the tumor rather than using cytotoxic agents which kill cells indiscriminately. Moreover, the advancements in genomics allowed for investigating the genetic background of tumors to identify the genetic alterations underlying tumorigenesis in each patient and determine the best therapeutic strategy, an approach known as personalized medicine.

The best representation of personalized medicine in the context of cancer treatment, is the exploitation of a phenomenon called synthetic lethality, where two mutations with viable phenotype for each one of them cause lethality if they are present together. As such, identifying pathways or genetic alterations that underlie tumor formation and targeting their synthetic lethal partners represents a promising therapeutic approach. This rationale paved the way for the discovery of the synthetic lethal interaction between Breast Cancer Susceptibility protein (BRCA) and PARP inhibitors (PARPi).

BRCA1 and BRCA2 are tumor suppressors crucial for the functionality of the double strand breaks (DSB) repair pathway, homologous recombination (HR) which ensures faithful repair of these lesions, therefore, preserving genomic integrity. Loss of either BRCA1 or BRCA2 impairs HR and predisposes to several cancers, mainly breast and ovarian cancers.

PARPi mainly inhibit an enzyme called PARP1. PARP1 catalyzes the posttranslational modification, ADP-ribosylation. Moreover, it has a crucial role in the repair of single-stranded DNA (ssDNA) breaks. Upon damage induction, PARP1 recruits to the site of DNA damage and mediates ADP-ribosylation of itself and nearby proteins, resulting in chromatin relaxation and facilitating recruitment of DNA repair factors, before its timely dissociation from the lesion site. PARPi not only block ADP-ribosylation, but also increase the retention time of PARP1 at the damage site causing a so-called “PARP trapping” phenomenon. The “trapped PARP1” at the site of DNA lesion hinders its repair and could be transformed to DSB upon collision with ongoing replication forks. These DSB can be faithfully repaired through HR. However, in HR-deficient backgrounds, such as BRCA1- or BRCA2-deficient

tumors, the cells rely on the error-prone non-homologous end joining (NHEJ) pathway to repair the DSB, leading to genomic instability and eventually cell death.

This model explains the synthetic lethal interaction between BRCA deficiency and PARPi treatment which led to the FDA-approval of PARPi to be used in the clinics to treat patients of breast and ovarian cancers with BRCA-deficiency. Continuous research allowed for the expansion of PARPi usage to tumors that are deficient of HR regardless of their BRCA status, a term known as BRCAness. Although PARPi have improved treatment outcomes for patients significantly, cases of acquired resistance started to emerge. Extensive research have identified different molecular mechanisms that could underlie PARPi resistance. Importantly, restoration of HR functionality is the main resistance mechanism that was identified not only at the bench but also in clinical cases. Altogether, efforts have been focused on identifying genetic alterations that could enhance PARPi sensitivity and overcome acquired resistance.

To identify genetic targets that could be used to induce sensitivity to PARPi treatment, we carried out previously a genome-wide CRISPR knockout screen with the PARPi, Olaparib. This approach permitted the identification of a large dataset of genes, which when knocked out, the cells become sensitive to Olaparib. Among these genes are the oncogenic chromatin remodeler ALC1, and the accessory subunits of DNA polymerase epsilon POLE3 and POLE4.

In this work, we utilized CRISPR/Cas9 technology to generate ALC1 KO, POLE3 KO and POLE4 KO cells, we also validated their sensitivity to different clinically-approved PARPi and demonstrated that this sensitivity depended on the presence of PARP1 as the main target of these inhibitors. Furthermore, we investigated the molecular mechanisms by which loss of ALC1 or POLE4 resulted in PARPi sensitivity.

ALC1 is a chromatin remodeler directly recruited to the sites of DNA damage by active ADP-ribosylation to facilitate chromatin relaxation allowing for repair factors to be recruited and mediate the resolving of genomic lesions. Moreover, ALC1 is an oncogene that is overexpressed in different types of cancer and associated with poor prognosis. In this project, we revealed that knocking out ALC1 impaired the release of PARP1 from the sites of DNA damage. This phenotype was further potentiated when PARPi were introduced, resulting in enhanced PARP1 trapping on the chromatin which hindered the repair of DNA lesions

leading to accumulation of DSB which underlined the cytotoxicity of PARPi in ALC1 KO. Importantly, we demonstrated that ALC1 functioned upstream of the DSB repair choice between HR and NHEJ, therefore, restoration of HR functionality, a common mechanism of PARPi resistance, did not rescue PARPi sensitivity in ALC1 KO cells. Additionally, we uncovered that ALC1 overexpression, a phenomenon observed in several cancers, induced PARPi resistance. This observation is crucial to direct medical intervention in these tumors to ensure maximum and timely benefits for the patients.

Similar to ALC1 KO, sensitivity of POLE4 KO to PARPi was HR-independent. Along with this notion, we proved that targeting both POLE4 and BRCA1 enhanced PARPi sensitivity and bypassed acquired resistance associated with rewiring of HR pathway. A phenotype that could hold significant implications for clinical applications. Mechanistically, we illustrated that while POLE4 did not impact PARP1 dynamics on the sites of DNA damage, it held an important role in replication stress tolerance. Loss of POLE4 slowed down replication speed and resulted in replication stress and upregulation of ATR activity. These phenotypes were further exacerbated upon PARPi treatment leading to replication catastrophe phenotype mediated by increased activity of both ATR and DNA-PK. Importantly, we revealed that POLE4 KO suffering from replication stress are sensitive to ATR inhibitor and combining both Olaparib and ATRi caused premature mitotic entry of stressed POLE4 KO which had synergistic killing effect on these cells.

Taken together, this work identified genetic alterations that modulate PARPi sensitivity and postulated the molecular mechanisms underlying this modulation. Beside the importance of these discoveries in terms of understanding mechanisms of PARPi sensitivity and resistance, they could hold significant clinical benefits, either by probing for these genetic alterations in tumor samples to facilitate informed medical interventions, or by potentially encouraging the development of novel inhibitors against these genes.

7. Összefoglaló

A rákterápiák célja a rosszindulatú sejtek eltávolítása úgy, hogy közben a lehető legkevesebb mellékhatást okozzák. Sajnos, a citotoxikus szerek általában nem tesznek különbséget az egészséges és transzformált sejtek között, válogatás nélkül pusztítják el az osztódó sejteket. Ezért célszerűbb új típusú terápiák kifejlesztése, amelyek a tumorsejtek számára nélkülözhetetlen útvonalakat specifikusan gátolják. A genomika fejlődése lehetővé tette a daganatok genetikai hátterének vizsgálatát, az egyes betegekben bekövetkező genetikai változások meghatározását, aminek köszönhetően kiválasztható a legalkalmasabb terápiás stratégia és megvalósítható a személyre szabott orvoslás.

A személyre szabott orvoslás legjobb példája a szintetikus letalitásnak nevezett jelenség kiaknázása. A szintetikus letalitás alapja, hogy két, önmagában életképes fenotípusú mutáció együttesen sejtthalált okoz. Ha sikerül azonosítani a tumorfejlődéshez vezető útvonalakat, genetikai változásokat és megtalálni szintetikus letális partnereiket, akkor azok gátlása ígéretes terápiás megközelítés lehet. Sikertörténetként említhetjük az emlőrákra érzékenyítő fehérje (Breast Cancer Susceptibility Protein, BRCA) és a PARP inhibitorok (PARPi) közötti szintetikus halálos kölcsönhatás azonosítását, amely megnyitotta az utat a PARPi klinikai használata előtt. A BRCA1 és BRCA2 tumorszuppresszorok, amelyek elengedhetetlenek a DNS kettős száltörés (DSB) javítási útvonalának, a homológ rekombinációnak (HR) működéséhez. A HR biztosítja ezeknek a sérüléseknek hibamentes javítását és ez által megőrzi a genomi integritást. A BRCA1 vagy BRCA2 mutációi esetében a HR útvonal károsodik, ami számos ráktípusra, főként emlő- és petefészekrákra hajlamosít. A PARPi elsősorban a PARP1 nevű enzimet gátolja. A PARP1 katalizálja az ADP-ribozilációt, ami fehérjék és nukleinsavak poszttranszlációs módosítása. A PARP1 döntő szerepet játszik az egyszálú DNS (ssDNS) törések javításában: a DNS-károsodás helyére toborozódik, ezáltal aktiválódik, önmagát és más fehérjéket ADP-ribozilál. Ennek hatására a kromatin fellazul, a PARP1 disszociál a DNS sérülés helyéről, míg más DNS hibajavító faktorok odakötődnek és aktiválódnak. A PARPi nemcsak blokkolja az ADP-ribozilációt, hanem növeli a PARP1 retenciós idejét a károsodás helyén, ami úgynevezett "PARP csapdázási" jelenséget okoz. A DNS-lézió helyén lévő "csapdába esett PARP1" akadályozza annak javítását, és a folyamatban lévő replikációs villákkal való ütközés esetén DSB-vé alakulhat. Ezek a DSB-

k hibamentesen javíthatók a HR-val, de a BRCA1- vagy BRCA2-hiányos daganatokban a sejtek a hibára hajlamos nem homolog végcsatlakozási (NHEJ) útvonalra támaszkodnak a DSB javításához, ami genomi instabilitáshoz és végül sejthalálhoz vezet. Ezzel a modellel magyarázható a BRCA-hiány és a PARPi-kezelés közötti szintetikus halálos kölcsönhatás, ennek alapján hagyta jóvá az Egyesült Államok Élelmiszer- és Gyógyszerügyi Hivatala (Food and Drug Administration, FDA) a BRCA-hiányos emlő- és petefészekrákos betegek PARPi kezelését. Az intenzív kutatásoknak köszönhetően a PARPi használata kiterjeszhető egyéb olyan daganatokra is, amelyekben a HR útvonal a BRCA státuszuktól függetlenül hiányos. Habár a PARPi jelentősen javította a betegek terápiás esélyeit, bizonyos esetekben ún. szerzett rezisztencia alakulhat ki. A PARPi rezisztencia alapját képező különböző molekuláris mechanizmusok azonosítása érdekében kiterjedt kutatások folynak. A fő mechanizmusnak a HR funkcionalitás helyreállítása bizonyul, amelyet nemcsak laboratóriumi kísérletekben, de klinikai esetekben is azonosítottak. Hatalmas erőfeszítések folynak olyan genetikai változások azonosítására, amelyek növelhetik a PARPi érzékenységet és leküzdhetik a szerzett rezisztenciát.

Annak érdekében, hogy új genetikai célpontokat azonosítsunk a PARPi-kezeléssel szembeni érzékenység kiváltásához, genomszintű CRISPR knockout szűrést végeztünk egy PARPi, az Olaparib segítségével. Ezzel a megközelítéssel azonosítottuk azt a génkészletet, amelyek kiütésekor a sejtek érzékennyé válnak Olaparibra. Ezek közé a gének közé tartozik a kromatin-átrendezőben részt vevő onkogén fehérje, az ALC1, valamint a DNS-polimeráz epsilon POLE3 és POLE4 járulékos alegységei.

Jelen munkában CRISPR/Cas9 technológiát alkalmaztunk ALC1, POLE3 és POLE4 hiányos sejtek (KO) előállítására, validáltuk érzékenységüket különböző klinikailag jóváhagyott PARPi-ra, és kimutattuk, hogy ez az érzékenység a PARP1 jelenlététől függ. Továbbá megvizsgáltuk azokat a molekuláris mechanizmusokat, amelyek révén az ALC1 vagy POLE4 elvesztése PARPi érzékenységet eredményezett. Az ALC1 egy kromatin átrendező fehérje, amely a poli-ADP-ribóz közvetlen kötése révén felhalmozódik a DNS-károsodás helyszínén, ahol a kromatin fellazításával lehetővé válik a DNS hibajavító faktorok kötődése és a genomikus léziók helyreállítása. Az ALC1 onkogénnek tekinthető, amely túltermelődése a különböző ráktípusban rossz prognózissal jár. Ebben a projektben feltártuk, hogy az ALC1

hiányában lassul a PARP1 leválása a DNS-károsodás helyéről. Ez a fenotípus tovább erősödik a PARPi jelenlétében, ami fokozott PARP1 csapdázást eredményez a kromatinon, akadályozva a DNS-léziók javítását, DSB felhalmozódáshoz vezet, végül sejthalált vált ki az ALC1 KO-ban. Kimutattuk, hogy az ALC1 a HR és az NHEJ hibajavítási útvonalak közötti választást megelőzően működik, ezért a HR működésének helyreállítása, ami PARPi rezisztencia alapja, nem mentette meg az ALC1 hiányos sejteket a PARPi-okozta sejthaláltól. Ezen kívül feltártuk, hogy az ALC1 túlműködése, amely számos rákban megfigyelhető jelenség, PARPi rezisztenciához vezet. Ez a megfigyelés hozzájárul ahhoz, hogy ezekben a daganatokban az ALC1 célzásával közvetlen és előnyös orvosi beavatkozást végezzenek. Az ALC1 KO-hoz hasonlóan a POLE4 KO PARPi-ra való érzékenysége is HR-független. Kimutattuk, hogy mind a POLE4, mind a BRCA1 gátlása növelte a PARPi érzékenységet, ráadásul a POLE4 hiánya esetén a HR útvonal újrarahozásával járó szerzett ellenállás is megkerülhető. Ennek a fenotípusnak nagy jelentősége lehet a klinikai alkalmazásokban. A molekuláris mechanizmust illetően kimutattuk, hogy bár a POLE4 nem befolyásolja a PARP1 dinamikáját a DNS-károsodás helyén, de fontos szerepet játszik a replikációs stressz kivédésében. A POLE4 elvesztése lelassítja a replikációs sebességet, replikációs stresszhez és az ATR (Ataxia-telangiectasia mutated and RAD3-related) kináz aktiválódásához vezet. Ezek a folyamatok tovább erősödtek a PARPi kezelés hatására, ami replikációs katasztrófához vezetett, amelyben mind az ATR, mind a DNA-PK (DNA-dependent protein kinase) fokozott aktivitása szerepet játszott. Emellett kimutattuk, hogy a replikációs stresszben szenvedő POLE4 KO érzékeny az ATR kináz gátlószerére (ATRi), valamint az Olaparib és az ATRi kombinálása a POLE4 KO sejteknek a mitózisba való korai belépését okozza, és ez által szinergikusan gyilkos hatást gyakorol ezekre a sejtekre.

Összefoglalva, jelen munkában olyan genetikai változásokat azonosítottunk, amelyek fokozzák a PARPi érzékenységet, és megállapítottuk a szenzitivitás alapjául szolgáló molekuláris mechanizmusokat. Amellett, hogy ezek a felfedezések fontosak a PARPi érzékenység és rezisztencia mechanizmusainak megértése szempontjából, jelentős klinikai előnyökkel járhatnak, akár azáltal, hogy ezekre a genetikai változásokra szűrve lehetővé teszik a személyre szabott orvosi beavatkozásokat, vagy potenciálisan ösztönzik új inhibitorok kifejlesztését ezen gének ellen.

8. Acknowledgment

I would like to express my sincere gratitude to my supervisor, Dr. Gyula Timinszky, for giving me the opportunity to work on this exciting topic, and for his unwavering support, and continuous encouragement throughout my doctoral studies. His expertise, patience, scientific curiosity and insightful feedback have been instrumental in shaping this work and my scientific journey.

I also would like to thank my co-supervisor, Dr. Roberta Fajka-Boja for her significant contributions to this work. Her extensive knowledge, technical skills, and scientific rigor were an example to follow throughout this doctoral journey.

I extend my sincere thanks to the members of our research group for their support and shared enthusiasm. Their contributions and discussions have enriched this research and made the academic environment stimulating and enjoyable.

I am also grateful for our collaborators who participated in this work for sharing their expertise, time and resources to contribute to the completion of this study, and I would like to highlight Prof. Sébastien Huet at the Institut de génétique et développement de Rennes and Dr. Andrew Bowman at Warwick medical school for hosting me in their labs as part of an EMBO advanced collaboration grant (10265) and providing the possibility to learn essential techniques.

My appreciation is extended to Dr. Éva Bálint and Dr. Péter Burkovics for dedicating their time to review and improve my PhD thesis and to be part of my process to obtain the degree.

I would like to acknowledge the support from the Institute of Genetics of the Biological Research Centre and its administration for providing the infrastructure and financial support which were crucial to complete this work.

I am also grateful to the Faculty of Science and Informatics and the Doctoral School of Biology of the University of Szeged, including all the teaching staff and administrators for making every possible effort to ensure my ability to pursue my doctoral studies.

My heartfelt appreciation and love go to my family not only for their support and encouragement all the way but importantly for planting the seeds of scientific curiosity providing the basis upon which my academic accomplishments have been built.

Last but certainly not least, my love and gratitude are to those who were always there for me providing support, advice, joy and love especially (Dina, Hani, Erika, Mahmood, Huda, Tamam, George and Monzer).

The work was supported by the National Research Development and Innovation Office (K143248) and (K128239), the Hungarian Academy of Sciences (LP2017-11/2017), as well as an EMBO advanced collaboration grant (10265).

9. References

1. Hajdu,S.I. (2011) A note from history: landmarks in history of cancer, part 1. *Cancer*, **117**, 1097–1102.
2. Faguet,G.B. (2015) A brief history of cancer: age-old milestones underlying our current knowledge database. *Int J Cancer*, **136**, 2022–2036.
3. DeVita,V.T. and Chu,E. (2008) A history of cancer chemotherapy. *Cancer Res*, **68**, 8643–8653.
4. Hanahan,D. and Weinberg,R.A. (2000) The hallmarks of cancer. *Cell*, **100**, 57–70.
5. Hanahan,D. and Weinberg,R.A. (2011) Hallmarks of cancer: the next generation. *Cell*, **144**, 646–674.
6. Fouad,Y.A. and Aanei,C. (2017) Revisiting the hallmarks of cancer. *Am J Cancer Res*, **7**, 1016–1036.
7. Ginsburg,G.S. and McCarthy,J.J. (2001) Personalized medicine: revolutionizing drug discovery and patient care. *Trends Biotechnol*, **19**, 491–496.
8. Personalized Medicine. <https://www.genome.gov/genetics-glossary/Personalized-Medicine>
9. Krzyszczyk,P., Acevedo,A., Davidoff,E.J., Timmins,L.M., Marrero-Berrios,I., Patel,M., White,C., Lowe,C., Sherba,J.J., Hartmanshenn,C., *et al.* (2018) The growing role of precision and personalized medicine for cancer treatment. *Technology (Singap World Sci)*, **6**, 79–100.
10. Pagliarini,R., Shao,W. and Sellers,W.R. (2015) Oncogene addiction: pathways of therapeutic response, resistance, and road maps toward a cure. *EMBO Rep*, **16**, 280–296.
11. O’Neil,N.J., Bailey,M.L. and Hieter,P. (2017) Synthetic lethality and cancer. *Nat Rev Genet*, **18**, 613–623.
12. Lucchesi,J.C. (1968) Synthetic lethality and semi-lethality among functionally related mutants of *Drosophila melanogaster*. *Genetics*, **59**, 37–44.
13. Bender,A. and Pringle,J.R. (1991) Use of a screen for synthetic lethal and multicopy suppressor mutants to identify two new genes involved in morphogenesis in *Saccharomyces cerevisiae*. *Mol Cell Biol*, **11**, 1295–1305.
14. Hartwell,L.H., Szankasi,P., Roberts,C.J., Murray,A.W. and Friend,S.H. (1997) Integrating genetic approaches into the discovery of anticancer drugs. *Science*, **278**, 1064–1068.

15. Ryan,C.J., Bajrami,I. and Lord,C.J. (2018) Synthetic Lethality and Cancer - Penetrance as the Major Barrier. *Trends Cancer*, **4**, 671–683.
16. Bryant,H.E., Schultz,N., Thomas,H.D., Parker,K.M., Flower,D., Lopez,E., Kyle,S., Meuth,M., Curtin,N.J. and Helleday,T. (2005) Specific killing of BRCA2-deficient tumours with inhibitors of poly(ADP-ribose) polymerase. *Nature*, **434**, 913–917.
17. Farmer,H., McCabe,N., Lord,C.J., Tutt,A.N.J., Johnson,D.A., Richardson,T.B., Santarosa,M., Dillon,K.J., Hickson,I., Knights,C., *et al.* (2005) Targeting the DNA repair defect in BRCA mutant cells as a therapeutic strategy. *Nature*, **434**, 917–921.
18. Tubbs,A. and Nussenzweig,A. (2017) Endogenous DNA Damage as a Source of Genomic Instability in Cancer. *Cell*, **168**, 644–656.
19. Loeb,L.A. and Harris,C.C. (2008) Advances in chemical carcinogenesis: a historical review and prospective. *Cancer Res*, **68**, 6863–6872.
20. Saxena,S. and Zou,L. (2022) Hallmarks of DNA replication stress. *Mol Cell*, **82**, 2298–2314.
21. Prakash,R., Zhang,Y., Feng,W. and Jasin,M. (2015) Homologous recombination and human health: the roles of BRCA1, BRCA2, and associated proteins. *Cold Spring Harb Perspect Biol*, **7**, a016600.
22. Daley,J.M., Niu,H., Miller,A.S. and Sung,P. (2015) Biochemical mechanism of DSB end resection and its regulation. *DNA Repair (Amst)*, **32**, 66–74.
23. Verma,P. and Greenberg,R.A. (2016) Noncanonical views of homology-directed DNA repair. *Genes Dev*, **30**, 1138–1154.
24. Blackford,A.N. and Jackson,S.P. (2017) ATM, ATR, and DNA-PK: The Trinity at the Heart of the DNA Damage Response. *Mol Cell*, **66**, 801–817.
25. San Filippo,J., Sung,P. and Klein,H. (2008) Mechanism of eukaryotic homologous recombination. *Annu Rev Biochem*, **77**, 229–257.
26. Feng,W. and Jasin,M. (2017) Homologous Recombination and Replication Fork Protection: BRCA2 and More! *Cold Spring Harb Symp Quant Biol*, **82**, 329–338.
27. Rickman,K. and Smogorzewska,A. (2019) Advances in understanding DNA processing and protection at stalled replication forks. *J Cell Biol*, **218**, 1096–1107.
28. Ira,G., Pelliccioli,A., Balijja,A., Wang,X., Fiorani,S., Carotenuto,W., Liberi,G., Bressan,D., Wan,L., Hollingsworth,N.M., *et al.* (2004) DNA end resection, homologous recombination and DNA damage checkpoint activation require CDK1. *Nature*, **431**, 1011–1017.

29. Huertas,P., Cortés-Ledesma,F., Sartori,A.A., Aguilera,A. and Jackson,S.P. (2008) CDK targets Sae2 to control DNA-end resection and homologous recombination. *Nature*, **455**, 689–692.
30. Sharan,S.K., Morimatsu,M., Albrecht,U., Lim,D.S., Regel,E., Dinh,C., Sands,A., Eichele,G., Hasty,P. and Bradley,A. (1997) Embryonic lethality and radiation hypersensitivity mediated by Rad51 in mice lacking Brca2. *Nature*, **386**, 804–810.
31. Yu,V.P., Koehler,M., Steinlein,C., Schmid,M., Hanakahi,L.A., van Gool,A.J., West,S.C. and Venkitaraman,A.R. (2000) Gross chromosomal rearrangements and genetic exchange between nonhomologous chromosomes following BRCA2 inactivation. *Genes Dev*, **14**, 1400–1406.
32. Jensen,R.B., Carreira,A. and Kowalczykowski,S.C. (2010) Purified human BRCA2 stimulates RAD51-mediated recombination. *Nature*, **467**, 678–683.
33. Liu,J., Doty,T., Gibson,B. and Heyer,W.-D. (2010) Human BRCA2 protein promotes RAD51 filament formation on RPA-covered single-stranded DNA. *Nat Struct Mol Biol*, **17**, 1260–1262.
34. Thorslund,T., McIlwraith,M.J., Compton,S.A., Lekomtsev,S., Petronczki,M., Griffith,J.D. and West,S.C. (2010) The breast cancer tumor suppressor BRCA2 promotes the specific targeting of RAD51 to single-stranded DNA. *Nat Struct Mol Biol*, **17**, 1263–1265.
35. Sung,P. and Klein,H. (2006) Mechanism of homologous recombination: mediators and helicases take on regulatory functions. *Nat Rev Mol Cell Biol*, **7**, 739–750.
36. Mazin,A.V., Zaitseva,E., Sung,P. and Kowalczykowski,S.C. (2000) Tailed duplex DNA is the preferred substrate for Rad51 protein-mediated homologous pairing. *EMBO J*, **19**, 1148–1156.
37. Baumann,P., Benson,F.E. and West,S.C. (1996) Human Rad51 protein promotes ATP-dependent homologous pairing and strand transfer reactions in vitro. *Cell*, **87**, 757–766.
38. Carreira,A., Hilario,J., Amitani,I., Baskin,R.J., Shivji,M.K.K., Venkitaraman,A.R. and Kowalczykowski,S.C. (2009) The BRC repeats of BRCA2 modulate the DNA-binding selectivity of RAD51. *Cell*, **136**, 1032–1043.
39. Solinger,J.A., Kiiianitsa,K. and Heyer,W.-D. (2002) Rad54, a Swi2/Snf2-like recombinational repair protein, disassembles Rad51:dsDNA filaments. *Mol Cell*, **10**, 1175–1188.
40. Sung,P. and Robberson,D.L. (1995) DNA strand exchange mediated by a RAD51-ssDNA nucleoprotein filament with polarity opposite to that of RecA. *Cell*, **82**, 453–461.

41. Scully,R., Chen,J., Plug,A., Xiao,Y., Weaver,D., Feunteun,J., Ashley,T. and Livingston,D.M. (1997) Association of BRCA1 with Rad51 in mitotic and meiotic cells. *Cell*, **88**, 265–275.
42. Bhattacharyya,A., Ear,U.S., Koller,B.H., Weichselbaum,R.R. and Bishop,D.K. (2000) The breast cancer susceptibility gene BRCA1 is required for subnuclear assembly of Rad51 and survival following treatment with the DNA cross-linking agent cisplatin. *J Biol Chem*, **275**, 23899–23903.
43. Huber,L.J., Yang,T.W., Sarkisian,C.J., Master,S.R., Deng,C.X. and Chodosh,L.A. (2001) Impaired DNA damage response in cells expressing an exon 11-deleted murine Brca1 variant that localizes to nuclear foci. *Mol Cell Biol*, **21**, 4005–4015.
44. Wu,W., Nishikawa,H., Fukuda,T., Vittal,V., Asano,M., Miyoshi,Y., Kleivit,R.E. and Ohta,T. (2015) Interaction of BARD1 and HP1 Is Required for BRCA1 Retention at Sites of DNA Damage. *Cancer Res*, **75**, 1311–1321.
45. Zhong,Q., Chen,C.F., Li,S., Chen,Y., Wang,C.C., Xiao,J., Chen,P.L., Sharp,Z.D. and Lee,W.H. (1999) Association of BRCA1 with the hRad50-hMre11-p95 complex and the DNA damage response. *Science*, **285**, 747–750.
46. Moynahan,M.E., Pierce,A.J. and Jasin,M. (2001) BRCA2 is required for homology-directed repair of chromosomal breaks. *Mol Cell*, **7**, 263–272.
47. Xia,F., Taghian,D.G., DeFrank,J.S., Zeng,Z.C., Willers,H., Iliakis,G. and Powell,S.N. (2001) Deficiency of human BRCA2 leads to impaired homologous recombination but maintains normal nonhomologous end joining. *Proc Natl Acad Sci U S A*, **98**, 8644–8649.
48. Tarsounas,M. and Sung,P. (2020) The antitumorigenic roles of BRCA1-BARD1 in DNA repair and replication. *Nat Rev Mol Cell Biol*, **21**, 284–299.
49. Wong,A.K., Pero,R., Ormonde,P.A., Tavtigian,S.V. and Bartel,P.L. (1997) RAD51 interacts with the evolutionarily conserved BRC motifs in the human breast cancer susceptibility gene brca2. *J Biol Chem*, **272**, 31941–31944.
50. Malacaria,E., Honda,M., Franchitto,A., Spies,M. and Pichierri,P. (2020) Physiological and Pathological Roles of RAD52 at DNA Replication Forks. *Cancers (Basel)*, **12**, 402.
51. Sugiyama,T., Kantake,N., Wu,Y. and Kowalczykowski,S.C. (2006) Rad52-mediated DNA annealing after Rad51-mediated DNA strand exchange promotes second ssDNA capture. *EMBO J*, **25**, 5539–5548.
52. Liao,H., Ji,F., Helleday,T. and Ying,S. (2018) Mechanisms for stalled replication fork stabilization: new targets for synthetic lethality strategies in cancer treatments. *EMBO Rep*, **19**, e46263.

53. Li,X. and Heyer,W.-D. (2008) Homologous recombination in DNA repair and DNA damage tolerance. *Cell Res*, **18**, 99–113.
54. Zellweger,R., Dalcher,D., Mutreja,K., Berti,M., Schmid,J.A., Herrador,R., Vindigni,A. and Lopes,M. (2015) Rad51-mediated replication fork reversal is a global response to genotoxic treatments in human cells. *J Cell Biol*, **208**, 563–579.
55. Chen,C.-C., Feng,W., Lim,P.X., Kass,E.M. and Jasin,M. (2018) Homology-Directed Repair and the Role of BRCA1, BRCA2, and Related Proteins in Genome Integrity and Cancer. *Annu Rev Cancer Biol*, **2**, 313–336.
56. Scully,R., Chen,J., Ochs,R.L., Keegan,K., Hoekstra,M., Feunteun,J. and Livingston,D.M. (1997) Dynamic changes of BRCA1 subnuclear location and phosphorylation state are initiated by DNA damage. *Cell*, **90**, 425–435.
57. Wang,Y., Cortez,D., Yazdi,P., Neff,N., Elledge,S.J. and Qin,J. (2000) BASC, a super complex of BRCA1-associated proteins involved in the recognition and repair of aberrant DNA structures. *Genes Dev*, **14**, 927–939.
58. Schlacher,K., Christ,N., Siaud,N., Egashira,A., Wu,H. and Jasin,M. (2011) Double-strand break repair-independent role for BRCA2 in blocking stalled replication fork degradation by MRE11. *Cell*, **145**, 529–542.
59. Taglialatela,A., Alvarez,S., Leuzzi,G., Sannino,V., Ranjha,L., Huang,J.-W., Madubata,C., Anand,R., Levy,B., Rabadan,R., *et al.* (2017) Restoration of Replication Fork Stability in BRCA1- and BRCA2-Deficient Cells by Inactivation of SNF2-Family Fork Remodelers. *Mol Cell*, **68**, 414-430.e8.
60. Liu,W., Krishnamoorthy,A., Zhao,R. and Cortez,D. (2020) Two replication fork remodeling pathways generate nuclease substrates for distinct fork protection factors. *Sci Adv*, **6**, eabc3598.
61. Lemaçon,D., Jackson,J., Quinet,A., Brickner,J.R., Li,S., Yazinski,S., You,Z., Ira,G., Zou,L., Mosammaparast,N., *et al.* (2017) MRE11 and EXO1 nucleases degrade reversed forks and elicit MUS81-dependent fork rescue in BRCA2-deficient cells. *Nat Commun*, **8**, 860.
62. Mijic,S., Zellweger,R., Chappidi,N., Berti,M., Jacobs,K., Mutreja,K., Ursich,S., Ray Chaudhuri,A., Nussenzweig,A., Janscak,P., *et al.* (2017) Replication fork reversal triggers fork degradation in BRCA2-defective cells. *Nat Commun*, **8**, 859.
63. Ying,S., Hamdy,F.C. and Helleday,T. (2012) Mre11-dependent degradation of stalled DNA replication forks is prevented by BRCA2 and PARP1. *Cancer Res*, **72**, 2814–2821.
64. Ray Chaudhuri,A., Callen,E., Ding,X., Gogola,E., Duarte,A.A., Lee,J.-E., Wong,N., Lafarga,V., Calvo,J.A., Panzarino,N.J., *et al.* (2016) Replication fork stability confers chemoresistance in BRCA-deficient cells. *Nature*, **535**, 382–387.

65. Murphy,A.K., Fitzgerald,M., Ro,T., Kim,J.H., Rabinowitsch,A.I., Chowdhury,D., Schildkraut,C.L. and Borowiec,J.A. (2014) Phosphorylated RPA recruits PALB2 to stalled DNA replication forks to facilitate fork recovery. *J Cell Biol*, **206**, 493–507.
66. Buisson,R., Niraj,J., Pauty,J., Maity,R., Zhao,W., Coulombe,Y., Sung,P. and Masson,J.-Y. (2014) Breast cancer proteins PALB2 and BRCA2 stimulate polymerase η in recombination-associated DNA synthesis at blocked replication forks. *Cell Rep*, **6**, 553–564.
67. Hamperl,S. and Cimprich,K.A. (2016) Conflict Resolution in the Genome: How Transcription and Replication Make It Work. *Cell*, **167**, 1455–1467.
68. Hatchi,E., Skourti-Stathaki,K., Ventz,S., Pinello,L., Yen,A., Kamieniarz-Gdula,K., Dimitrov,S., Pathania,S., McKinney,K.M., Eaton,M.L., *et al.* (2015) BRCA1 recruitment to transcriptional pause sites is required for R-loop-driven DNA damage repair. *Mol Cell*, **57**, 636–647.
69. Hill,S.J., Rolland,T., Adelmant,G., Xia,X., Owen,M.S., Dricot,A., Zack,T.I., Sahni,N., Jacob,Y., Hao,T., *et al.* (2014) Systematic screening reveals a role for BRCA1 in the response to transcription-associated DNA damage. *Genes Dev*, **28**, 1957–1975.
70. Tacconi,E.M., Lai,X., Folio,C., Porru,M., Zonderland,G., Badie,S., Michl,J., Sechi,I., Rogier,M., Matía García,V., *et al.* (2017) BRCA1 and BRCA2 tumor suppressors protect against endogenous acetaldehyde toxicity. *EMBO Mol Med*, **9**, 1398–1414.
71. Kim,H. and D’Andrea,A.D. (2012) Regulation of DNA cross-link repair by the Fanconi anemia/BRCA pathway. *Genes Dev*, **26**, 1393–1408.
72. Miki,Y., Swensen,J., Shattuck-Eidens,D., Futreal,P.A., Harshman,K., Tavtigian,S., Liu,Q., Cochran,C., Bennett,L.M. and Ding,W. (1994) A strong candidate for the breast and ovarian cancer susceptibility gene BRCA1. *Science*, **266**, 66–71.
73. Tavtigian,S.V., Simard,J., Rommens,J., Couch,F., Shattuck-Eidens,D., Neuhausen,S., Merajver,S., Thorlacius,S., Offit,K., Stoppa-Lyonnet,D., *et al.* (1996) The complete BRCA2 gene and mutations in chromosome 13q-linked kindreds. *Nat Genet*, **12**, 333–337.
74. Wooster,R., Neuhausen,S.L., Mangion,J., Quirk,Y., Ford,D., Collins,N., Nguyen,K., Seal,S., Tran,T. and Averill,D. (1994) Localization of a breast cancer susceptibility gene, BRCA2, to chromosome 13q12-13. *Science*, **265**, 2088–2090.
75. Chen,S. and Parmigiani,G. (2007) Meta-analysis of BRCA1 and BRCA2 penetrance. *J Clin Oncol*, **25**, 1329–1333.
76. Zhang,Y., Wang,J., Ding,M. and Yu,Y. (2013) Site-specific characterization of the Asp- and Glu-ADP-ribosylated proteome. *Nat Methods*, **10**, 981–984.

77. Palazzo,L., Leidecker,O., Prokhorova,E., Dauben,H., Matic,I. and Ahel,I. (2018) Serine is the major residue for ADP-ribosylation upon DNA damage. *Elife*, **7**, e34334.
78. Yan,F., Huang,C., Wang,X., Tan,J., Cheng,S., Wan,M., Wang,Z., Wang,S., Luo,S., Li,A., *et al.* (2020) Threonine ADP-Ribosylation of Ubiquitin by a Bacterial Effector Family Blocks Host Ubiquitination. *Mol Cell*, **78**, 641-652.e9.
79. Vandekerckhove,J., Schering,B., Bärman,M. and Aktories,K. (1987) Clostridium perfringens iota toxin ADP-ribosylates skeletal muscle actin in Arg-177. *FEBS Lett*, **225**, 48–52.
80. Koch-Nolte,F., Petersen,D., Balasubramanian,S., Haag,F., Kahlke,D., Willer,T., Kastelein,R., Bazan,F. and Thiele,H.G. (1996) Mouse T cell membrane proteins Rt6-1 and Rt6-2 are arginine/protein mono(ADPriboseyl)transferases and share secondary structure motifs with ADP-ribosylating bacterial toxins. *J Biol Chem*, **271**, 7686–7693.
81. Vyas,S., Matic,I., Uchima,L., Rood,J., Zaja,R., Hay,R.T., Ahel,I. and Chang,P. (2014) Family-wide analysis of poly(ADP-ribose) polymerase activity. *Nat Commun*, **5**, 4426.
82. Belousova,E.A., Ishchenko,A.A. and Lavrik,O.I. (2018) Dna is a New Target of Parp3. *Sci Rep*, **8**, 4176.
83. Gros Lambert,J., Prokhorova,E. and Ahel,I. (2021) ADP-ribosylation of DNA and RNA. *DNA Repair (Amst)*, **105**, 103144.
84. Munir,A., Banerjee,A. and Shuman,S. (2018) NAD⁺-dependent synthesis of a 5'-phospho-ADP-ribosylated RNA/DNA cap by RNA 2'-phosphotransferase Tpt1. *Nucleic Acids Res*, **46**, 9617–9624.
85. Munnur,D., Bartlett,E., Mikolčević,P., Kirby,I.T., Rack,J.G.M., Mikoč,A., Cohen,M.S. and Ahel,I. (2019) Reversible ADP-ribosylation of RNA. *Nucleic Acids Res*, **47**, 5658–5669.
86. Wolfram-Schauerte,M., Pozhydaieva,N., Grawenhoff,J., Welp,L.M., Silber,I., Wulf,A., Billau,F.A., Glatter,T., Urlaub,H., Jäschke,A., *et al.* (2023) A viral ADP-ribosyltransferase attaches RNA chains to host proteins. *Nature*, **620**, 1054–1062.
87. Lüscher,B., Ahel,I., Altmeyer,M., Ashworth,A., Bai,P., Chang,P., Cohen,M., Corda,D., Dantzer,F., Daugherty,M.D., *et al.* (2022) ADP-ribosyltransferases, an update on function and nomenclature. *FEBS J*, **289**, 7399–7410.
88. Cohen,M.S. and Chang,P. (2018) Insights into the biogenesis, function, and regulation of ADP-ribosylation. *Nat Chem Biol*, **14**, 236–243.
89. Barkauskaite,E., Brassington,A., Tan,E.S., Warwicker,J., Dunstan,M.S., Banos,B., Lafite,P., Ahel,M., Mitchison,T.J., Ahel,I., *et al.* (2013) Visualization of poly(ADP-

- ribose) bound to PARG reveals inherent balance between exo- and endo-glycohydrolase activities. *Nat Commun*, **4**, 2164.
90. Rack, J.G.M., Liu, Q., Zorzini, V., Voorneveld, J., Ariza, A., Honarmand Ebrahimi, K., Reber, J.M., Krassnig, S.C., Ahel, D., van der Marel, G.A., *et al.* (2021) Mechanistic insights into the three steps of poly(ADP-ribosylation) reversal. *Nat Commun*, **12**, 4581.
91. Slade, D., Dunstan, M.S., Barkauskaite, E., Weston, R., Lafite, P., Dixon, N., Ahel, M., Leys, D. and Ahel, I. (2011) The structure and catalytic mechanism of a poly(ADP-ribose) glycohydrolase. *Nature*, **477**, 616–620.
92. Sharifi, R., Morra, R., Appel, C.D., Tallis, M., Chioza, B., Jankevicius, G., Simpson, M.A., Matic, I., Ozkan, E., Golia, B., *et al.* (2013) Deficiency of terminal ADP-ribose protein glycohydrolase TARG1/C6orf130 in neurodegenerative disease. *EMBO J*, **32**, 1225–1237.
93. Jankevicius, G., Hassler, M., Golia, B., Rybin, V., Zacharias, M., Timinszky, G. and Ladurner, A.G. (2013) A family of macrodomain proteins reverses cellular mono-ADP-ribosylation. *Nat Struct Mol Biol*, **20**, 508–514.
94. Rosenthal, F., Feijs, K.L.H., Frugier, E., Bonalli, M., Forst, A.H., Imhof, R., Winkler, H.C., Fischer, D., Caflisch, A., Hassa, P.O., *et al.* (2013) Macrodomain-containing proteins are new mono-ADP-ribosylhydrolases. *Nat Struct Mol Biol*, **20**, 502–507.
95. Gupte, R., Liu, Z. and Kraus, W.L. (2017) PARPs and ADP-ribosylation: recent advances linking molecular functions to biological outcomes. *Genes Dev*, **31**, 101–126.
96. O’Sullivan, J., Tedim Ferreira, M., Gagné, J.-P., Sharma, A.K., Hendzel, M.J., Masson, J.-Y. and Poirier, G.G. (2019) Emerging roles of eraser enzymes in the dynamic control of protein ADP-ribosylation. *Nat Commun*, **10**, 1182.
97. Oka, S., Kato, J. and Moss, J. (2006) Identification and characterization of a mammalian 39-kDa poly(ADP-ribose) glycohydrolase. *J Biol Chem*, **281**, 705–713.
98. Fontana, P., Bonfiglio, J.J., Palazzo, L., Bartlett, E., Matic, I. and Ahel, I. (2017) Serine ADP-ribosylation reversal by the hydrolase ARH3. *Elife*, **6**, e28533.
99. Huang, D. and Kraus, W.L. (2022) The expanding universe of PARP1-mediated molecular and therapeutic mechanisms. *Mol Cell*, **82**, 2315–2334.
100. Caldecott, K.W. (2014) Protein ADP-ribosylation and the cellular response to DNA strand breaks. *DNA Repair (Amst)*, **19**, 108–113.
101. Smith, R., Zentout, S., Rother, M., Bigot, N., Chapuis, C., Mihut, A., Zobel, F.F., Ahel, I., van Attikum, H., Timinszky, G., *et al.* (2023) HPF1-dependent histone ADP-ribosylation triggers chromatin relaxation to promote the recruitment of repair factors at sites of DNA damage. *Nat Struct Mol Biol*, **30**, 678–691.

102. Ahel,D., Horejsí,Z., Wiechens,N., Polo,S.E., Garcia-Wilson,E., Ahel,I., Flynn,H., Skehel,M., West,S.C., Jackson,S.P., *et al.* (2009) Poly(ADP-ribose)-dependent regulation of DNA repair by the chromatin remodeling enzyme ALC1. *Science*, **325**, 1240–1243.
103. Gottschalk,A.J., Timinszky,G., Kong,S.E., Jin,J., Cai,Y., Swanson,S.K., Washburn,M.P., Florens,L., Ladurner,A.G., Conaway,J.W., *et al.* (2009) Poly(ADP-ribosylation) directs recruitment and activation of an ATP-dependent chromatin remodeler. *Proc Natl Acad Sci U S A*, **106**, 13770–13774.
104. Gibbs-Seymour,I., Fontana,P., Rack,J.G.M. and Ahel,I. (2016) HPF1/C4orf27 Is a PARP-1-Interacting Protein that Regulates PARP-1 ADP-Ribosylation Activity. *Mol Cell*, **62**, 432–442.
105. Maya-Mendoza,A., Moudry,P., Merchut-Maya,J.M., Lee,M., Strauss,R. and Bartek,J. (2018) High speed of fork progression induces DNA replication stress and genomic instability. *Nature*, **559**, 279–284.
106. Hanzlikova,H., Kalasova,I., Demin,A.A., Pennicott,L.E., Cihlarova,Z. and Caldecott,K.W. (2018) The Importance of Poly(ADP-Ribose) Polymerase as a Sensor of Unligated Okazaki Fragments during DNA Replication. *Mol Cell*, **71**, 319-331.e3.
107. Cong,K., Peng,M., Kousholt,A.N., Lee,W.T.C., Lee,S., Nayak,S., Krais,J., VanderVere-Carozza,P.S., Pawelczak,K.S., Calvo,J., *et al.* (2021) Replication gaps are a key determinant of PARP inhibitor synthetic lethality with BRCA deficiency. *Mol Cell*, **81**, 3227.
108. Simoneau,A., Xiong,R. and Zou,L. (2021) The trans cell cycle effects of PARP inhibitors underlie their selectivity toward BRCA1/2-deficient cells. *Genes Dev*, **35**, 1271–1289.
109. Suskiewicz,M.J., Prokhorova,E., Rack,J.G.M. and Ahel,I. (2023) ADP-ribosylation from molecular mechanisms to therapeutic implications. *Cell*, **186**, 4475–4495.
110. Curtin,N.J. and Szabo,C. (2020) Poly(ADP-ribose) polymerase inhibition: past, present and future. *Nat Rev Drug Discov*, **19**, 711–736.
111. Rudolph,J., Jung,K. and Luger,K. (2022) Inhibitors of PARP: Number crunching and structure gazing. *Proc Natl Acad Sci U S A*, **119**, e2121979119.
112. Curtin,N.J. (2005) PARP inhibitors for cancer therapy. *Expert Rev Mol Med*, **7**, 1–20.
113. Ferraris,D.V. (2010) Evolution of poly(ADP-ribose) polymerase-1 (PARP-1) inhibitors. From concept to clinic. *J Med Chem*, **53**, 4561–4584.
114. Thomas,H.D., Calabrese,C.R., Batey,M.A., Canan,S., Hostomsky,Z., Kyle,S., Maegley,K.A., Newell,D.R., Skalitzky,D., Wang,L.-Z., *et al.* (2007) Preclinical

- selection of a novel poly(ADP-ribose) polymerase inhibitor for clinical trial. *Mol Cancer Ther*, **6**, 945–956.
115. Calabrese,C.R., Almassy,R., Barton,S., Batey,M.A., Calvert,A.H., Canan-Koch,S., Durkacz,B.W., Hostomsky,Z., Kumpf,R.A., Kyle,S., *et al.* (2004) Anticancer chemosensitization and radiosensitization by the novel poly(ADP-ribose) polymerase-1 inhibitor AG14361. *J Natl Cancer Inst*, **96**, 56–67.
 116. Plummer,R., Jones,C., Middleton,M., Wilson,R., Evans,J., Olsen,A., Curtin,N., Boddy,A., McHugh,P., Newell,D., *et al.* (2008) Phase I study of the poly(ADP-ribose) polymerase inhibitor, AG014699, in combination with temozolomide in patients with advanced solid tumors. *Clin Cancer Res*, **14**, 7917–7923.
 117. Lesueur,P., Chevalier,F., Austry,J.-B., Waissi,W., Burckel,H., Noël,G., Habrand,J.-L., Saintigny,Y. and Joly,F. (2017) Poly-(ADP-ribose)-polymerase inhibitors as radiosensitizers: a systematic review of pre-clinical and clinical human studies. *Oncotarget*, **8**, 69105–69124.
 118. Evers,B., Drost,R., Schut,E., de Bruin,M., van der Burg,E., Derksen,P.W.B., Holstege,H., Liu,X., van Drunen,E., Beverloo,H.B., *et al.* (2008) Selective inhibition of BRCA2-deficient mammary tumor cell growth by AZD2281 and cisplatin. *Clin Cancer Res*, **14**, 3916–3925.
 119. Powell,C., Mikropoulos,C., Kaye,S.B., Nutting,C.M., Bhide,S.A., Newbold,K. and Harrington,K.J. (2010) Pre-clinical and clinical evaluation of PARP inhibitors as tumour-specific radiosensitisers. *Cancer Treat Rev*, **36**, 566–575.
 120. Lindahl,T., Satoh,M.S., Poirier,G.G. and Klungland,A. (1995) Post-translational modification of poly(ADP-ribose) polymerase induced by DNA strand breaks. *Trends Biochem Sci*, **20**, 405–411.
 121. Saleh-Gohari,N., Bryant,H.E., Schultz,N., Parker,K.M., Cassel,T.N. and Helleday,T. (2005) Spontaneous homologous recombination is induced by collapsed replication forks that are caused by endogenous DNA single-strand breaks. *Mol Cell Biol*, **25**, 7158–7169.
 122. Venkitaraman,A.R. (2001) Functions of BRCA1 and BRCA2 in the biological response to DNA damage. *J Cell Sci*, **114**, 3591–3598.
 123. Prokhorova,E., Agnew,T., Wondisford,A.R., Tellier,M., Kaminski,N., Beijer,D., Holder,J., Gros Lambert,J., Suskiewicz,M.J., Zhu,K., *et al.* (2021) Unrestrained poly-ADP-ribosylation provides insights into chromatin regulation and human disease. *Mol Cell*, **81**, 2640-2655.e8.
 124. Murai,J., Huang,S.N., Das,B.B., Renaud,A., Zhang,Y., Doroshow,J.H., Ji,J., Takeda,S. and Pommier,Y. (2012) Trapping of PARP1 and PARP2 by Clinical PARP Inhibitors. *Cancer Res*, **72**, 5588–5599.

125. Zandarashvili,L., Langelier,M.-F., Velagapudi,U.K., Hancock,M.A., Steffen,J.D., Billur,R., Hannan,Z.M., Wicks,A.J., Krastev,D.B., Pettitt,S.J., *et al.* (2020) Structural basis for allosteric PARP-1 retention on DNA breaks. *Science*, **368**, eaax6367.
126. Arnold,M.R., Langelier,M.-F., Gartrell,J., Kirby,I.T., Sanderson,D.J., Bejan,D.S., Šileikytė,J., Sundalam,S.K., Nagarajan,S., Marimuthu,P., *et al.* (2022) Allosteric regulation of DNA binding and target residence time drive the cytotoxicity of phthalazinone-based PARP-1 inhibitors. *Cell Chem Biol*, **29**, 1694-1708.e10.
127. Ryan,K., Bolaños,B., Smith,M., Palde,P.B., Cuenca,P.D., VanArsdale,T.L., Niessen,S., Zhang,L., Behenna,D., Ornelas,M.A., *et al.* (2021) Dissecting the molecular determinants of clinical PARP1 inhibitor selectivity for tankyrase1. *J Biol Chem*, **296**, 100251.
128. Stojanovic,P., Luger,K. and Rudolph,J. (2023) Slow Dissociation from the PARP1-HPF1 Complex Drives Inhibitor Potency. *Biochemistry*, **62**, 2382–2390.
129. Cancer Genome Atlas Research Network (2011) Integrated genomic analyses of ovarian carcinoma. *Nature*, **474**, 609–615.
130. Waddell,N., Pajic,M., Patch,A.-M., Chang,D.K., Kassahn,K.S., Bailey,P., Johns,A.L., Miller,D., Nones,K., Quek,K., *et al.* (2015) Whole genomes redefine the mutational landscape of pancreatic cancer. *Nature*, **518**, 495–501.
131. Carnevale,J. and Ashworth,A. (2015) Assessing the Significance of BRCA1 and BRCA2 Mutations in Pancreatic Cancer. *J Clin Oncol*, **33**, 3080–3081.
132. Mateo,J., Carreira,S., Sandhu,S., Miranda,S., Mossop,H., Perez-Lopez,R., Nava Rodrigues,D., Robinson,D., Omlin,A., Tunariu,N., *et al.* (2015) DNA-Repair Defects and Olaparib in Metastatic Prostate Cancer. *N Engl J Med*, **373**, 1697–1708.
133. Gelmon,K.A., Tischkowitz,M., Mackay,H., Swenerton,K., Robidoux,A., Tonkin,K., Hirte,H., Huntsman,D., Clemons,M., Gilks,B., *et al.* (2011) Olaparib in patients with recurrent high-grade serous or poorly differentiated ovarian carcinoma or triple-negative breast cancer: a phase 2, multicentre, open-label, non-randomised study. *Lancet Oncol*, **12**, 852–861.
134. Mukhopadhyay,A., Elattar,A., Cerbinskaite,A., Wilkinson,S.J., Drew,Y., Kyle,S., Los,G., Hostomsky,Z., Edmondson,R.J. and Curtin,N.J. (2010) Development of a functional assay for homologous recombination status in primary cultures of epithelial ovarian tumor and correlation with sensitivity to poly(ADP-ribose) polymerase inhibitors. *Clin Cancer Res*, **16**, 2344–2351.
135. Konstantinopoulos,P.A., Spentzos,D., Karlan,B.Y., Taniguchi,T., Fountzilias,E., Francoeur,N., Levine,D.A. and Cannistra,S.A. (2010) Gene expression profile of BRCAness that correlates with responsiveness to chemotherapy and with outcome in patients with epithelial ovarian cancer. *J Clin Oncol*, **28**, 3555–3561.

136. Lord,C.J. and Ashworth,A. (2016) BRCAness revisited. *Nat Rev Cancer*, **16**, 110–120.
137. Alexandrov,L.B., Nik-Zainal,S., Wedge,D.C., Aparicio,S.A.J.R., Behjati,S., Biankin,A.V., Bignell,G.R., Bolli,N., Borg,A., Børresen-Dale,A.-L., *et al.* (2013) Signatures of mutational processes in human cancer. *Nature*, **500**, 415–421.
138. Nik-Zainal,S., Davies,H., Staaf,J., Ramakrishna,M., Glodzik,D., Zou,X., Martincorena,I., Alexandrov,L.B., Martin,S., Wedge,D.C., *et al.* (2016) Landscape of somatic mutations in 560 breast cancer whole-genome sequences. *Nature*, **534**, 47–54.
139. Polak,P., Kim,J., Braunstein,L.Z., Tiao,G., Karlic,R., Rosebrock,D., Livitz,D., Kübler,K., Mouw,K.W., Haradhvala,N.J., *et al.* (2017) A mutational signature reveals alterations underlying deficient homologous recombination repair in breast cancer. *Nat Genet*, **49**, 1476–1486.
140. Beltran,H., Yelensky,R., Frampton,G.M., Park,K., Downing,S.R., MacDonald,T.Y., Jarosz,M., Lipson,D., Tagawa,S.T., Nanus,D.M., *et al.* (2013) Targeted next-generation sequencing of advanced prostate cancer identifies potential therapeutic targets and disease heterogeneity. *Eur Urol*, **63**, 920–926.
141. Graeser,M., McCarthy,A., Lord,C.J., Savage,K., Hills,M., Salter,J., Orr,N., Parton,M., Smith,I.E., Reis-Filho,J.S., *et al.* (2010) A marker of homologous recombination predicts pathologic complete response to neoadjuvant chemotherapy in primary breast cancer. *Clin Cancer Res*, **16**, 6159–6168.
142. Vaitsiankova,A., Burdova,K., Sobol,M., Gautam,A., Benada,O., Hanzlikova,H. and Caldecott,K.W. (2022) PARP inhibition impedes the maturation of nascent DNA strands during DNA replication. *Nat Struct Mol Biol*, **29**, 329–338.
143. Baxter,J.S., Zatreanu,D., Pettitt,S.J. and Lord,C.J. (2022) Resistance to DNA repair inhibitors in cancer. *Mol Oncol*, **16**, 3811–3827.
144. Edwards,S.L., Brough,R., Lord,C.J., Natrajan,R., Vatcheva,R., Levine,D.A., Boyd,J., Reis-Filho,J.S. and Ashworth,A. (2008) Resistance to therapy caused by intragenic deletion in BRCA2. *Nature*, **451**, 1111–1115.
145. Swisher,E.M., Sakai,W., Karlan,B.Y., Wurz,K., Urban,N. and Taniguchi,T. (2008) Secondary BRCA1 mutations in BRCA1-mutated ovarian carcinomas with platinum resistance. *Cancer Res*, **68**, 2581–2586.
146. Sakai,W., Swisher,E.M., Karlan,B.Y., Agarwal,M.K., Higgins,J., Friedman,C., Villegas,E., Jacquemont,C., Farrugia,D.J., Couch,F.J., *et al.* (2008) Secondary mutations as a mechanism of cisplatin resistance in BRCA2-mutated cancers. *Nature*, **451**, 1116–1120.
147. Waks,A.G., Cohen,O., Kochupurakkal,B., Kim,D., Dunn,C.E., Buendia Buendia,J., Wander,S., Helvie,K., Lloyd,M.R., Marini,L., *et al.* (2020) Reversion and non-

reversion mechanisms of resistance to PARP inhibitor or platinum chemotherapy in BRCA1/2-mutant metastatic breast cancer. *Ann Oncol*, **31**, 590–598.

148. Tobalina,L., Armenia,J., Irving,E., O’Connor,M.J. and Forment,J.V. (2021) A meta-analysis of reversion mutations in BRCA genes identifies signatures of DNA end-joining repair mechanisms driving therapy resistance. *Ann Oncol*, **32**, 103–112.
149. Pettitt,S.J., Frankum,J.R., Punta,M., Lise,S., Alexander,J., Chen,Y., Yap,T.A., Haider,S., Tutt,A.N.J. and Lord,C.J. (2020) Clinical BRCA1/2 Reversion Analysis Identifies Hotspot Mutations and Predicted Neoantigens Associated with Therapy Resistance. *Cancer Discov*, **10**, 1475–1488.
150. Kondrashova,O., Nguyen,M., Shield-Artin,K., Tinker,A.V., Teng,N.N.H., Harrell,M.I., Kuiper,M.J., Ho,G.-Y., Barker,H., Jasin,M., *et al.* (2017) Secondary Somatic Mutations Restoring RAD51C and RAD51D Associated with Acquired Resistance to the PARP Inhibitor Rucaparib in High-Grade Ovarian Carcinoma. *Cancer Discov*, **7**, 984–998.
151. Goodall,J., Mateo,J., Yuan,W., Mossop,H., Porta,N., Miranda,S., Perez-Lopez,R., Dolling,D., Robinson,D.R., Sandhu,S., *et al.* (2017) Circulating Cell-Free DNA to Guide Prostate Cancer Treatment with PARP Inhibition. *Cancer Discov*, **7**, 1006–1017.
152. Siravegna,G., Mussolin,B., Venesio,T., Marsoni,S., Seoane,J., Dive,C., Papadopoulos,N., Kopetz,S., Corcoran,R.B., Siu,L.L., *et al.* (2019) How liquid biopsies can change clinical practice in oncology. *Ann Oncol*, **30**, 1580–1590.
153. Knijnenburg,T.A., Wang,L., Zimmermann,M.T., Chambwe,N., Gao,G.F., Cherniack,A.D., Fan,H., Shen,H., Way,G.P., Greene,C.S., *et al.* (2018) Genomic and Molecular Landscape of DNA Damage Repair Deficiency across The Cancer Genome Atlas. *Cell Rep*, **23**, 239-254.e6.
154. Min,A., Kim,K., Jeong,K., Choi,S., Kim,S., Suh,K.J., Lee,K.-H., Kim,S. and Im,S.-A. (2020) Homologous repair deficiency score for identifying breast cancers with defective DNA damage response. *Sci Rep*, **10**, 12506.
155. Min,A., Im,S.-A., Yoon,Y.-K., Song,S.-H., Nam,H.-J., Hur,H.-S., Kim,H.-P., Lee,K.-H., Han,S.-W., Oh,D.-Y., *et al.* (2013) RAD51C-deficient cancer cells are highly sensitive to the PARP inhibitor olaparib. *Mol Cancer Ther*, **12**, 865–877.
156. Kondrashova,O., Topp,M., Nestic,K., Lieschke,E., Ho,G.-Y., Harrell,M.I., Zapparoli,G.V., Hadley,A., Holian,R., Boehm,E., *et al.* (2018) Methylation of all BRCA1 copies predicts response to the PARP inhibitor rucaparib in ovarian carcinoma. *Nat Commun*, **9**, 3970.
157. Jamal,K., Galbiati,A., Armenia,J., Illuzzi,G., Hall,J., Bentouati,S., Barrell,D., Ahdesmäki,M., Functional Genomics Centre Group, O’Connor,M.J., *et al.* (2022) Drug-gene Interaction Screens Coupled to Tumor Data Analyses Identify the Most

Clinically Relevant Cancer Vulnerabilities Driving Sensitivity to PARP Inhibition. *Cancer Res Commun*, **2**, 1244–1254.

158. Patch,A.-M., Christie,E.L., Etemadmoghadam,D., Garsed,D.W., George,J., Fereday,S., Nones,K., Cowin,P., Alsop,K., Bailey,P.J., *et al.* (2015) Whole-genome characterization of chemoresistant ovarian cancer. *Nature*, **521**, 489–494.
159. Hurley,R.M., McGehee,C.D., Nestic,K., Correia,C., Weiskittel,T.M., Kelly,R.L., Venkatachalam,A., Hou,X., Pathoulas,N.M., Meng,X.W., *et al.* (2021) Characterization of a RAD51C-silenced high-grade serous ovarian cancer model during development of PARP inhibitor resistance. *NAR Cancer*, **3**, zcab028.
160. Castroviejo-Bermejo,M., Cruz,C., Llop-Guevara,A., Gutiérrez-Enríquez,S., Ducey,M., Ibrahim,Y.H., Gris-Oliver,A., Pellegrino,B., Bruna,A., Guzmán,M., *et al.* (2018) A RAD51 assay feasible in routine tumor samples calls PARP inhibitor response beyond BRCA mutation. *EMBO Mol Med*, **10**, e9172.
161. ter Brugge,P., Kristel,P., van der Burg,E., Boon,U., de Maaker,M., Lips,E., Mulder,L., de Rooter,J., Moutinho,C., Gevensleben,H., *et al.* (2016) Mechanisms of Therapy Resistance in Patient-Derived Xenograft Models of BRCA1-Deficient Breast Cancer. *JNCI: Journal of the National Cancer Institute*, **108**, djw148.
162. Aly,A. and Ganesan,S. (2011) BRCA1, PARP, and 53BP1: conditional synthetic lethality and synthetic viability. *J Mol Cell Biol*, **3**, 66–74.
163. Bunting,S.F., Callén,E., Wong,N., Chen,H.-T., Polato,F., Gunn,A., Bothmer,A., Feldhahn,N., Fernandez-Capetillo,O., Cao,L., *et al.* (2010) 53BP1 inhibits homologous recombination in Brca1-deficient cells by blocking resection of DNA breaks. *Cell*, **141**, 243–254.
164. Bouwman,P., Aly,A., Escandell,J.M., Pieterse,M., Bartkova,J., van der Gulden,H., Hiddingh,S., Thanasoula,M., Kulkarni,A., Yang,Q., *et al.* (2010) 53BP1 loss rescues BRCA1 deficiency and is associated with triple-negative and BRCA-mutated breast cancers. *Nat Struct Mol Biol*, **17**, 688–695.
165. Cao,L., Xu,X., Bunting,S.F., Liu,J., Wang,R.-H., Cao,L.L., Wu,J.J., Peng,T.-N., Chen,J., Nussenzweig,A., *et al.* (2009) A selective requirement for 53BP1 in the biological response to genomic instability induced by Brca1 deficiency. *Mol Cell*, **35**, 534–541.
166. Gupta,R., Somyajit,K., Narita,T., Maskey,E., Stanlie,A., Kremer,M., Typas,D., Lammers,M., Mailand,N., Nussenzweig,A., *et al.* (2018) DNA Repair Network Analysis Reveals Shieldin as a Key Regulator of NHEJ and PARP Inhibitor Sensitivity. *Cell*, **173**, 972-988.e23.
167. Noordermeer,S.M., Adam,S., Setiaputra,D., Barazas,M., Pettitt,S.J., Ling,A.K., Olivieri,M., Álvarez-Quilón,A., Moatti,N., Zimmermann,M., *et al.* (2018) The shieldin complex mediates 53BP1-dependent DNA repair. *Nature*, **560**, 117–121.

168. Xu,G., Chapman,J.R., Brandsma,I., Yuan,J., Mistrik,M., Bouwman,P., Bartkova,J., Gogola,E., Warmerdam,D., Barazas,M., *et al.* (2015) REV7 counteracts DNA double-strand break resection and affects PARP inhibition. *Nature*, **521**, 541–544.
169. Zimmermann,M., Murina,O., Reijns,M.A.M., Agathangelou,A., Challis,R., Tarnauskaitė,Ž., Muir,M., Fluteau,A., Aregger,M., McEwan,A., *et al.* (2018) CRISPR screens identify genomic ribonucleotides as a source of PARP-trapping lesions. *Nature*, **559**, 285–289.
170. Clements,K.E., Schleicher,E.M., Thakar,T., Hale,A., Dhoonmoon,A., Tolman,N.J., Sharma,A., Liang,X., Imamura Kawasawa,Y., Nicolae,C.M., *et al.* (2020) Identification of regulators of poly-ADP-ribose polymerase inhibitor response through complementary CRISPR knockout and activation screens. *Nat Commun*, **11**, 6118.
171. Su,D., Feng,X., Colic,M., Wang,Y., Zhang,C., Wang,C., Tang,M., Hart,T. and Chen,J. (2020) CRISPR/CAS9-based DNA damage response screens reveal gene-drug interactions. *DNA Repair (Amst)*, **87**, 102803.
172. Shalem,O., Sanjana,N.E., Hartenian,E., Shi,X., Scott,D.A., Mikkelsen,T., Heckl,D., Ebert,B.L., Root,D.E., Doench,J.G., *et al.* (2014) Genome-Scale CRISPR-Cas9 Knockout Screening in Human Cells. *Science*, **343**, 84–87.
173. Juhász,S., Smith,R., Schauer,T., Spekhardt,D., Mamar,H., Zentout,S., Chapuis,C., Huet,S. and Timinszky,G. (2020) The chromatin remodeler ALC1 underlies resistance to PARP inhibitor treatment. *Sci Adv*, **6**, eabb8626.
174. Lehmann,L.C., Hewitt,G., Aibara,S., Leitner,A., Marklund,E., Maslen,S.L., Maturi,V., Chen,Y., van der Spoel,D., Skehel,J.M., *et al.* (2017) Mechanistic Insights into Autoinhibition of the Oncogenic Chromatin Remodeler ALC1. *Mol Cell*, **68**, 847-859.e7.
175. Singh,H.R., Nardoza,A.P., Möller,I.R., Knobloch,G., Kistemaker,H.A.V., Hassler,M., Harrer,N., Blessing,C., Eustermann,S., Kotthoff,C., *et al.* (2017) A Poly-ADP-Ribose Trigger Releases the Auto-Inhibition of a Chromatin Remodeling Oncogene. *Mol Cell*, **68**, 860-871.e7.
176. Sellou,H., Lebeaupin,T., Chapuis,C., Smith,R., Hegele,A., Singh,H.R., Kozlowski,M., Bultmann,S., Ladurner,A.G., Timinszky,G., *et al.* (2016) The poly(ADP-ribose)-dependent chromatin remodeler Alc1 induces local chromatin relaxation upon DNA damage. *Mol Biol Cell*, **27**, 3791–3799.
177. Tsuda,M., Cho,K., Ooka,M., Shimizu,N., Watanabe,R., Yasui,A., Nakazawa,Y., Ogi,T., Harada,H., Agama,K., *et al.* (2017) ALC1/CHD1L, a chromatin-remodeling enzyme, is required for efficient base excision repair. *PLoS One*, **12**, e0188320.
178. Pines,A., Vrouwe,M.G., Marteiijn,J.A., Typas,D., Luijsterburg,M.S., Cansoy,M., Hensbergen,P., Deelder,A., de Groot,A., Matsumoto,S., *et al.* (2012) PARP1

- promotes nucleotide excision repair through DDB2 stabilization and recruitment of ALC1. *J Cell Biol*, **199**, 235–249.
179. Ma,N.-F., Hu,L., Fung,J.M., Xie,D., Zheng,B.-J., Chen,L., Tang,D.-J., Fu,L., Wu,Z., Chen,M., *et al.* (2008) Isolation and characterization of a novel oncogene, amplified in liver cancer 1, within a commonly amplified region at 1q21 in hepatocellular carcinoma. *Hepatology*, **47**, 503–510.
180. Cheng,W., Su,Y. and Xu,F. (2013) CHD1L: a novel oncogene. *Mol Cancer*, **12**, 170.
181. Li,Y., He,L.-R., Gao,Y., Zhou,N.-N., Liu,Y., Zhou,X.-K., Liu,J.-F., Guan,X.-Y., Ma,N.-F. and Xie,D. (2019) CHD1L contributes to cisplatin resistance by upregulating the ABCB1-NF- κ B axis in human non-small-cell lung cancer. *Cell Death Dis*, **10**, 99.
182. He,W.-P., Zhou,J., Cai,M.-Y., Xiao,X.-S., Liao,Y.-J., Kung,H.-F., Guan,X.-Y., Xie,D. and Yang,G.-F. (2012) CHD1L protein is overexpressed in human ovarian carcinomas and is a novel predictive biomarker for patients survival. *BMC Cancer*, **12**, 437.
183. Burgers,P.M.J. and Kunkel,T.A. (2017) Eukaryotic DNA Replication Fork. *Annu Rev Biochem*, **86**, 417–438.
184. Pursell,Z.F. and Kunkel,T.A. (2008) DNA Polymerase ϵ : A Polymerase Of Unusual Size (and Complexity). *Prog Nucleic Acid Res Mol Biol*, **82**, 101–145.
185. Aksenova,A., Volkov,K., Maceluch,J., Pursell,Z.F., Rogozin,I.B., Kunkel,T.A., Pavlov,Y.I. and Johansson,E. (2010) Mismatch repair-independent increase in spontaneous mutagenesis in yeast lacking non-essential subunits of DNA polymerase ϵ . *PLoS Genet*, **6**, e1001209.
186. Puddu,F., Piergiovanni,G., Plevani,P. and Muzi-Falconi,M. (2011) Sensing of replication stress and Mec1 activation act through two independent pathways involving the 9-1-1 complex and DNA polymerase ϵ . *PLoS Genet*, **7**, e1002022.
187. Bellelli,R., Borel,V., Logan,C., Svendsen,J., Cox,D.E., Nye,E., Metcalfe,K., O’Connell,S.M., Stamp,G., Flynn,H.R., *et al.* (2018) Pol ϵ Instability Drives Replication Stress, Abnormal Development, and Tumorigenesis. *Mol Cell*, **70**, 707-721.e7.
188. Yu,C., Gan,H., Serra-Cardona,A., Zhang,L., Gan,S., Sharma,S., Johansson,E., Chabes,A., Xu,R.-M. and Zhang,Z. (2018) A mechanism for preventing asymmetric histone segregation onto replicating DNA strands. *Science*, **361**, 1386–1389.
189. Li,Z., Hua,X., Serra-Cardona,A., Xu,X., Gan,S., Zhou,H., Yang,W.-S., Chen,C.-L., Xu,R.-M. and Zhang,Z. (2020) DNA polymerase α interacts with H3-H4 and facilitates the transfer of parental histones to lagging strands. *Sci Adv*, **6**, eabb5820.

190. Iida,T. and Araki,H. (2004) Noncompetitive counteractions of DNA polymerase epsilon and ISW2/yCHRAC for epigenetic inheritance of telomere position effect in *Saccharomyces cerevisiae*. *Mol Cell Biol*, **24**, 217–227.
191. He,H., Li,Y., Dong,Q., Chang,A.-Y., Gao,F., Chi,Z., Su,M., Zhang,F., Ban,H., Martienssen,R., *et al.* (2017) Coordinated regulation of heterochromatin inheritance by Dpb3-Dpb4 complex. *Proc Natl Acad Sci U S A*, **114**, 12524–12529.
192. Hucl,T., Rago,C., Gallmeier,E., Brody,J.R., Gorospe,M. and Kern,S.E. (2008) A syngeneic variance library for functional annotation of human variation: application to BRCA2. *Cancer Res*, **68**, 5023–5030.
193. Lim,K.S., Li,H., Roberts,E.A., Gaudiano,E.F., Clairmont,C., Sambel,L.A., Ponninselvan,K., Liu,J.C., Yang,C., Kozono,D., *et al.* (2018) USP1 Is Required for Replication Fork Protection in BRCA1-Deficient Tumors. *Mol Cell*, **72**, 925-941.e4.
194. Bairoch,A. (2018) The Cellosaurus, a Cell-Line Knowledge Resource. *J Biomol Tech*, **29**, 25–38.
195. Ran,F.A., Hsu,P.D., Wright,J., Agarwala,V., Scott,D.A. and Zhang,F. (2013) Genome engineering using the CRISPR-Cas9 system. *Nat Protoc*, **8**, 2281–2308.
196. Smith,R., Sellou,H., Chapuis,C., Huet,S. and Timinszky,G. (2018) CHD3 and CHD4 recruitment and chromatin remodeling activity at DNA breaks is promoted by early poly(ADP-ribose)-dependent chromatin relaxation. *Nucleic Acids Res*, **46**, 6087–6098.
197. Carpenter,A.E., Jones,T.R., Lamprecht,M.R., Clarke,C., Kang,I.H., Friman,O., Guertin,D.A., Chang,J.H., Lindquist,R.A., Moffat,J., *et al.* (2006) CellProfiler: image analysis software for identifying and quantifying cell phenotypes. *Genome Biol*, **7**, R100.
198. Olive,P.L. and Banáth,J.P. (2006) The comet assay: a method to measure DNA damage in individual cells. *Nat Protoc*, **1**, 23–29.
199. Schindelin,J., Arganda-Carreras,I., Frise,E., Kaynig,V., Longair,M., Pietzsch,T., Preibisch,S., Rueden,C., Saalfeld,S., Schmid,B., *et al.* (2012) Fiji: an open-source platform for biological-image analysis. *Nat Methods*, **9**, 676–682.
200. Mórocz,M., Gali,H., Raskó,I., Downes,C.S. and Haracska,L. (2013) Single cell analysis of human RAD18-dependent DNA post-replication repair by alkaline bromodeoxyuridine comet assay. *PLoS One*, **8**, e70391.
201. Jg,J., A,T.-S., G,H., H,G., A,H., F,J., K,E., Z,L., Lh,M., L,H., *et al.* (2009) Separate domains of Rev1 mediate two modes of DNA damage bypass in mammalian cells. *Molecular and cellular biology*, **29**.

202. Thomas,A., Murai,J. and Pommier,Y. The evolving landscape of predictive biomarkers of response to PARP inhibitors. *J Clin Invest*, **128**, 1727–1730.
203. Patel,A.G., Sarkaria,J.N. and Kaufmann,S.H. (2011) Nonhomologous end joining drives poly(ADP-ribose) polymerase (PARP) inhibitor lethality in homologous recombination-deficient cells. *Proc Natl Acad Sci U S A*, **108**, 3406–3411.
204. Belotserkovskaya,R., Raga Gil,E., Lawrence,N., Butler,R., Clifford,G., Wilson,M.D. and Jackson,S.P. (2020) PALB2 chromatin recruitment restores homologous recombination in BRCA1-deficient cells depleted of 53BP1. *Nat Commun*, **11**, 819.
205. Jaspers,J.E., Kersbergen,A., Boon,U., Sol,W., van Deemter,L., Zander,S.A., Drost,R., Wientjens,E., Ji,J., Aly,A., *et al.* (2013) Loss of 53BP1 causes PARP inhibitor resistance in Brca1-mutated mouse mammary tumors. *Cancer Discov*, **3**, 68–81.
206. Hustedt,N., Álvarez-Quilón,A., McEwan,A., Yuan,J.Y., Cho,T., Koob,L., Hart,T. and Durocher,D. (2019) A consensus set of genetic vulnerabilities to ATR inhibition. *Open Biol*, **9**, 190156.
207. Lin,X., Jiang,W., Rudolph,J., Lee,B.J., Luger,K. and Zha,S. (2022) PARP inhibitors trap PARP2 and alter the mode of recruitment of PARP2 at DNA damage sites. *Nucleic Acids Res*, **50**, 3958–3973.
208. Langelier,M.-F., Lin,X., Zha,S. and Pascal,J.M. Clinical PARP inhibitors allosterically induce PARP2 retention on DNA. *Sci Adv*, **9**, eadf7175.
209. Buchfellner,A., Yurlova,L., Nüske,S., Scholz,A.M., Bogner,J., Ruf,B., Zolghadr,K., Drexler,S.E., Drexler,G.A., Girst,S., *et al.* (2016) A New Nanobody-Based Biosensor to Study Endogenous PARP1 In Vitro and in Live Human Cells. *PLoS One*, **11**, e0151041.
210. Zeman,M.K. and Cimprich,K.A. (2014) Causes and consequences of replication stress. *Nat Cell Biol*, **16**, 2–9.
211. Liu,S., Shiotani,B., Lahiri,M., Maréchal,A., Tse,A., Leung,C.C.Y., Mark Glover,J.N., Yang,X.H. and Zou,L. (2011) ATR Autophosphorylation as a Molecular Switch for Checkpoint Activation. *Mol Cell*, **43**, 192–202.
212. Maréchal,A. and Zou,L. (2015) RPA-coated single-stranded DNA as a platform for post-translational modifications in the DNA damage response. *Cell Res*, **25**, 9–23.
213. Buisson,R., Boisvert,J.L., Benes,C.H. and Zou,L. (2015) Distinct but Concerted Roles of ATR, DNA-PK, and Chk1 in Countering Replication Stress during S Phase. *Mol Cell*, **59**, 1011–1024.
214. Cybulla,E. and Vindigni,A. (2023) Leveraging the replication stress response to optimize cancer therapy. *Nat Rev Cancer*, **23**, 6–24.

215. Byrum,A.K., Vindigni,A. and Mosammaparast,N. (2019) Defining and Modulating ‘BRCAness’. *Trends Cell Biol*, **29**, 740–751.
216. Tirkkonen,M., Tanner,M., Karhu,R., Kallioniemi,A., Isola,J. and Kallioniemi,O.P. (1998) Molecular cytogenetics of primary breast cancer by CGH. *Genes Chromosomes Cancer*, **21**, 177–184.
217. Kudoh,K., Takano,M., Koshikawa,T., Hirai,M., Yoshida,S., Mano,Y., Yamamoto,K., Ishii,K., Kita,T., Kikuchi,Y., *et al.* (1999) Gains of 1q21-q22 and 13q12-q14 are potential indicators for resistance to cisplatin-based chemotherapy in ovarian cancer patients. *Clin Cancer Res*, **5**, 2526–2531.
218. Blessing,C., Mandemaker,I.K., Gonzalez-Leal,C., Preisser,J., Schomburg,A. and Ladurner,A.G. (2020) The Oncogenic Helicase ALC1 Regulates PARP Inhibitor Potency by Trapping PARP2 at DNA Breaks. *Mol Cell*, **80**, 862-875.e6.
219. Verma,P., Zhou,Y., Cao,Z., Deraska,P.V., Deb,M., Arai,E., Li,W., Shao,Y., Puentes,L., Li,Y., *et al.* (2021) ALC1 links chromatin accessibility to PARP inhibitor response in homologous recombination-deficient cells. *Nat Cell Biol*, **23**, 160–171.
220. Hewitt,G., Borel,V., Segura-Bayona,S., Takaki,T., Ruis,P., Bellelli,R., Lehmann,L.C., Sommerova,L., Vancevska,A., Tomas-Loba,A., *et al.* (2021) Defective ALC1 nucleosome remodeling confers PARPi sensitization and synthetic lethality with HRD. *Molecular Cell*, **81**, 767-783.e11.
221. Prigaro,B.J., Esquer,H., Zhou,Q., Pike,L.A., Awolade,P., Lai,X.-H., Abraham,A.D., Abbott,J.M., Matter,B., Kompella,U.B., *et al.* (2022) Design, Synthesis, and Biological Evaluation of the First Inhibitors of Oncogenic CHD1L. *J Med Chem*, **65**, 3943–3961.
222. Abbott,J.M., Zhou,Q., Esquer,H., Pike,L., Broneske,T.P., Rinaldetti,S., Abraham,A.D., Ramirez,D.A., Lunghofer,P.J., Pitts,T.M., *et al.* (2020) First-in-Class Inhibitors of Oncogenic CHD1L with Preclinical Activity against Colorectal Cancer. *Mol Cancer Ther*, **19**, 1598–1612.
223. Johannes,J.W., Balazs,A., Barratt,D., Bista,M., Chuba,M.D., Cosulich,S., Critchlow,S.E., Degorce,S.L., Di Fruscia,P., Edmondson,S.D., *et al.* (2021) Discovery of 5-{4-[(7-Ethyl-6-oxo-5,6-dihydro-1,5-naphthyridin-3-yl)methyl]piperazin-1-yl}-N-methylpyridine-2-carboxamide (AZD5305): A PARP1-DNA Trapper with High Selectivity for PARP1 over PARP2 and Other PARPs. *J Med Chem*, **64**, 14498–14512.
224. Illuzzi,G., Staniszewska,A.D., Gill,S.J., Pike,A., McWilliams,L., Critchlow,S.E., Cronin,A., Fawell,S., Hawthorne,G., Jamal,K., *et al.* (2022) Preclinical Characterization of AZD5305, A Next-Generation, Highly Selective PARP1 Inhibitor and Trapper. *Clin Cancer Res*, **28**, 4724–4736.

225. Navas,T.A., Zhou,Z. and Elledge,S.J. (1995) DNA polymerase epsilon links the DNA replication machinery to the S phase checkpoint. *Cell*, **80**, 29–39.
226. Araki,H., Leem,S.H., Phongdara,A. and Sugino,A. (1995) Dpb11, which interacts with DNA polymerase II(epsilon) in *Saccharomyces cerevisiae*, has a dual role in S-phase progression and at a cell cycle checkpoint. *Proc Natl Acad Sci U S A*, **92**, 11791–11795.
227. Bellelli,R., Youds,J., Borel,V., Svendsen,J., Pavicic-Kaltenbrunner,V. and Boulton,S.J. (2020) Synthetic Lethality between DNA Polymerase Epsilon and RTEL1 in Metazoan DNA Replication. *Cell Rep*, **31**, 107675.
228. Borel,V., Boeing,S., Van Wietmarschen,N., Sridharan,S., Hill,B.R., Ombrato,L., Perez-Lloret,J., Jackson,D., Goldstone,R., Boulton,S.J., *et al.* (2022) Disrupted control of origin activation compromises genome integrity upon destabilization of Pol ϵ and dysfunction of the TRP53-CDKN1A/P21 axis. *Cell Reports*, **39**, 110871.
229. Smirnova,M. and Klein,H.L. (2003) Role of the error-free damage bypass postreplication repair pathway in the maintenance of genomic stability. *Mutation Research/Fundamental and Molecular Mechanisms of Mutagenesis*, **532**, 117–135.
230. Cimprich,K.A. and Cortez,D. (2008) ATR: an essential regulator of genome integrity. *Nat Rev Mol Cell Biol*, **9**, 616–627.
231. Zou,L. and Elledge,S.J. (2003) Sensing DNA damage through ATRIP recognition of RPA-ssDNA complexes. *Science*, **300**, 1542–1548.
232. Zhao,H. and Piwnicka-Worms,H. (2001) ATR-mediated checkpoint pathways regulate phosphorylation and activation of human Chk1. *Mol Cell Biol*, **21**, 4129–4139.
233. Liu,Q., Guntuku,S., Cui,X.S., Matsuoka,S., Cortez,D., Tamai,K., Luo,G., Carattini-Rivera,S., DeMayo,F., Bradley,A., *et al.* (2000) Chk1 is an essential kinase that is regulated by Atr and required for the G(2)/M DNA damage checkpoint. *Genes Dev*, **14**, 1448–1459.
234. Menolfi,D., Lee,B.J., Zhang,H., Jiang,W., Bowen,N.E., Wang,Y., Zhao,J., Holmes,A., Gershik,S., Rabadan,R., *et al.* (2023) ATR kinase supports normal proliferation in the early S phase by preventing replication resource exhaustion. *Nat Commun*, **14**, 3618.
235. Kim,H., George,E., Ragland,R., Rafail,S., Zhang,R., Krepler,C., Morgan,M., Herlyn,M., Brown,E. and Simpkins,F. (2017) Targeting the ATR/CHK1 Axis with PARP Inhibition Results in Tumor Regression in BRCA-Mutant Ovarian Cancer Models. *Clin Cancer Res*, **23**, 3097–3108.
236. Schoonen,P.M., Kok,Y.P., Wierenga,E., Bakker,B., Foiijer,F., Spierings,D.C.J. and van Vugt,M.A.T.M. (2019) Premature mitotic entry induced by ATR inhibition potentiates olaparib inhibition-mediated genomic instability, inflammatory

- signaling, and cytotoxicity in BRCA2-deficient cancer cells. *Mol Oncol*, **13**, 2422–2440.
237. Zimmermann,M., Bernier,C., Kaiser,B., Fournier,S., Li,L., Desjardins,J., Skeldon,A., Rimkunas,V., Veloso,A., Young,J.T.F., *et al.* (2022) Guiding ATR and PARP inhibitor combinations with chemogenomic screens. *Cell Rep*, **40**, 111081.
238. Miao,C., Tsujino,T., Takai,T., Gui,F., Tsutsumi,T., Sztupinski,Z., Wang,Z., Azuma,H., Szallasi,Z., Mouw,K.W., *et al.* (2022) RB1 loss overrides PARP inhibitor sensitivity driven by RNASEH2B loss in prostate cancer. *Sci Adv*, **8**, eab19794.
239. Jette,N.R., Radhamani,S., Arthur,G., Ye,R., Goutam,S., Bolyos,A., Petersen,L.F., Bose,P., Bebb,D.G. and Lees-Miller,S.P. (2019) Combined poly-ADP ribose polymerase and ataxia-telangiectasia mutated/Rad3-related inhibition targets ataxia-telangiectasia mutated-deficient lung cancer cells. *Br J Cancer*, **121**, 600–610.
240. Lloyd,R.L., Wijnhoven,P.W.G., Ramos-Montoya,A., Wilson,Z., Illuzzi,G., Falenta,K., Jones,G.N., James,N., Chabbert,C.D., Stott,J., *et al.* (2020) Combined PARP and ATR inhibition potentiates genome instability and cell death in ATM-deficient cancer cells. *Oncogene*, **39**, 4869–4883.
241. Haince,J.-F., Kozlov,S., Dawson,V.L., Dawson,T.M., Hendzel,M.J., Lavin,M.F. and Poirier,G.G. (2007) Ataxia telangiectasia mutated (ATM) signaling network is modulated by a novel poly(ADP-ribose)-dependent pathway in the early response to DNA-damaging agents. *J Biol Chem*, **282**, 16441–16453.
242. Bryant,H.E. and Helleday,T. (2006) Inhibition of poly (ADP-ribose) polymerase activates ATM which is required for subsequent homologous recombination repair. *Nucleic Acids Res*, **34**, 1685–1691.

10. List of Publications

MTMT Number: 10076533

Mandatory peer-reviewed international publications for the fulfilment of the doctoral process and on which this thesis is based:

- **Hasan Mamar***, Roberta Fajka-Boja*, Mónika Mórocz, Eva Pinto Jurado, Siham Zentout, Alexandra Mihał, Anna Georgina Kopasz, Mihály Mérey, Rebecca Smith, Abhishek Bharadwaj Sharma, Nicholas D. Lakin, Andrew James Bowman, Lajos Haracska, Sébastien Huet and Gyula Timinszky. The loss of DNA polymerase epsilon accessory subunits POLE3-POLE4 leads to BRCA1-independent PARP inhibitor sensitivity. *Nucleic Acids Research* (2024). doi: <https://doi.org/10.1093/nar/gkae439>. (* Shared first authors). **Impact factor: 14.9**
- Szilvia Juhász*, Rebecca Smith*, Tamás Schauer, Dóra Spekhardt, **Hasan Mamar**, Siham Zentout, Catherine Chapuis, Sébastien Huet, and Gyula Timinszky. The chromatin remodeler ALC1 underlies resistance to PARP inhibitor treatment. *Science Advances*. (2020). DOI: <https://doi.org/10.1126/sciadv.abb8626>. (* Shared first authors). **Impact factor: 15.4**

Awarded fellowship:

- **EMBO short-term fellowship** at University of Warwick, UK. (2023)

Conferences:

- Poster Presentation at **Characterization of posttranslational modifications in cellular signaling**, Odense, Denmark. (2023)
- Selected Talk at **FEBS Advances Lectures Course PARP 2023**, Hvar, Croatia. (2023)
- Selected Talk at **Straub days**, Szeged, Hungary. (2023)
- Selected Talk at **The Biochemistry Global Summit**, Lisbon, Portugal. (2022)
- Poster Presentation at **Young Scientist Forum**, Vimeiro, Portugal. (2022)
- Poster Presentation at **Hungarian Molecular Life Sciences**, Eger, Hungary. (2021)

11. Appendix

TABLES AND THEIR LEGENDS

Table S1. Dharmacon smart pool siRNA

Target	Name	Reference
CTRL	ON-TARGET plus Non-targeting Control siRNAs	D-001810-01-20
PARP1	ON-TARGET plus Human PARP1 siRNA	L-006656-03-0005
PARP2	ON-TARGET plus Human PARP2 siRNA	L-010127-02-0005
BRCA1	ON-TARGET plus Human BRCA1 siRNA	L-003461-00-0005
53BP1	ON-TARGET plus Human TP53BP1 siRNA	L-003548-00-0005
POLE4	ON-TARGET plus Human POLE4 siRNA	L-009850-02-0005
POLE3	ON-TARGET plus Human POLE3 siRNA	L-008460-01-0005

Table S2. Antibodies and antibody-like reagents used in this study

Target	Host	Company	Reference	Dilution in IF	Dilution in FACS	Dilution in WB
53BP1	Rabbit	Abcam	ab36823	-	-	1:3000
Actin	Mouse	Abcam	Ab14128	-	-	1:5000
ALC1	Rabbit	Abcam	ab213929	-	-	1:1000
Beta-Actin	Mouse	Thermo Fisher Scientific	MA5-15739	-	-	1:5000
BrdU	Mouse	Santacruz	sc-32323	1:200	1:200	-
BrdU	Mouse	Becton Dickinson	347580	1:400	-	-
BrdU	Rat	Abcam	6326	1:400	-	-
BRCA1	Rabbit	Proteintech	22362-1-AP	-	-	1:1000
BRCA1	Rabbit	Abcam	ab213929	-	-	1:1000
CHRAC15	Rabbit	ABclonal	A14896	-	-	1:1000
gamma H2AX (phospho S139)	Rabbit	Abcam	ab81299	-	1:250	-

GAPDH	Rabbit	Thermo Fisher	PA1-16777	-	-	1:4000
Ku 70	Mouse	Santa Cruz	sc-5309	-	-	1:1000
mCherry	Mouse	CliniScienes	E-AB- 20015-200	-	-	1:2000
PARP1	Rabbit	Abcam	ab32138	-	-	1:2000
PARP2	Rabbit	Proteintech	55149-1-AP	-	-	1:2000
pATM	Rabbit	Abcam	ab81292	-	-	1:5000
pATR (T1989)	Rabbit	Abcam	ab223258	-	-	1:1000
pDNAPK	Rabbit	Invitrogen	PA5-78130	-	-	1:1000
p-Histone H3(Ser10)	Mouse	Invitrogen	MA5-15220	-	1:200	-
POLE3	Rabbit	ABclonal	A6469	-	-	1:1000
POLE4	Rabbit	ABclonal	A9882	-	-	1:1000
pRPA (S33)	Rabbit	Fortis Life sciences	A300-249A	-	-	1:1000
pRPA (T21)	Rabbit	Abcam	ab109394	-	1:2000	-
Rad51	Rabbit	Abcam	ab133534	1:1000	-	-
Tubulin	Mouse	Thermo Fisher	sc #62204	-	-	1:2000
Secondary antibodies						
Alexa Fluor 488 anti-rabbit IgG	Goat	Invitrogen	A11008	1:500	1:500	-
Alexa Fluor 488 anti-mouse IgG	Goat	Invitrogen	A11001	1:500	1:500	-

Alexa Fluor 488 anti-rat IgG	Goat	Biotium	200023	1:500	-	-
Alexa Fluor 555 anti-rabbit IgG	Goat	Invitrogen	A21428	1:500	1:500	-
Alexa Fluor 555 anti-mouse IgG	Goat	Invitrogen	A21422	1:500	1:500	-
Alexa-Fluor- 546 anti-mouse IgG	Goat	Thermo Fisher	A21123	1:500	-	-
Alexa Fluor 647 anti-mouse IgG	Goat	Invitrogen	A21235	-	1:500	-
Anti-Mouse IgG-HRP	Goat	Invitrogen	A16066	-	-	1:5000
Anti-Rabbit IgG-HRP	Goat	Thermo Fisher	G-21234	-	-	1:5000

Table S3. Inhibitors used in this study

Inhibitor	Commercial name	Company	Reference
ABT-888	Veliparib	Selleck Chemicals	S1004
AG014699	Rucaparib	MedChem Express	HY-10617A
AZD2281	Olaparib	Selleck Chemicals	S1060
BMN-673	Talazoparib	MedChem Express	HY-16106
KU-55933	ATMi	Selleck Chemicals	S1092
MK-4827	Niraparib	Selleck Chemicals	S2741
NU7441	DNAPKi	Selleck Chemicals	S2638
VE-821	ATRi	Selleck Chemicals	S8007

12. Declaration

I declare as the supervisor and the corresponding author of the below listed publications, that the contribution of Hasan Mamar was significant in these publications and that the doctoral process is based on these publications. The results reported in the PhD dissertation were not used to acquire any PhD degree in the past and will not be used in the future either.

- Hasan Mamar*, Roberta Fajka-Boja*, Mónika Mórocz, Eva Pinto Jurado, Siham Zentout, Alexandra Mihuț, Anna Georgina Kopasz, Mihály Mérey, Rebecca Smith, Abhishek Bharadwaj Sharma, Nicholas D. Lakin, Andrew James Bowman, Lajos Haracska, Sébastien Huet and Gyula Timinszky. **The loss of DNA polymerase epsilon accessory subunits POLE3-POLE4 leads to BRCA1-independent PARP inhibitor sensitivity.** *Nucleic Acids Research* (2024). doi: <https://doi.org/10.1093/nar/gkae439>. (* Shared first authors). **Impact factor: 14.9**
- Szilvia Juhász*, Rebecca Smith*, Tamás Schauer, Dóra Spekhardt, Hasan Mamar, Siham Zentout, Catherine Chapuis, Sébastien Huet, and Gyula Timinszky. **The chromatin remodeler ALC1 underlies resistance to PARP inhibitor treatment.** *Science Advances*. (2020). DOI: <https://doi.org/10.1126/sciadv.abb8626>. (* Shared first authors). **Impact factor: 15.4**

Szeged, 27.05.2024

Gyula Timinszky, M.D., Ph.D.

13. Co-authors declaration


We declare that the data used in the thesis written by Hasan Mamar reflect the contribution of the doctoral candidate to the articles:

- Hasan Mamar*, Roberta Fajka-Boja*, Mónika Mórocz, Eva Pinto Jurado, Siham Zentout, Alexandra Mihuț, Anna Georgina Kopasz, Mihály Mérey, Rebecca Smith, Abhishek Bharadwaj Sharma, Nicholas D. Lakin, Andrew James Bowman, Lajos Haracska, Sébastien Huet and Gyula Timinszky. **The loss of DNA polymerase epsilon accessory subunits POLE3-POLE4 leads to BRCA1-independent PARP inhibitor sensitivity.** *Nucleic Acids Research* (2024). doi: <https://doi.org/10.1093/nar/gkae439>. (* Shared first authors). **Impact factor: 14.9**
- Szilvia Juhász*, Rebecca Smith*, Tamás Schauer, Dóra Spekhardt, Hasan Mamar, Siham Zentout, Catherine Chapuis, Sébastien Huet, and Gyula Timinszky. **The chromatin remodeler ALC1 underlies resistance to PARP inhibitor treatment.** *Science Advances*. (2020). DOI: <https://doi.org/10.1126/sciadv.abb8626>. (* Shared first authors). **Impact factor: 15.4**

The results reported in the Ph.D. thesis and the publications were not used to acquire any Ph.D. degree previously. We further declare that the candidate has made a significant contribution to the creation of the above-mentioned publications.

Szeged, 27.05.2024


Roberta Fajka-Boja, Ph.D.


Gyula Timinszky, M.D., Ph.D.